Studies on optimization of membrane properties of chlorinated poly(vinyl chloride) flat-sheet membrane in application for membrane bioreactor

March 2022

Sano Toshio

Graduate School of Science and Technology

Kumamoto University

Contents

Chapter I
Introduction
I.1 Expectation for a new role of membrane bioreactors ……..…... 1
I.2 Membrane bioreactor and their issues ……..…… 3
I.3 Membrane fouling in membrane bioreactors ……...……...……. 4
I.4 Modification of membrane by blending with amphiphilic polymers ……...…… 7
I.5 Strategy to further popularize membrane bioreactor ……...……. 8
I.6 Purpose of this study …….....…..….. 9
References ……..…… 10

Chapter II
Effect of structural vulnerability of flat-sheet membrane on fouling development in continuous submerged membrane bioreactors
II.1 Introduction ……... 29
II.2 Materials and methods …… 31
II.2.1 Membranes and flat-sheet membrane modules used ……...…….. 31
II.2.2 Configuration and operation of laboratory-scale submerged membrane bioreactor .....… 32
II.2.3 Analytical methods ……..….. 35
II.3 Results ……...…… 36
II.3.1 Changes in transmembrane pressure and mixed liquor suspended solid concentration in laboratory-scale submerged membrane ……..……..……..……...… 36
II.3.2 Contribution of membrane surface vulnerability to fouling behavior depending on membrane fabrication process ……..……...……... 38
II.3.3 Comparison of characteristics of suspension liquids from laboratory-scale submerged membrane, night-soil treatment plant with an membrane bioreactor, and sewage treatment plant with a common aeration tank ……...…… 42
II.4 Discussion ……... 46
II.5 Conclusions ……..……..…….. 50
References …….....……... 50

Chapter III
Mechanical durability and fouling development of flat-sheet membranes in a submerged membrane bioreactor
III.1 Introduction ……..... 57
III.2 Materials and methods ……..…. 59
III.2.1 Flat-sheet membranes used in this study ……..…. 59

Contents

III.2.2 Operation of laboratory-scale submerged membrane bioreactor experiment and membrane cleaning …….. 60
III.2.3 Analysis of membrane property ……..… 61
III.2.4 Filtration resistance measurement ……...……...……. 63
III.3 Results ……. 64
III.3.1 Changes in membrane property before and after membrane bioreactor operations …...……. 64
III.3.2 Changes in membrane morphology before and after membrane bioreactor operations ..…… 69
III.3.3 Filtration resistance of the fouled membranes ……...…...……... 69
III.4 Discussion ……...…… 72
III.5 Conclusion ……...…… 74
References ……...…… 75

Chapter IV
Direct and indirect effects of membrane pore size on fouling development in a submerged membrane bioreactor with a symmetric chrolinated poly(vinyl chrolide) flat-sheet membrane

IV.1 Introduction ……. 81
IV.2 Materials and methods …….. 84
IV.2.1 Materials ……...…… 84
IV.2.2 Membrane preparation with different pore sizes …….. 84
IV.2.3 Membrane module fabrication and setup of a laboratory-scale submerged membrane bioreactor ……..... 85
IV.2.4 Synthetic wastewater and membrane bioreactor operating condition ……..…… 87
IV.2.5 Analytical methods ……...…… 88
IV.2.5.1 Characterization of prepared membranes …….…. 88
IV.2.5.2 Characterization of suspension liquid in membrane bioreactor ……..…….. 89
IV.2.5.3 Measurement and evaluation of filtration resistance ……. 90
IV.2.5.4 Gel layer observation ……...…. 92
IV.3 Results ……...…….. 92
IV.3.1 Preparation and characterization of chlorinated poly(vinyl chloride) membranes with different pore size ……...……... 92
IV.3.2 Changes in transmembrane pressure and mixed liquor suspended solids concentrations in a laboratory-scale submerged membrane bioreactor ……. 94
IV.3.3 Filtration resistance of the fouled membranes ……...…….. 98
IV.3.4 Gel layer observation on the membrane surface …….… 100
IV.4 Discussion ……..... 101
IV.5 Conclusion ……...…… 107
References ……..... 108

Contents

Chapter V
Effect of surface hydrophilicity of symmetric polytetrafluoroetylene flat-sheet membranes on membrane fouling in a submerged membrane bioreactor
V.1 Introduction …… 117
V.2 Materials and methods ……..…… 119
V.2.1 Membrane and module fabrication ……..…. 119
V.2.2 Setup of laboratory-scale submerged membrane bioreactor …… 120
V.2.3 Synthetic wastewater and operation condition ……..... 121
V.2.4 Analytical methods …….. 123
V.2.5 Membrane resistance measurement ……. 124
V.3 Results ……...……. 125
V.3.1 Membrane characterization ……. 125
V.3.2 Changes in transmembrane pressure during continuous operation of laboratory-scale submerged membrane bioreactor ……..……..…… 126
V.3.3 Membrane resistance of hydrophilic and hydrophobic membranes …….…… 128
V.4 Discussion …….. 131
V.5 Conclusions ……...…. 134
References ……..... 135

Chapter VI
Effects of Pluronic TR-702 on chlorinated poly(vinyl chloride) flat-sheet membranes prepared by water vapor induced phase separation
VI.1 Introduction ……..……. 141
VI.2 Materials and methods ……..……. 144
VI.2.1 Materials …… 144
VI.2.2 Membrane preparation ……... 145
VI.2.3 Membrane characterization ……...…… 146
VI.2.3.1 Membrane thickness ……...… 146
VI.2.3.2 Pure water permeability …….. 147
VI.2.3.3 Pore size and distribution …… 147
VI.2.3.4 Membrane morphology and porosity ……..…. 148
VI.3 Results ……..…… 148
VI.3.1 Turbidity of the dope solutions ……....……... 148
VI.3.2 Effect of Pluronic TR-702 concentration on the thickness of the prepared membranes …… 149
VI.3.3 Effect of Pluronic TR-702 concentration on the pure water permeability of the prepared membranes ……...…… 149
VI.3.4 Effect of Pluronic TR-702 concentration on the pore size and distribution of the prepared membranes ……...…… 150
VI.3.5 Effect of Pluronic TR-702 concentration on the morphology of the prepared membranes … 151
VI.4 Discussion ……. 154

VI.5 Conclusions 157
References 157

Chapter VII
Fabrication of high-performance chlorinated poly(vinyl chloride) flat-sheet membranes using commercially available fluoropolymers as membrane- property modifiers
VII.1 Introduction 165
VII.2 Materials and methods 166
VII.2.1 Materials 166
VII.2.2 Membrane fabrication 167
VII.2.3 Membrane characterization 168
VII.2.3.1 Surface hydrophilicity 168
VII.2.3.2 Pure water permeability 168
VII.2.3.3 Pore size and distribution 169
VII.2.3.4 Surface morphology and porosity 169
VII.2.3.5 Surface roughness 170
VII.3 Results 170
VII.3.1 Viscosities of dope solutions 170
VII.3.2 Hydrophilicities of fabricated membranes 170
VII.3.3 Pure water permeability of fabricated membranes 171
VII.3.4 Pore size and distribution of fabricated membranes 172
VII.3.5 Surface morphologies and porosities of fabricated membranes 173
VII.3.6 Surface roughness of fabricated membranes 175
VII.4 Discussion 177
VII.5 Conclusions 179
References 180

Chapter VIII
Conclusions
..... 183

Publication related to this dissertation
..... 189

Acknowledgement
..... 193

Chapter I

Introduction

I.1 Expectation for a new role of membrane bioreactors

We release a large amount of sewage such as domestic wastewater and human sewage in our daily lives. Since sewage water contains many organic substances, it causes pathogenic bacteria and a putrid odor. Therefore, if released, it may adversely affect our lives and natural ecosystems. Sewage treatment plants are facilities that collect sewage and rainwater, treat it to below specified water quality standards, and then return it to the natural environment such as river water and seawater. This allows us to live a sanitary life. At the end of 2019, approximately 2,100 sewage treatment plants were found in Japan. Further, two main treatment processes exist: the standard activated sludge process and the oxidation ditch process, which account for most of the total plants.

As a new technology for wastewater treatment, membrane bioreactors (MBRs) have been developed and advanced for more than three decades [1]. Over the years, MBRs have gained widespread attention, were put to practical use, and have been used all over the world [2-14]. MBRs have been widely used for treating municipal and industrial wastewater because of their numerous advantages, including high-quality effluent, small footprint requirements, and ease of operation, in contrast to conventional activated sludge systems, which use settling tanks [15-17]. MBRs also show high pollutant removal performance because suspended solids, including valuable microorganisms, remain inside the reactor [17]. Thus, MBRs have been widely adopted at various wastewater treatment plants worldwide [18,19]. However, as mentioned above,

the standard activated sludge method and the oxidation ditch method are the main methods for wastewater treatment in Japan. Thus, it cannot be declared that MBRs are widespread despite their advantages in Japan.

Plastics are now indispensable substances for maintaining our lives, and we encounter them in food and drink containers, stationaries, clothing, and shopping bags every day. Some of these plastics eventually reach the ocean and cause marine pollution. Because the complete mineralization of plastics commonly requires many years, they are currently the most common and persistent pollutants in the oceans worldwide [20,21]. Two types of plastics exist in marine pollution categorized according to their size, microplastics and macroplastics [22]. Microplastics, commonly defined as plastic particles smaller than 5 mm, have received great attention as substances that may harm ecosystems and human health in recent years [23-25]. Current studies have revealed that the influence of microplastics on marine ecosystems has become more serious [26-37]. Furthermore, several studies on the sources of microplastics have been conducted [38-40]. One of the important sources of microplastics is artificial fiber from laundry washing using washing machines [41-48]. Browne et al. reported that over 1900 types of fibers were generated from domestic washing machines [41], and Hartline et al. reported that a single wash of polyester fleece produced up to 2 g of microfiber [44]. De Falco et al. reported that the number of microfibers released from a typical 5 kg load of polyester fabrics exceeded 6,000,000, depending on the type of detergent used [48]. In addition, personal care products such as facial cleansers contain polyethylene microbeads, which are also well known to be a source of microplastics [22,34,49-52]. These microfibers and microbeads eventually reach wastewater treatment plants (WWTPs) via the sewer system [42], and more than 90% of microplastics are removed in WWTPs [53-56]. However, this

means that almost 10% of microplastics slip through WWTPs and flow into the water environment [57-61]. Therefore, conventional WWTPs are insufficient facilities for microplastic removal. MBR, which is an advanced wastewater treatment technology, has excellent removal performance for microplastics as compared with conventional WWTPs [23,62-64]. Lares et al. reported that MBRs were able to remove 99.4% of microplastics [62]. Li et al. reported that no microplastics were found in the MBR permeate from scanning electron microscopy observations [64]. This suggests that MBRs are a promising solution to marine pollution caused by microplastics. Therefore, MBRs can be expected to play a new role not only as a wastewater treatment system but also as a means to solve one of the environmental problems (SDGs Goal 14).

I.2 Membrane bioreactors and their issues

MBRs are wastewater treatment processes that combine a solid-liquid separation process using membranes and a biological degradation process using activated sludge. Compared with the conventional activated sludge process, MBR eliminates the need for multiple tanks such as the primary settling tank and final settling tank, and in an extreme case, only an aeration tank. Therefore, MBRs have the advantage that the footprint of the processing equipment can be reduced [65,66]. Furthermore, because the membrane can prevent suspended solids and *Escherichia coli*, clear and hygienic treated water can be obtained [67]. However, compared to the conventional activated sludge process, MBRs incur higher operating costs for two main reasons. One is the energy consumption used for membrane aeration [68-72]. Fenu et al. reported that the energy cost of municipal full-scale MBR in Schilde (Belgium) with Zenon hollow fiber membranes was 0.64 kWh/m^3 of permeate [73]. There were some similar reports, which showed more than double the

energy costs for MBRs than for conventional activated sludge with an energy cost of 0.3 kWh/m^3 of permeate [74-76]. In recent years, many efforts have been made to reduce the energy consumption of MBRs and have been successful [9,77]. In the immediate future, the energy cost is expected to be comparable to that of the conventional activated sludge process.

The other is due to the decline in water permeability caused by membrane fouling [68,78-80]. Membrane fouling is a phenomenon by which suspended matter is deposited on the membrane surface and/or captured in membrane pores, and the filtration resistance increases over time [81]. When serious membrane fouling is observed, membrane module cleaning or replacement is needed, but this leads to an increase in operating and maintenance costs [4,18]. Therefore, the reduction of fouling development is still a big issue for the further application of MBRs in the future. Many studies have focused on mitigating membrane fouling in MBRs [82-85], but a definite and effective technique has not been established.

I.3 Membrane fouling in membrane bioreactors

In general, membrane fouling occurs when solutes and solids as foulants contained in the raw water are adsorbed and accumulated on the surface and inside of the membrane, which clogs the pores and reduces the water permeability. Membrane fouling causes various problems, such as an increased operating cost and decreased membrane life [86]. Membrane fouling in MBRs is believed to be due to both pore clogging inside the membrane and the accumulation of sludge cake on the membrane, which is the main fouling component [87]. The factors affecting membrane fouling can be divided into multiple groups such as membrane properties, characteristics of feed water,

characteristics of activated sludge, and operating conditions [17-19,88-100]. The multiple effects of these factors further complicate membrane fouling phenomena [101,102]. For the case of membrane properties among these factors, previous studies reported that membrane material, surface hydrophilicity, membrane morphology, surface charge, pure water permeability, pore size and distribution, porosity, and surface roughness were important factors for the development of membrane fouling [82,103-111]. However, the relationship between the properties of the membrane material and membrane fouling phenomena is still unclear owing to many conflicting results.

Generally, a hydrophobic membrane develops more membrane fouling than hydrophilic membrane due to hydrophobic interactions between foulants, such as extracellular polymeric substances secreted from activated sludge, in the suspension liquid and membrane surface [18,19,106,112-114]. For this reason, many studies have focused on the hydrophilicity of membrane surfaces in the development of antifouling membranes [110,115-117]. However, contradictory results have been reported. For instance, Miyoshi et al. reported that the fouling rate increased in the order of cellulose acetate butyrate (CAB) > polyvinylidene fluoride (PVDF) > polyvinyl butyral (PVB) membranes although PVDF was extremely hydrophobic [109]. Chen et al. reported that the flux diminishing rate was in the order of cellulose acetate (CA) > PVDF > polyethersulfone (PES) membranes although CA was the most hydrophilic among them [118]; similar results have also been reported by other researchers [104,119]. The above studies [104,106,109,110,113,114,118,119] used membranes with different hydrophilicity and other membrane properties for the experiments. This means there is a possibility that the effect of membrane hydrophilicity on membrane fouling was much smaller than the other membrane properties such as pore size and surface roughness,

which led to misinterpretation of the results. Therefore, I considered it necessary to carry out comparative experiments using membranes with similar membrane properties, except hydrophilicity, to confirm the effect of hydrophilicity on membrane fouling, as only a few previous similar studies [108].

In addition to the relationship between the hydrophilicity of the membrane and the membrane fouling propensity, many contradictory results have been reported on the relationship between membrane pore size and membrane fouling propensity [106,107,109,120]. For instance, Miyoshi et al. investigated the relationship between the pore size of the membrane and the development of membrane fouling using membranes made of different materials and a bench-scale MBR. They suggested that the optimal membrane pore size that prevents membrane fouling depends on the membrane material. For PVDF, the larger the pore size, the greater the degree of suppression, whereas the opposite result was obtained in the case of CAB [109]. However, to date, only a few studies have investigated the relationship between membrane pore size and fouling phenomena by comparing membranes made from the same membrane material, which have similar membrane properties but different pore sizes [106,107,120]. Jin et al. investigated the relationship between membrane pore size and membrane fouling using ceramic membranes with four different pore sizes and a laboratory-scale MBR. They found that membranes with the smallest pore size exhibited the slowest membrane fouling, whereas the membrane with the largest pore size exhibited the fastest membrane fouling [107]. However, Nittami et al., obtained opposite results. They investigated the relationship between membrane pore size and membrane fouling using symmetrical hydrophobic polytetrafluoroethylene (PTFE) membranes with different pore sizes and a laboratory-scale MBR and reported that the membrane with the smallest pore size

exhibited the fastest membrane fouling [120]. These results also suggest that the relationship between membrane pore size and fouling propensity depends on the membrane material; thus, this relationship should be investigated using individual membranes made from the same material.

On the contrary, regarding the relationship between the surface roughness of the membrane and the fouling propensity, the results are generally in agreement, and it was reported that the larger the surface roughness, the easier the membrane fouling [111,118,121,122].

As described above, it cannot be said that the relationship between the membrane properties and the membrane fouling propensity has been demonstrated in MBRs. Therefore, the relationship between the individual membrane properties and the membrane fouling propensity for each membrane material should be investigated, and the range of optimum membrane properties that can mitigate membrane fouling should be clarified. From the results, I believe that a membrane suitable for MBRs can be determined.

I.4 Modification of membrane by blending with amphiphilic polymers

In recent years, to fabricate membrane with hydrophilicity and antifouling properties, many attempts have been made to prepare modified membranes blended with amphiphilic polymers such as Pluronic F127 and Tween-80 [123-129]. In these studies, effects other than tuning the hydrophilicity of the membrane have also been reported. Zhao et al. reported that the pore sizes of the skin layer on PES ultrafiltration membranes blended with Pluronic F127 increased with an increase in Pluronic F127 content [126]. Liu et al. reported that the pore size and surface roughness of polyvinyl chloride (PVC)

ultrafiltration membranes blended with Pluronic F127 decreased compared to the membrane without it [127]. Furthermore, Rabiee et al. reported that pure water flux on PVC ultrafiltration membranes blended with Tween-20 and Tween-80 increased continuously with the addition of Tween because of the higher surface hydrophilicity and higher porosity [128]. As described above, the addition of amphiphilic polymers can not only provide hydrophilicity to the membrane surface but can also tune the membrane surface and internal structures, such as pore size, surface roughness and pure water permeability. Therefore, by applying this technique to membrane preparation, membranes with antifouling properties suitable for MBR applications can be prepared.

Most of the amphiphilic polymers added for membrane modification, including those in the studies mentioned above, have been limited to polymers such as Pluronic, Tween and polyvinylpyrrolidone (PVP) [123-132]. However, apart from these polymers, numerous other polymers are commercially available and can be used as polymer additives in membranes. Among the many commercially available polymers, fluoropolymers are attractive materials. Since fluoropolymers have a perfluoroalkyl group, their surface tension is small owing to the intermolecular force of the group [133,134]. Because of this function, the fluoropolymers are expected to make the surface of the membrane smoother. As mentioned in Section I.3, a membrane with a smoother surface is superior in terms of membrane fouling. In this respect, fluoropolymers are promising additives.

I.5 Strategy to further popularize membrane bioreactor

The majority of membranes applied in MBRs are polymeric membranes prepared by the phase inversion method or stretching method [101]. Polymeric

membranes are classified into hollow fiber membranes and flat-sheet membranes according to their shapes. In this study, the target was limited to flat-sheet membranes. In flat-sheet membranes, the membrane materials used for MBRs are mainly PVDF [87, 135-140], PTFE [105,108,120,141], PES [142-146], and chlorinated polyvinyl chloride (CPVC) [110,147-152], polyacrylonitrile (PAN) [153,154], and polyethylene (PE) [82] are the most popular at present. In particular, CPVC flat-sheet microfiltration membranes with non-woven polyester fabric as a support layer have been widely applied in MBRs because of their excellent chemical and mechanical properties [9,147,155].

The study aims to provide new value for the further popularization of MBRs using CPVC flat-sheet membranes with excellent chemical and mechanical properties. For this purpose, it is necessary to demonstrate that the CPVC flat-sheet membrane has durability and fouling resistance suitable for removing microplastics in wastewater treatment plants, and to determine the optimum membrane properties for mitigating membrane fouling. Therefore, it is necessary to establish a technique for preparing CPVC membranes with optimum membrane properties.

I.6 Purpose of this study

This dissertation focuses on investigating the membranes taht are suitable for MBRs and suggests processes for preparing such membranes. The membrane suitable for MBRs referred to here is a membrane with durability that is unlikely to be a source of microplastics and low fouling propensity.

This dissertation is composed of three parts:, Chapters II and III of the first part clarified the durability and fouling resistance of the membrane in a lab-scale MBR using commercially available flat-sheet membranes. Chapters IV and V of the middle part

revealed the membrane properties of CPVC membranes with a low fouling propensity for application to MBRs. In Chapters VI and VII of the final part, I found a simple technique for CPVC membranes with the preparation of the revealed membrane properties.

References

[1] K. Yamamoto, M. Hiasa, T. Mahmood and T. Matsuo, Direct solid-liquid separation using hollow fiber membrane in an activated sludge aeration tank, *Water Sci. Technol.*, 21(4-5), 43-54 (1989).

[2] B. Jefferson, A.L. Laine, S.J. Judd and T. Stephenson, Membrane bioreactors and their role in wastewater reuse, *Water Sci. Technol.*, 41(1), 197-204 (2000).

[3] C. Visvanathan, R.B. Aim and K. Parameshwaran, Membrane separation bioreactors for wastewater treatment, *Crit. Rev. Environ. Sci. Technol.*, 30, 1-48 (2000).

[4] W. Yang, N. Cicek and J. Ilg, State-of-the-art of membrane bioreactors: worldwide research and commercial applications in North America, *J. Membr. Sci.*, 270, 201-211 (2006).

[5] S. Judd, The status of membrane bioreactor technology, *Trends Biotechnol.*, 26(2), 109-116 (2007).

[6] B. Lesjean and E.H. Huisjes, Survey of the European MBR market: trends and perspectives, *Desalination*, 231, 71-81 (2008).

[7] Z. Wang, Z. Wu, S. Mai, G. Yang, X. Wang, Y. An and Z. Zhou, Research and applications of membrane bioreactors in China: progress and prospect, *Sep. Purif. Technol.*, 62, 249-263 (2008).

[8] X. Huang, K. Xiao and Y.X. Shen, Recent advances in membrane bioreactor technology for wastewater treatment in China, *Front. Environ. Sci. Eng. China*, 4, 245-

271 (2010).

[9] M. Tokushima, Development for energy-saving MBR technology, *membrane*, 37, 235-239 (2012).

[10] L. Huang and D.-J. Lee, Membrane bioreactor: a mini review on recent R&D works, *Bioresour. Technol.*, 194, 383-388 (2015).

[11] S. Judd, The status of industrial and municipal effluent treatment with membrane bioreactor technology, *Chem. Eng. J.*, 305, 37-45 (2016).

[12] P. Krzeminski, L. Leverette, S. Malamis and E. Katsou, Membrane bioreactors-a review on recent developments in energy reduction, fouling, control, novel configurations, LCA and market prospects, *J. Membr. Sci.*, 527, 207-227 (2017).

[13] H. Lin, W. Gao, F. Meng, B.-Q. Liao, K.-T. Leung, L. Zhao, J. Chen and H. Hong, Membrane bioreactors for industrial wastewater treatment: a critical review, *Crit. Rev. Environ. Sci. Technol.*, 42, 677-740 (2021).

[14] K. Xiao, Y. Xu, S. Liang, T. Lei, J. Sun, X. Wen, H. Zhang, C. Chen and X. Huang, Engineering application of membrane bioreactor for wastewater treatment in China: current state and future prospect, *Front. Environ. Sci. Eng.*, 8, 805-819 (2014).

[15] L. Deng, W. Guo, H.H. Ngo, H. Zhang, J. Li, S. Xia and Y. Wu, Biofouling and control approaches in membrane bioreactors, *Bioresour. Technol.*, 221, 656-665 (2016).

[16] V. Jegatheesan, B.K. Pramanik, J. Chen, D. Navaratna, C.Y. Chang and L. Shu, Treatment of textile wastewater with membrane bioreactor: a critical review, *Bioresour. Technol.*, 204, 202-212 (2016).

[17] F. Meng, S. Zhang, Y. Oh, Z. Zhou, H.S. Shin and S.R. Chae, Fouling in membrane bioreactors: an updated review, *Water Res.*, 147, 393-402 (2017).

[18] P. Le-Clech, V. Chen and T.A.G. Fane, Fouling in membrane bioreactors used in

wastewater treatment, *J. Membr. Sci.*, 284, 17-53 (2006).

[19] F. Meng, S.-R. Chae, A. Drews, M. Kraume, H.-S. Shin and F. Yang, Recent advances in membrane bioreactors (MBRs): membrane fouling and membrane material, *Water Res.*, 43, 1489-1512 (2009).

[20] C.J. Moore, Synthetic polymers in the marine environment: a rapidly increasing, long-term threat, *Environ. Res.*, 108, 131-139 (2008).

[21] A. Shrivastava, 7-Environmental aspects of plastics, in: A. Shrivastava (Ed.), Introduction to Plastics Engineering, William Andrew Publishing, Oxford UK (2018).

[22] L.S. Fendall and M.A. Sewell, Contributing to marine pollution by washing your face: microplastics in facial cleansers, *Mar. Pollut. Bull.*, 58, 1225-1228 (2009).

[23] K. Xiao, S. Liang, X. Wang, C. Chen and X. Huang, Current state and challenges of full-scale membrane bioreactor applications: a critical review, *Bioresour. Technol.*, 271, 473-481 (2019).

[24] A. Collignon, J.-H. Hecq, F. Galgani, F. Collard and A. Goffart, Annual variation in neustonic micro- and meso-plastic particles and zooplankton in the Bay of Calvi (Mediterranean-Corsica), *Mar. Pollut. Bull.*, 79, 293-298 (2014).

[25] Y. Otsuka, H. Takada, Y. Nihei, Y. Kameda and K. Nishikawa, Current status and issues of microplastic pollution research, *J. Jpn. Soc. Water Environ.*, 44, 35-42 (2021).

[26] R. Yamashita, H. Takada, M. Fukuwaka and Y. Watanuki, Physical and chemical effects of ingested plastic debris on short-tailed shearwaters, Puffinus tenuirostris, in the North Pacific Ocean, *Mar. Pollut. Bull.*, 62, 2845-2849 (2011).

[27] L.V. Cauwenberghe and C.R. Janssen, Microplastics in bivalves cultured for human consumption, *Environ. Pollut.*, 193, 65-70 (2014).

[28] J.R. Jambeck, R. Geyer, C. Wilcox, T.R. Siegler, M. Perryman, A. Andrady, R.

Narayan and K.L. Law, Plastic waste inputs from land into the ocean, *Science*, 347, 768-771 (2015).

[29] S. Rezania, J. Park, M.F.M. Din, S.M. Taib, A. Talaiekhozani, K.K. Yadav and H. Kamyab, Microplastics pollution in different aquatic environments and biota: a review of recent studies, *Mar. Pollut. Bull.*, 133, 191-208 (2018).

[30] D. Xanthos and T.R. Walker, International policies to reduce plastic marine pollution from single-use plastics (plastic bags and microbeads): a review, *Mar. Pollut. Bull.*, 118, 17-26 (2017).

[31] J.A. Ivar do Sul and M.F. Costa, The present and future of microplastic pollution in the marine environment, *Environ. Pollut.*, 185, 352-364 (2014).

[32] L.G.A. Barboza and B.C.G. Gimenez, Microplastics in the marine environment: current trends and future perspectives, *Mar. Pollut. Bull.*, 97, 5-12 (2015).

[33] J. Li, D. Yang, L. Li, K. Jabeen and H. Shi, Microplastics in commercial bivalves from China, *Environ. Pollut.*, 207, 190-195 (2015).

[34] K. Tanaka and H. Takada, Microplastic fragments and microbeads in digestive tracts of planktivorous fish from urban coastal waters, *Sci. Rep.*, 6, 34351 (2016).

[35] N. González-Sotoa, J. Hatfield, A. Katsumiti, N. Duroudier, J.M. Lacave, E. Bilbao, A. Orbea, E. Navarro and M.P. Cajaraville, Impacts of dietary exposure to different sized polystyrene microplastics alone and with sorbed benzo[a]pyrene on biomarkers and whole organism responses in mussels *Mytilus galloprovincialis*, *Sci. Total Environ.*, 684, 548-566 (2019).

[36] L.G.A. Barboza, C. Lopes, P. Oliveria, F. Bessa, V. Otero, B. Henriques, J. Raimundo, M. Caetano, C. Vale and L. Guihermino, Microplastics in wild fish from North East Atlantic Ocean and its potential for causing neurotoxic effects, lipid oxidative damage,

and human health risks associated with ingestion exposure, *Sci. Total Environ.*, 717, 134625 (2020).

[37] J.L. Lavers, I. Hutton and A.L. Bond, Clinical pathology of plastic ingestion in marine birds and relationships with blood chemistry, *Environ. Sci. Technol.*, 53, 9224-9231 (2019).

[38] R.R. Leads and J.E. Weinstein, Occurrence of tire wear particles and other microplastics within the tributaries of the Charleston Harbor Estuary, South Carolina, USA, *Mar. Pollut. Bull.*, 145, 569-582 (2019).

[39] S. Yukioka, S. Tanaka, Y. Nabetani, Y. Suzuki, T. Ushijima, S. Fujii, H. Takada, Q. Van Tran and S. Singh, Occurrence and characteristics of microplastics in surface road dust in Kusatsu (Japan), Da Nang (Vietnam), and Kathmandu (Nepal), *Environ. Pollut.*, 256, 113447 (2020).

[40] D. Xanthos and T.R. Walker, International policies to reduce plastic marine pollution from single-use plastics (plastic bags and microbeads): a review, *Mar. Pollut. Bull.*, 118, 17-26 (2017).

[41] M.A. Browne, P. Crump, S.J. Niven, E. Teuten, A. Tonkin, T. Galloway, R. Thompson, Accumulation of microplastic on shorelines worldwide sources and sinks, *Environ. Sci. Technol.*, 45, 9175-9179 (2011).

[42] R. Dris, J. Gasperi, V. Rocher, M. Saad, N. Renault, B. Tassin, Microplastic contamination in an urban area: a case study in Greater Paris, *Environ. Chem.*, 12, 592-599 (2015).

[43] I.E. Napper, R.C. Thomson, Release of synthetic microplastic plastic fibres from domestic washing machines: effects of fabric type and washing condition, *Mar. Pollut. Bull.*, 112, 39-45 (2016).

[44] N.L. Hartline, N.J. Bruce, S.N. Karba, E.O. Ruff, S.U. Sonar, P.A. Holden, Microfiber masses recovered from conventional machine washing of new or aged garments, *Environ. Sci. Technol.*, 50, 11532-11538 (2016).

[45] E. Hernandez, B. Nowack, D.M. Mitrano, Polyester textiles as a source of microplastics from households: a mechanistic study to understand microfiber release during washing, *Environ. Sci Technol.*, 51, 7036-7046 (2017).

[46] L. Yang, F. Qiao, K. Lei, H. Li, Y. Kang, S. Cui and L. An, Microfiber release from different fabrics during washing, *Environ. Pollut.*, 249, 136-143 (2019).

[47] B.M.C. Almroth, L. Åström, S. Roslund, H. Petersson, M. Johansson and N.K. Persson, Quantifying shedding of synthetic fibers from textiles; a source of microplastics released into the environment, *Environ. Sci. Pollut. Res.*, 25, 1191-1199 (2018).

[48] F. De Falco, M.P. Gullo, G. Gentile, E. Di Pace, M. Cocca, L. Gelabert, M. Brouta-Agnésa, A. Rovira, R. Escudero, R. Villalba, R. Mossotti, A. Montarsolo, S. Gavignano, C. Tonin and M. Avella, Evaluation of microplastic release caused by textile washing processes of synthetic fabrics, *Environ. Pollut.*, 236, 916-925 (2018).

[49] P.K. Cheung, L. Fok, Evidence of microbeads from personal care product contaminating the sea, *Mar. Pollut. Bull.*, 109, 582-585 (2016).

[50] A.G. Anderson, J. Grose, S. Pahl, R.C. Thompson, K.J. Wyles, Microplastics in personal care products: exp;oring perceptions of environmentalists, beauticians and students, *Mar. Pollut. Bull.*, 113, 454-460 (2016).

[51] L. Anagnosi, A. Varvaresou, P. Pavlou, E. Protopapa, V. Carayanni, Worldwide actions against plastic pollution from microbeads and microplastics in cosmetics focusing on European policies. Has the issue been handled effectively?, *Mar. Pollut. Bull.*, 162, 111883 (2021).

[52] C.M. Rochman, S.K. Kross, J.B. Armstrong, M.T. Bogan, E.S. Darling, S.J. Green, A.R. Smyth, D. Verissimo, Scientific evidence supports a ban on microbeads, *Environ. Sci. Technol.*, 49, 10759-10761 (2015).

[53] R.M. Blair, S. Waldron, C. Gauchotte-Lindsay, Average daily flow of microplastics through a tertiary wastewater treatment plant over a ten-month period, *Water Res.*, 163, 114909 (2019).

[54] J. Bayo, S. Olmos, J. López-Castellanos, Microplastics in an urban wastewater treatment plant: the influence of physicochemical parameters and environmental factors, *Chemosphere*, 238, 124593 (2020).

[55] C. Edo, M. González-Pleiter, F. Leganés, F. Fernández-Piñas, R. Rosal, Fate of microplastics in wastewater treatment plants and their environmental dispersion with effluent and sludge, *Environ. Pollut.*, 259, 113837 (2020).

[56] P. Masia, D. Sol, A. Ardura, A. Laca, Y. J. Borrell, E. Dopico, A. Laca, G. Machado-Schiaffino, M. Díaz, E. Garcia-Vazquez, Bioremediation as a promising strategy for microplastics removal in wastewater treatment plants, *Mar. Pollut. Bull.*, 156, 111252 (2020).

[57] S. Carr, J. Liu, A. G. Tesoro, Transport and fate of microplastic particles in wastewater treatment plants, *Water Res.*, 91, 174-182 (2016).

[58] F. Murphy, C. Ewins, F. Carbonnier, B. Quinn, Wastewater treatment works (WwTW) as a source of microplastics in the aquatic environment, *Environ. Sci. Technol.*, 50, 5800-5808 (2016).

[59] A.M. Mahon, B. O'Connell, M.G. Healy, I. O'Connor, R. Officer, R. Nash, L. Morrison, Microplastics in sewage sludge: effects of treatment, *Environ. Sci. Technol.*, 51, 810-818 (2017).

[60] J. Talvitie, M. Heinonen, J-P. Pääkkönen, E. Vahtera, A. Mikola, O. Setälä, R. Vahala, Do wastewater treatment plants act as a potential point source of microplastics? Preliminary study in the coastal Gulf of Finland, Baltic Sea, *Water Sci. Technol.*, 72, 1495-1504 (2015).

[61] A.A. Horton, A. Walton, D.J. Spurgeon, E. Lahive, C. Sevendsen, Microplastics in freshwater and terrestrial environments: evaluating the current understanding to identify the knowledge gaps and future research priorities, *Sci. Total Environ.*, 586, 127-141 (2017).

[62] M. Lares, M.C. Ncibi, M. Sillanpää, M. Silanpää, Occurrence, identification and removal of microplastic particles and fibers in conventional activated sludge process and advanced MBR technology, *Water Res.*, 133, 236-246 (2018).

[63] J. Talvitie, A. Mikola, A. Koistinen, O. Setälä, Solutions to microplastic pollution - removal of microplastics from wastewater effluent with advanced wastewater treatment technologies, *Water Res.*, 123, 401-407 (2017).

[64] L. Li, D. Liu, K. Song, Y. Zhou, Performance evaluation of MBR in treating microplastics polyvinylchloride contaminated polluted surface water, *Mar. Pollut. Bull.*, 150, 110724 (2020).

[65] N. Suzuki and K. Okada, Development of the control technology for membrane fouling by the biological approaches, *Kubota Technical Report*, 46, 42-47 (2012).

[66] K. Kawasaki, Utilization of membrane in the wastewater treatment, *membrane*, 39, 8-13 (2014).

[67] N. Engelhardt, W. Firk and W. Warnken, Integration of membrane filtration into the activated sludge process in municipal wastewater treatment, *Water Sci. Technol.*, 38, 429-436 (1998).

[68] A. Drews, Membrane fouling in membrane bioreactors-characterization, contradictions, cause and cures, *J. Membr. Sci.*, 363, 1-28 (2010).

[69] A. Joss, M. Böhler, D. Wedi and H. Siegrist, Proposing a method for online permeability monitoring in membrane bioreactors, *Water Sci. Technol.*, 60, 497-506 (2009).

[70] B. Verrecht, S. Judd, G. Guglielmi, C. Brepols and J.W. Mulder, An aeration energy model for an immersed membrane bioreactor, *Water Res.*, 42, 4761-4770 (2008).

[71] J.-P. Nywening and H. Zhou, Influence of filtration conditions on membrane fouling and scouring aeration effectiveness in submerged membrane bioreactors to treat municipal wastewater, *Water Res.*, 43, 3548-3558 (2009).

[72] M. Kraume and A. Drews, Membrane bioreactors in waste water treatment – status and trends, *Chem. Eng. Technol.*, 33, 1251-1259 (2010).

[73] A. Fenu, J. Roels, T. Wambecq, K. De Gussem, C. Thoeye, G. De Gurldre and B. Van De Steene, Energy audit of a full scale MBR system, *Desalination*, 262, 121-128 (2010).

[74] P. Cornel and S. Krause, State of the art of MBR in Europe, *Technical Note of National Institute for Land and Infrastructure Management*, 186, 151-162 (2004).

[75] J.A. Gil, L Túa, A. Rueda, B. Montaño, M. Rodríguez and D. Prats, Monitoring and analysis of the energy cost of an MBR, *Desalination*, 250, 997-1001 (2010).

[76] J.W. Mulder, Operational experiences with the hybrid MBR Heenvliet, a smart way of retrofitting, Book of Proceedings of final MBR Network workshop, 31 March-1 April, Berlin, Germany, 2009.

[77] H. Nagaoka, Future prospects of membrane bioreactors, *membrane*, 36, 217-221 (2011).

[78] P. Le-Clech, V. Chen, T.A.G. Fane, Fouling in membrane bioreactors used in wastewater treatment, *J. Membr. Sci.*, 284, 17-53 (2006).

[79] F. Meng, S.-R. Chae, A. Drews, M. Kraume, H.-S. Shin, F. Yang, Recent advances in membrane bioreactors (MBRs): Membrane fouling and membrane material, *Water Res.*, 43, 1489-1512 (2009).

[80] W. Yang, N. Cicek, J. Llg, State-of-the-art of membrane bioreactors: worldwide research and commercial applications in North America, *J. Membr. Sci.*, 270, 201-211 (2006).

[81] E. Iritani, Modeling and evaluation of pore clogging of membrane in membrane filtration, *Kagaku Kougaku Ronbunshu*, 35, 1-11 (2009).

[82] N. Yamato, K. Kimura, T. Miyoshi and Y. Watanabe, Difference in membrane fouling in membrane bioreactors (MBRs) caused by membrane polymer materials, *J. Membr. Sci.*, 280, 911-919 (2006).

[83] A. Kola, Y. Ye, P. Le-Clech and V. Chen, Transverse vibration as novel membrane fouling mitigation strategy in anaerobic membrane bioreactor applications, *J. Membr. Sci.*, 455, 320-329 (2014).

[84] T. Kurita, K. Kimura and Y. Watanabe, The influence of granular materials on the operation and membrane characteristics of submerged MBRs, *J. Membr. Sci.*, 469, 292-299 (2014).

[85] C. Niu, Y. Pan, X. Lu, S. Wang, Z. Zhang, C. Zheng, Y. Tan, G. Zhen, Y. Zhao and Y.-Y. Li, Mesophilic anaerobic digestion of thermally hydrolyzed sludge in anaerobic membrane bioreactor: Long-term performance, microbial community dynamics and membrane fouling mitigation, *J. Membr. Sci.*, 612, 118264 (2020).

[86] T. Maruyama, Visualization of membrane fouling, *Kobunshi*, 65, 181-184 (2016).

[87] J. Lee, W.-Y. Ahn and C.-H. Lee, Comparison of the filtration characteristics between attached and suspended growth microorganism in submerged membrane bioreactor, *Water Res.*, 35, 2435-2445 (2001).

[88] N.S.A. Mutamim, Z.Z. Noor, M.A.A. Hassan, A. Yuniarto and G. Olsson, Membrane bioreactor and limitations in treating high strength industrial wastewater, *Chem. Eng. J.*, 225, 109-119 (2013).

[89] M. Hashino, T. Katagiri, N. Kubota, Y. Ohmukai, T. Maruyama and H. Matsuyama, Effect of surface roughness of hollow fiber membranes with gear-shaped structure on membrane fouling by sodium alginate, *J. Membr. Sci.*, 366, 389-397 (2011).

[90] R. Van den Broeck, J. van Dierdonck, P. Nijskens, C. Dotremont, P. Krzeminski, J.H.J.M. van der Graaf, J.B. van Lier, J.F.M. van Impe and I.Y. Smets, The influence of solids retention time on activated sludge bioflocculation and membrane fouling in a membrane bioreactor (MBR), *J. Membr. Sci.*, 401, 48-55 (2012).

[91] L. Shen, Q. Lei, J. Chen, H. Hong, Y. He and H. Lin, Membrane fouling in a submerged bioreactor: impact of floc size, *Chem. Eng. J.*, 269, 328-334 (2015).

[92] R.S. Trussell, R.P. Merlo, S.W. Hermanowics and D. Jenkins, Influence of mixed liquor properties and aeration intensity on membrane fouling in a submerged membrane bioreactor at high mixed liquor suspended solids concentrations, *Water Res.*, 41, 947-958 (2007).

[93] J.Cho, K.-G. Song, S. Hyup Lee and K.-H. Ahn, Sequencing anoxic/anaerobic membrane bioreactor (SAM) pilot plant for advanced wastewater treatment, *Desalination*, 178, 219-225 (2005).

[94] L. Ji and J. Zhou, Influence of aeration on microbial polymers and membrane fouling in submerged MBRs, *J. Membr. Sci.*, 276, 168-177 (2006).

[95] Z. Ahmed, J. Cho, B.-R. Lim, K.-G. Song and K.-H. Ahn, Effects of sludge retention time on membrane fouling and microbial community structure in a membrane bioreactor, *J. Membr. Sci.*, 287, 211-218 (2007).

[96] F. Meng and F. Yang, Fouling mechanisms of deflocculated sludge, normal sludge; bulking sludge in membrane bioreactor, *J. Membr. Sci.*, 305, 48-56 (2007).

[97] S. Feng, N. Zhang, H. Liu, X. Du, Y. Liu and H. Lin, The effect of COD/N ratio on process performance and membrane fouling in a submerged bioreactor, *Desalination*, 285, 232-238 (2012).

[98] Z. Ma, X. Wen, F. Zhao, Y. Xia, X. Huang, D. Waite and J. Guan, Effect of temperature variation on membrane fouling and microbial community structure in membrane bioreactor, *Bioresour. Technol.*, 133, 462-468 (2013).

[99] N. Jang, H. Shon, X. Ren, S. Vigneswaran and I.S. Kim, Characteristics of bio-foulants in the membrane bioreactor, *Desalination*, 200, 201-202 (2006).

[100] A. Sweity, W. Ying, S. Belfer, G. Oron and M. Herzberg, pH effects on the adherence and fouling propensity of extracellular polymeric substances in a membrane bioreactor, *J. Membr. Sci.*, 378, 186-193 (2011).

[101] S. Judd, The MBR Book: Principles and Applications of Membrane Bioreactor for Water and Wastewater Treatment 2nd ed., Oxford, Elservier, 2011.

[102] H. Matsuyama, T. Takahashi and M. Yasukawa, Present situation and future prospects of water treatment technology with membrane, *membrane*, 39, 209-216 (2014).

[103] C.-C. Ho and A.L. Zydney, Effect of membrane morphology on the initial rate of protein fouling during microfiltration, *J. Membr. Sci.*, 155, 261-275 (1999).

[104] H.H.P. Fang and X. Shi, Pore fouling of microfiltration membranes by activated sludge, J. Membr. Sci., 161-166 (2005).

[105] J.-H. Choi and H.Y. Ng, Effect of membrane type and material on performance of a submerged membrane bioreactor, *Chemosphere*, 71, 853-859 (2008).

[106] P. van der Marel, A. Zwijnenburg, A. Kemperman, M. Wessling, H. Tenmink and W. van der Meer, Influnece of membrane properties on fouling in submerged membrane bioreactors, *J. Membr. Sci.*, 348, 66-74 (2010).

[107] L. Jin, S.L. Ong and H.Y. Ng, Comparison of foluing characteristics in different pore-sized submergd ceramic membrane bioreactors, *Water Res.*, 44, 5907-5918 (2010).

[108] T. Nittami, H. Tokunaga, A. Satoh, M. Takeda and K. Matsumoto, Influence of surface hydrophilicity on polytetrafluoroethylene flat sheet membrane fouling in a submerged membrane bioreactor using two activated sludges with different characteristics, *J. Membr. Sci.*, 463, 183-189 (2014).

[109] T. Miyoshi, K. Yuasa, T. Ishigami, S. Rajabzadeh, E. Kamio, Y. Ohmukai, D. Saeki, J. Ni and H. Matsuyama, Effect of membrane polymeric materials on relationship between surface pore size and membrane fouling in membrane bioreactors, *Appl. Surf. Sci.*, 330, 331-357 (2015).

[110] M. Higashi, J. Morita, N. Shimada and T. Kitagawa, Long-term-hydrophilic flat-sheet microfiltration membrane made from chlorinated poly (vinyl chloride), *J. Membr. Sci.*, 500, 180-189 (2016).

[111] T. Tsuyuhara, Y. Hanamoto, T. Miyoshi, K. Kimura and Y. Watanabe, Influence of membrane properties on physically reversible and irreversible fouling in membrane bioreactors, *Water Sci. Technol.*, 61, 2235-2240 (2010).

[112] O.T. Iorheman, R.A. Hamza and J.H. Tay, Membrane bioreactor (MBR) technology for wastewater treatment and reclamation: membrane fouling, *membranes*, 6, 33 (2016).

[113] N. Maximous, G. Nakhla and W. Wan, Comparative assessment of hydrophobic and

hydrophilic membrane fouling in wastewater applications, *J. Membr. Sci.*, 339, 93-99 (2009).

[114] I. Chang, S. Bag and C. Lee, Effects of membrane fouling on solute rejection during membrane filtration of activated sludge, *Process Biochem.*, 36, 855-860 (2001).

[115] H. Yu, M. Hu, Z. Xu, J. Wang and S. Wang, Surface modification of polypropylene microporous membranes to improve their antifouling property in MBR: NH_3 plasma treatment, *Sep. Purif. Technol.*, 45, 8-15 (2005).

[116] L. Liu, B. Shao and F. Yang, Polydopamine coating – surface modification of polyester filter and fouling reduction, *Sep. Purif. Technol.*, 118, 226-233 (2013).

[117] H. Minehara, K. Dan, Y. Ito, H. Takabatake and M. Henmi, Quantitative evaluation of fouling resistance of PVDF/PMMA-g-PEO polymer blend membranes for membrane bioreactor, *J. Membr. Sci.*, 466, 211-219 (2014).

[118] L. Chen, Y. Tian, C.Q. Cao, J. Zhang and Z.N. Li, Interaction energy evaluation of soluble microbial products (SMP) on different membrane surfaces: role of the reconstructed membrane technology, *Water Res.*, 46, 2693-2704 (2012).

[119] K.H. Choo and C.H. Lee, Effect of anaerobic digestion broth composition on membrane permeability, *Water Sci. Technol.*, 34, 173-179 (1996).

[120] T. Nittami, T. Hitomi, K. Matsumoto, K. Nakamura, T. Ikeda, Y. Setoguchi and M. Motoori, Comparison of polytetrafluoroethylene flat-sheet membranes with different pore sizes in application to submerged membrane bioreactor, *membranes*, 2, 228-236 (2012).

[121] M. Zhang, B.-q. Liao, X. Zhou, Y. He, H. Hong, H. Lin and J. Chen, Effects of hydrophilicity/hydrophobicity of membrane on membrane fouling in a submerged membrane bioreactor, *Bioresor. Technol.*, 175, 59-67 (2015).

[122] J.-H. Choi, S.-K Park and H.-Y. Ng, Membrane fouling in a submerged membrane bioreactor using track-etched and phase-inversed porous membranes, *Sep. Purif. Technol.*, 65, 184-192 (2009).

[123] B. Liu, C. Chen, W. Zhang, J. Crittenden and Y. Chen, Low-cost antifouling PVC ultrafiltration membrane fabrication with Pluronic F127: effect of additives on properties and performance, *Desalination*, 307, 26-33 (2012).

[124] C.H. Loh, R. Wang, L. Shi and A.G. Fane, Fabrication of high performance polyethersulfone UF hollow fiber membranes using amphiphilic Pluronic block copolymers as pore-forming additives, *J. Membr. Sci.*, 380, 114-123 (2011).

[125] H.-H. Chang, S.-C. Chen, D.-J. Lin and L.-P. Cheng, The effect of Tween-20 additive on the morphology and performance of PVDF membranes, *J. Membr. Sci.*, 466, 302-312 (2014).

[126] W. Zhao, Y. Su, C. Li, Q. Shi, X. Ning and Z. Jiang, Fabrication of antifoling polyestersulfone ultrafiltration membranes using Pluronic F127 as both surface modifier and pore-forming agent, *J. Membr. Sci.*, 318, 405-412 (2008).

[127] J. Liu, Y. Su, J. Peng, X. Zhao, Y. Zhang, Y. Dong and Z. Jiang, Preparation and performance of antifouling PVC/CPVC blend ultrafiltration membranes, *Ind. Eng. Chem. Res.*, 51, 8308-8314 (2012).

[128] H. Rabiee, S. M. S. Shahabadi, A. Mokhtare, H. Rabiei and N. Alvandifar, Enhancement in permeation and antifouling properties of PVC ultrafiltration membranes *Chem. Eng.*, 4, 4050-4061 (2016).

[129] T. Shibutani, T. Maruyama, T. Kitaura, X. Fu, N. Arahman, T. Sotani, S. Nakatsuka, T. Watabe and H. Matsuyama, Effect of amphiphilic additives on properties of hollow-fiber membranes of cellulose acetate butyrate prepared by thermally induced phase

separation, *Kagaku Kogaku Ronbunshu*, 35, 117-121 (2009).

[130] V.P. Khare, A.R. Greenberg and W.B. Krantz, Vapor-induced phase separation-effect of the humid air exposure step on membrane morphology Part I. Insights from mathematical modeling, *J. Membr. Sci.*, 258, 140-156 (2005).

[131] M.-H. Xu, R. Xie, X.-J. Ju, W. Wang, Z. Liu and L.-Y. Chu, Antifouling membranes with bi-continuous porous structures and high fluxes prepared by vapor-induced phase separation, *J. Membr. Sci.*, 611, 118256 (2020).

[132] T. Marino, E. Blasi, S. Tornaghi, E.D. Nicolo and A. Figoli, Polyethersulfone membranes prepared with Rhodiasolv ®Polaclean as water soluble green solvent, *J. Membr. Sci.*, 549, 192-204 (2018).

[133] S. Ohtoshi, Synthesis and specific properties of fluoro-surfactants, *Sekiyu Gakkaishi*, 32, 277-285 (1989).

[134] H.W. Fox, E.F. Hare and W.A. Zisman, The spreading of liquids on low-energy surface. VI. Branched-chain monolayers, aromatic surfaces, and thin liquid films, *J. Colloid Sci.*, 8, 194-203 (1953).

[135] J.-J. Qin, W.M. Nyunt, G. Tao, K.A. Kekre and H. Seah, Membrane bioreactor study for reclamation of mixed sewage mostly from industrial sources, *Sep. Purif. Technol.*, 53, 296-300 (2007).

[136] Y. Ye, P. Le-Clech, V. Chen, A.G. Fane and B. Jefferson, Fouling mechanisms of alginate solutions as model extracellular polymeric substances, *Desalination*, 175, 7-20 (2005).

[137] J. Teng, M. Zhang, K.-T. Leung, J. Chen, H. Hong, H. Lin and B.-Q. Liao, A unified thermodynamic mechanism underlying fouling behaviors of soluble microbial products (SMPs) in a membrane bioreactor, *Water Res.*, 149, 477-487 (2019).

[138] Y.-T. Huang, T.-H. Huang, J.-H. Yang and R.A. Damodar, Identifications and characterizations of proteins from fouled membrane surfaces of different materials, *Int. Biodeter. Biodegrade.*, 66, 47-52 (2012).

[139] H. Hong, M. Zhang, Y. He, J. Chen and H. Lin, Fouling mechanisms of gel layer in a submerged membrane bioreactor, *Bioresour. Technol.*, 166, 295-302 (2014).

[140] J. Chen, M. Zhang, F. Li, L. Qian, H. Lin, L. Yang, X. Wu, X. Zhou, Y. He and B-Q. Liao, Membrane fouling in a membrane bioreactor: high filtration resistance of gel layer and its underlying mechanism, *Water Res.*, 102, 82-89 (2016).

[141] E-J. Lee, K-Y. Kim, Y-S. Lee, J-W. Nam, Y-S. Lee, H-S. Kim and A. Jang, A study on high-flux MBR system using PTFE flat sheet membranes with chemical backwashing, *Desalination*, 306, 35-40 (2012).

[142] Y. He, P. Xu, C. Li and B. Zhang, High-concentration food wastewater treatment by an anaerobic membrane bioreactor, *Water Res.*, 39, 4110-4118 (2005).

[143] J.-G. Choi, T.-H. Bae, J.-H. Kim, T.-M. Tak and A.A. Randall, The behavior of membrane fouling initiation on the crossflow membrane bioreactor system, *J. Membr. Sci.*, 203, 103-113 (2002).

[144] Z. Wu, Z. Wang, S. Huang, S. Mai, C. Yang, X. Wang and Z. Zhou, Effects of various factors on critical flux in submerged membrane bioreactors for municipal wastewater treatment, *Sep. Purif. Technol.*, 62, 56-63 (2008).

[145] Z. Wang, Z. Wu and S. Tang, Extracellular polymeric substances (EPS) properties and their effects on membrane fouling in a submerged membrane bioreactor, *Water Res.*, 43, 2504-2512 (2009).

[146] Y. Zheng, W. Zhang, B. Tang, J. Ding, Y. Zheng and Z. Zhang, Membrane fouling mechanism of biofilm-membrane bioreactor (BF-MBR): pore blocking model and

membrane cleaning, *Bioresour. Technol.*, 250, 398-405 (2018).

[147] N. Shimada, J. Morita, M. Higashi, T. Kitagawa and J. Nakajima, Long term pilot MBR test for a newly development flat sheet membrane made from chlorinated polyvinyl chloride in treatment of kitchen wastewater from a cafeteria, *J. Water Environ. Technol.*, 14, 329-340 (2016).

[148] T. Uesaka, Membrane separation: MBR, *Kagakukougaku*, 73, 79-82 (2009).

[149] C. Nuengjamnong, J.H. Kweon, J. Cho, C. Polprasert and K-H. Ahn, Membrane fouling caused by extracellular polymeric substances during microfiltration processes, *Desalination*, 179, 117-124 (2005).

[150] H. Nagaoka and H. Akoh, Decomposition of EPS on the membrane surface and its influence on the fouling mechanism in MBRs, *Desalination*, 231, 150-155 (2008).

[151] C. Huyskens, S. Lenaerts, E. Brauns, L. Diels and H.D. Wever, Study of (ir)reversible fouling in MBRs under various operating conditions using new on-line fouling sensor, *Sep. Purif. Technol.*, 81, 208-215 (2011).

[152] C. Jacquin, G. Lesage, J. Traber, W. Pronk and M. Heran, Three-dimensional excitation and emission matrix fluorescence (3DEEM) for quick and pseudo-quantitative determination of protein- and humic-like substances in full-scale membrane bioreactor (MBR), *Water Res.*, 118, 82-92 (2017).

[153] A. Drews, J. Mante, V. Iversen, M. Vocks, B. Lesjean and M. Kraume, Impact of ambient conditions on SMP elimination and rejection in MBRs, *Water Res.*, 41, 3850-3858 (2007).

[154] C.G. Dosoretz and K.W. Böddeker, Removal of trace organics from water using a pumped bed-membrane bioreactor with powdered activated carbon, *J. Membr. Sci.*, 239, 81-90 (2004).

[155] Q.-V. Bach, V.T. Le, Y.S. Yoon, X.T. Bui. W. Chang, S.W. Chang, H.H. Ngo, W. Guo and D.D. Nguyen, A new hybrid sewage treatment system combining a rolled pipe system and membrane bioreactor to improve the biological nitrogen removal efficiency: a pilot study, *J. Clean. Prod.*, 178, 937-946 (2018).

Chapter II

Effects of structural vulnerability of flat-sheet membranes on fouling development in continuous submerged membrane bioreactors

---

II.1 Introduction

Membrane bioreactors (MBRs) have come to be used widely for treating various types of wastewater over the last 20 years because of their numerous advantages, including the high quality of the thus-treated water, their low space requirements, and their ease of operation compared to conventional activated sludge treatment processes, which use settling tank [1-3]. MBRs also show high pollutant removal performance because they allow for the ready control of the concentration of mixed liquor suspended solids (MLSSs) [3]. However, membrane fouling remains a matter of concern in actual wastewater treatment processes [2,3]. MBRs can be categorized into two classes based on the configuration of the membranes used: hollow-fiber membrane bioreactors [4-8] and flat-sheet membrane bioreactors [9-15]. Both types of MBRs experience fouling-related problems, though their configurations are different and there have been numerous studies to find suitable solutions for these problems [3]. At the time of the introduction of MBRs for biochemical water treatments, which was in the early 2000 s, it was already acknowledge that soluble microbial products and extracellular polymeric substances (EPSs) are responsible for membrane fouling. In particular, there had been several studies on the effects of their size and hydrophobicity [3,16,17]. Thus, there have been extensive efforts over the years to improve the hydrophobicity of membrane materials [18-21],

because it has recognized that the hydrophobic binding between the membrane material and the fouling matter is the primary reason for the irreversible fouling of membranes. In addition, there have been several studies from an engineering perspective to prevent or limit membrane fouling [3,22] by changing the operating conditions of MBRs, such as the MLSS concentration and composition [23], solid retention time (SRT) [24], filtration flux [25], and intensity of aeration [3,12]. The scouring and cleaning of the membranes can also help prevent fouling [26,27]. However, the relationship between the characteristics of membrane material used and the fouling phenomenon is still unclear. For instance, Miyoshi et al. investigated the relationship between membrane pore size and the development of membrane fouling using membranes of three different materials and a bench-scale MBR with activated sludge. They found that the optimal membrane pore size for preventing membrane fouling depends on the membrane material. For polyvinylidene fluoride (PVDF), the larger the pore size is, the greater is the degree of mitigation whereas in the case of cellulose acetate butyrate (CAB) membranes, the opposite is true [28]. That is, there is not even consistent in only one of the relationships between membrane characteristics and fouling development, thus in order to increase the applicability of MBRs for the treatment of real wastewater, additional studies on the above-mentioned relationship are needed.

On the other hand, in most previous studies, the focus was only on the properties of polymer themselves for making membranes and their degree of fouling, and there have been few reports on the effects of the structures of the membrane sheets and their supporting materials on the fouling propensity and how these structures vary with the membrane fabrication method used. However, the membrane sheets used in flat-sheet membrane MBRs are usually combined with a supporting material such as polyethylene

terephthalate (PET) [13,15,29]. Besides, membrane fouling generally occurs in the primary fouling mechanisms including adhesion/deposition mechanism [30-32] and filtration resistance caused by chemical potential mechanism [17,33-35]. Thus, not only the effects of the properties of the membrane material itself but also those of the fabricated membrane sheets on the fouling phenomenon in the primary fouling phenomena should be considered when analyzing the practical applications of MBRs.

From this perspective, the objectives of the comparative study intended to elucidate the fouling behavior of membranes in a bench-scale continuous MBR that treated synthetic wastewater using flat-sheet membranes of four different membrane materials, viz. PVDF, polyethersulfone (PES), polytetrafluoroethylene (PTFE), and chlorinated poly (vinyl chloride) (CPVC). In particular, this study focused on the properties of the flat-sheet membranes with PET as the supporting material and discuss the relationship between their properties and the fouling phenomenon. It was also investigated that other factors which contribute to fouling, such as the amounts of MLSSs, EPSs, and soluble matter present, determined based on the excitation-emission matrix (EEM). Besides, it was also investigated and compared the characteristics of the laboratory-scale submerged MBR in this study and two types of bioreactors at real wastewater treatment plants (MBR at an actual night-soil treatment plant and aeration tank at an actual sewage-treatment plant) in order to determine whether the knowledge obtained in this study can be extrapolated to actual wastewater treatment plants.

II.2 Materials and methods

II.2.1 Membranes and flat-sheet membrane modules used

As stated above, in this study, four different types of flat-sheet membranes were

used. These membranes are available commercially for use in actual wastewater treatment facilities worldwide and were obtained from their manufactures. Table 2-1 lists the physical and chemical characteristics of each membrane material. All the materials except for PES were hydrophobic before use. In other words, PVDF membrane was subjected to a hydrophilic treatment by the manufacture, whereas the modules of the CPVC and PTFE membranes were soaked in ethanol for 10 min in the laboratory to ensure that their surfaces adapted to water right before the start of the experiments. The modal flow rate-based pore sizes of the membranes were similar (0.16-0.25 μm) except for the PES membrane (< 0.05 μm). Further, the pure water permeability of the PES membrane was also lower than those of the other membranes; this was owing to differences in the structures of the membrane materials. PVDF and PES membranes are generally produced by a non-solvent induced phase separation (NIPS) method [36] and use a non-woven piece of PET fabric as the supporting layer, whereas CPVC flat-sheet membranes are produced by vapor-induced phase separation (VIPS) [37] and also use a piece of non-woven PET fabric as the supporting layer. On the other hand, in the case of PTFE flat-sheet membranes, first a thin film of PTFE is produced and stretched to induce micropores. It is then laminated with non-woven PET [38]. In this study, each flat-sheet membrane was fixed to a polyvinyl chloride frame using polyester spacers, and a plastic corrugated board was employed to form the membrane module for MBR (Fig. 2-1). The total effective filtration area of each membrane module was 0.11 m^2 (0.19 × 0.29 m × 2 sheets).

II.2.2 Configuration and operation of laboratory-scale submerged membrane bioreactor

A schematic of laboratory-scale submerged MBR (MBR/Lab) is shown in Fig. 2-2. MBR/Lab was made of clear polyvinyl chloride and had an effective working volume

Table 2-1 Membrane materials used and their characteristics

Material		PVDF	CPVC	PTFE	PES
Pore size	Specification (μm)*	0.05	0.2	0.1	0.05
	Modal flow-rate pore size (μm)	0.25	0.17	0.16	< 0.05
Hydrophilicity		Hydrophobic**	Hydrophobic	Hydrophobic	Hydrophilic
Structural symmetry		Asymmetric	Symmetric	Symmetric	Asymmetric
Pure water permeability (ml/cm^2 bar min)		105	17.0	20.2	2.66

* Information from manufacture.
** Membrane was subjected to hydrophilic treatment by manufacture.

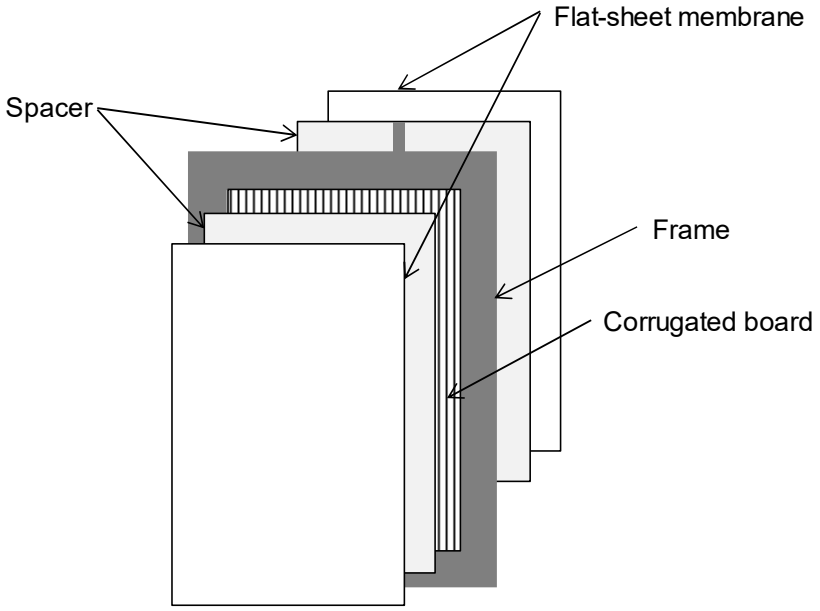

Fig. 2-1 Schematic of flat-sheet membrane module.

6.8 L. The membrane module was installed in the middle part of the reactor. Aeration was performed at the bottom of the reactor via tubular, porous air diffuser, and the air flow rate was controlled at 5.0 L/min using a pressure regulator with a gauge (SCO-4-115L, NIPPON FLOW CELL Co., Japan). The operational temperature was maintained at 23.0-27.0 ℃ (laboratory temperature). The synthetic wastewater used in the reactor was produced from seed sludge that had been obtained previously from a sewage

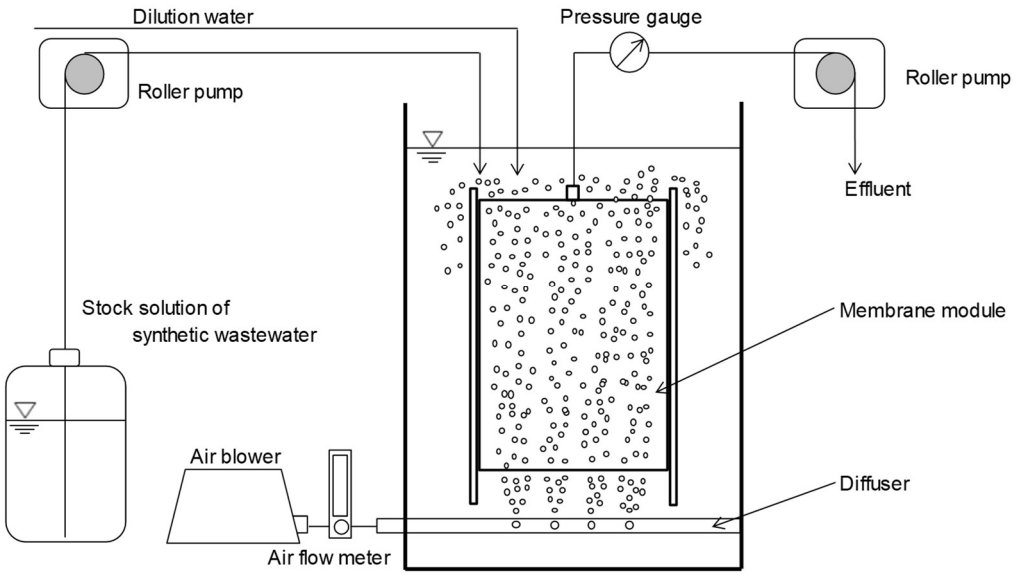

Fig. 2-2 Schematic of laboratory-scale MBR.

treatment plant in Kumamoto City and whose MLSS concentration had increased to more 10,000 mg/L using sequential batch culturing over three years. The synthetic wastewater than was continuously fed into removed from the reactor through the membrane using peristaltic pumps (MP-2000, TOKYO RIKAKIKAI Co. Ltd., Japan). The synthetic wastewater was prepared using the following components in order to emulate a sewage wastewater in Japan in reference to some literatures [39]: 250 mg/L D-glucose, 50 mg/L meat extract, 40 mg/L polypeptone, 50 mg/L K_2HPO_4, 20 mg/L $(NH_4)H_2PO_4$, 3.0 mg/L NaCl, 5.0 mg/L $MgSO_4 \cdot 7H_2O$, 2.5 mg/L $CaCl_2 \cdot 2H_2O$, and 0.5 mg/L $FeCl_3 \cdot 6H_2O$, and pH was adjusted at 7.2 ± 0.2 using a 2 mol/L NaOH solution. The total organic carbon (TOC) concentration of the synthetic wastewater was 120 mg/L, and the TOC removal efficiency was kept at more than 98% for all the cases in this study. The MLSS concentration of each reactor was measured periodically by drawing out an appropriate volume of the activated sludge (200-300 mL), in order to ensure that it remained constant.

The SRT was varied depending on the drawn volume of the activated sludge, but was generally thirty days. Every two days, all the suspension liquid in each reactor was removed and stirred and then returned to the reactor to ensure that the MLSS concentration was the same in each reactor. The degree of membrane fouling was evaluated based on the transmembrane pressure (TMP), which was measured periodically using a digital pressure gauge (GC31-174, NAGANO KEIKI Co, Ltd., Japan).

II.2.3 Analytical methods

The MLSS concentrations were measured following the standard method recommended by the American Public Health Association using 100 mL of the suspension liquid [40]. The particle size distributions of the suspended matters were measured with a laser differential scattering spectrophotometer (LA-950 V2-ADB, HORIBA Co. Ltd., Japan). The loosely bound EPSs (LB-EPS) and tightly bound EPSs (TB-EPS) were extracted using the following previously reported method [41,42]. To begin with, the suspension liquid (activated sludge) was centrifuged at 4000 g for 10 min. Next, the obtained pellet was suspended in physiological saline and incubated at 50 ℃ for 1 min. Then, the suspension liquid was centrifuged at 4000 g for 10 min, and the supernatant was recovered as the LB-EPS solution. Next, the obtained pellet was suspended in physiological saline and incubated at 60 ℃ for 30 min. Finally, the suspension liquid was centrifuged at 4000 g for 20 min, and the supernatant was recovered as the TB-EPS solution. The concentrations of carbohydrates and proteins, which are both primary components of the EPSs, were measured by the phenol-sulfuric acid method [40] while using glucose as the carbohydrate standard and a bicinchoninic acid (BCA) assay (TaKaRa BCA Protein Assay kit, Takara-bio Co., Japan) with bovine serum albumin as

the protein standard. The analysis of EPSs was duplicated and an average value was computed. The three-dimensional EEMs were measured with fluorescence spectrometer (F-2700, Hitachi High-Tech Science Co., Japan). The suspension liquids corresponding to two actual wastewater plants were obtained from a night-soil treatment plant with an MBR (MBR/NTP) in Kami-Amakusa City and a sewage treatment plant with a common aeration tank (AT/STP) in Kumamoto City. Their characteristics were compared to those of the suspension liquid in MBR/Lab.

II.3 Results

II.3.1 Changes in transmembrane pressure and mixed liquor suspended solid concentration in laboratory-scale submerged membrane bioreactor

Figure 2-3 shows the changes in the TMP and MLSS concentration over course of the experiment. The MLSS concentration remained within the 11000-12500 mg/L range, with its variation being within 0.71% for the four reactors. During the first operation, the TMP was low (< 1.0 kPa) at a flux of 0.3 $m^3/m^2 \cdot d$, which is a value used commonly in practical applications. However, when the flux was raised to 0.65 $m^3/m^2 \cdot d$, the TMP increased sharply initially and then plateaued over the course of 5 days. The highest TMP was observed for the PVDF membrane (30 kPa on day 16), which was followed by those for the CPVC, PES, and PTFE membranes (in that order), although the differences in the TMP values were within 3.0 kPa. Moreover, the difference in the TMP values for CPVC and PES membranes was small. Finally, when the flux was raised to 0.92 $m^3/m^2 \cdot d$, the TMP increased gradually and then plateaued over the course of 5 days. The order in the which the TMP values could be arranged was the same as that for a flux of 0.65 $m^3/m^2 \cdot d$. The differences between the TMPs for the various membranes

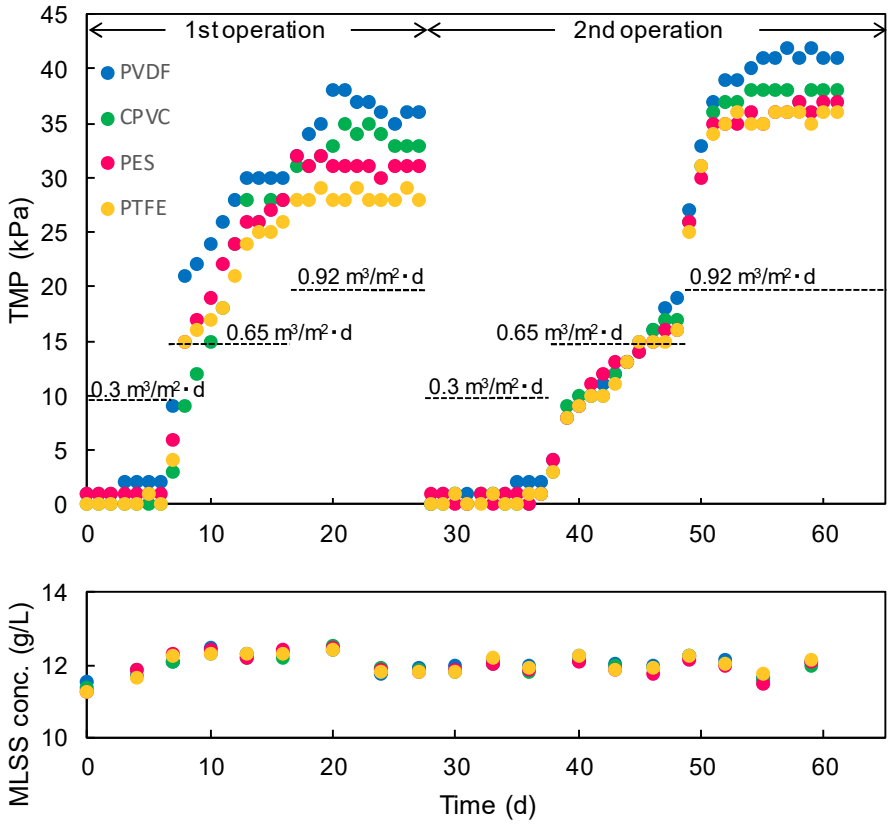

Fig. 2-3 Changes in TMP and MLSS concentrations over the course of the experiment.

were as high as 8.0 kPa in the steady state (on day 27). At this point, all the membrane modules were removed from the reactors, physically scoured with a sponge and water, and then soaked in a 0.5% hypochlorite solution for more than 2 h before commencing the second operation.

During the second operation, the TMP remained lower than 1.0 kPa at 0.3 $m^3/m^2 \cdot d$ for all the membranes. When the flux was raised to 0.65 $m^3/m^2 \cdot d$, the TMPs increased continuously over the course of 10 days in the same manner as that observed during the first operation although the rate of increase in the TMPs was slightly lower than that during the first operation. The differences between the TMP values were within

3.0 kPa, and the values after 11 days at 0.65 $m^3/m^2 \cdot d$ (on day 48) could be arranged in the same order as in the case of the first operation. However, when the flux was raised to 0.92 $m^3/m^2 \cdot d$, the TMP increased rapidly and exceeded 35 kPa within 4 days. This was the case for all the membranes. After the TMP values had reached a steady state, they could be arranged in the following order: PVDF > CPVC > PES > PTFE. The actual TMP values for all the membranes were higher than those during the first operation. Finally, the differences between the TMPs were only 5 kPa (on day 61) and smaller than those during the first operation.

II.3.2 Contribution of membrane surface vulnerability to fouling behavior depending on membrane fabrication process.

After the completion of all the MBR/Lab operations, the flat-sheet membranes were analyzed using scanning electron microscopy (SEM) to elucidate the effects of the MBR/Lab operations on the membrane structure. The original structure of each membrane is illustrated in the literatures [36-38].

The SEM images of the conditions of the surfaces and cross-sections of the flat-sheet membranes before and after the operations are shown in Fig. 2-4 and Fig. 2-5, respectively. There was little to no change in the surface properties of the PTFE, CPVC, and PES membranes after operations. However, the surface of the PVDF membrane showed significant changes. The PVDF layer of the membrane had been removed almost completely, leaving the non-woven PET layer (i.e., the supporting layer) almost bare. Surface deterioration was observed in the other membranes as well. However, their surface structures remained unchanged. Table 2-2 shows the contact angles of the various membranes, measured before and after operations. The contact angle of the flat-sheet of

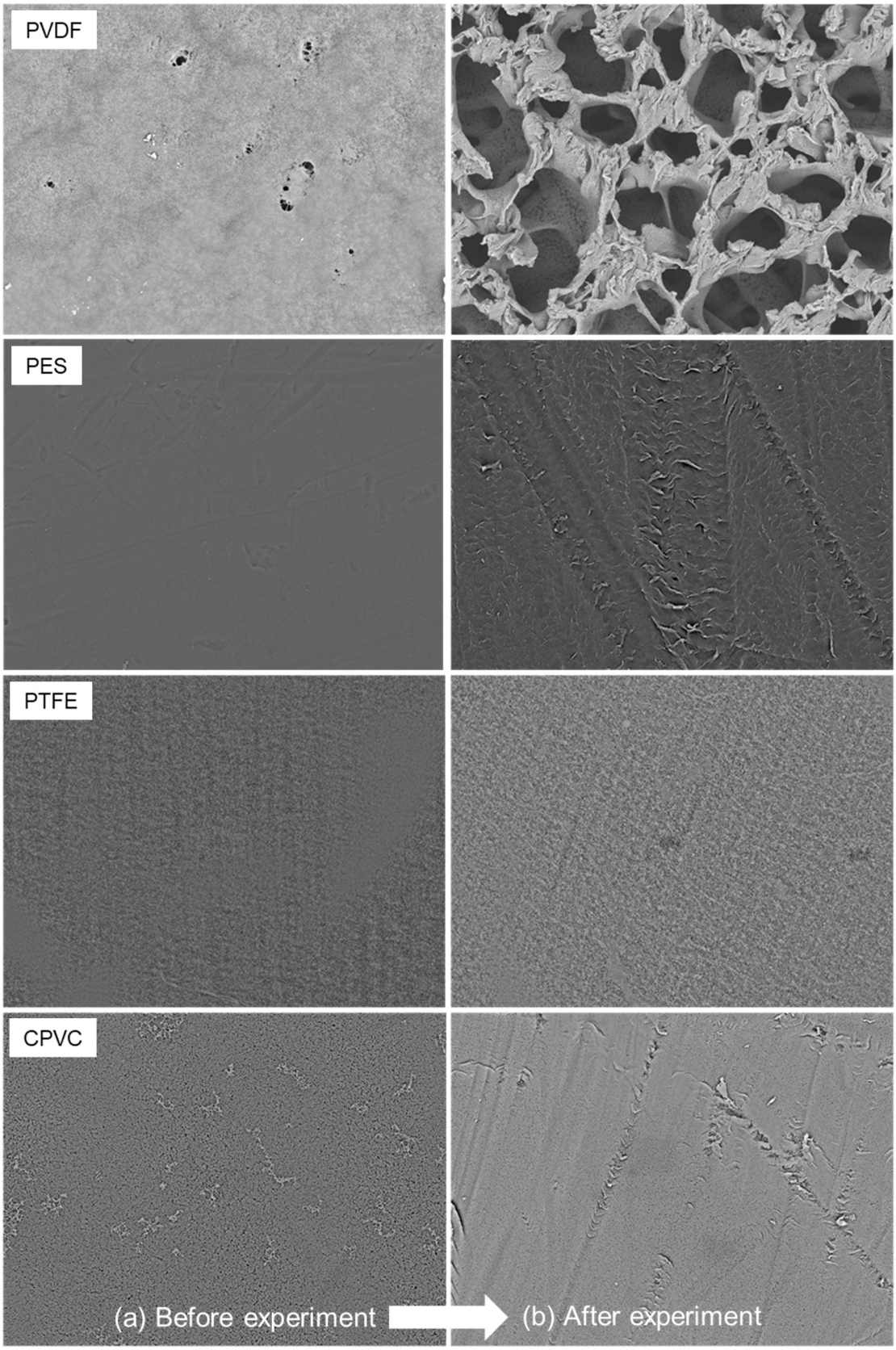

Fig. 2-4 SEM images of surfaces of flat-sheet membranes (a) before and (b) after experiment.

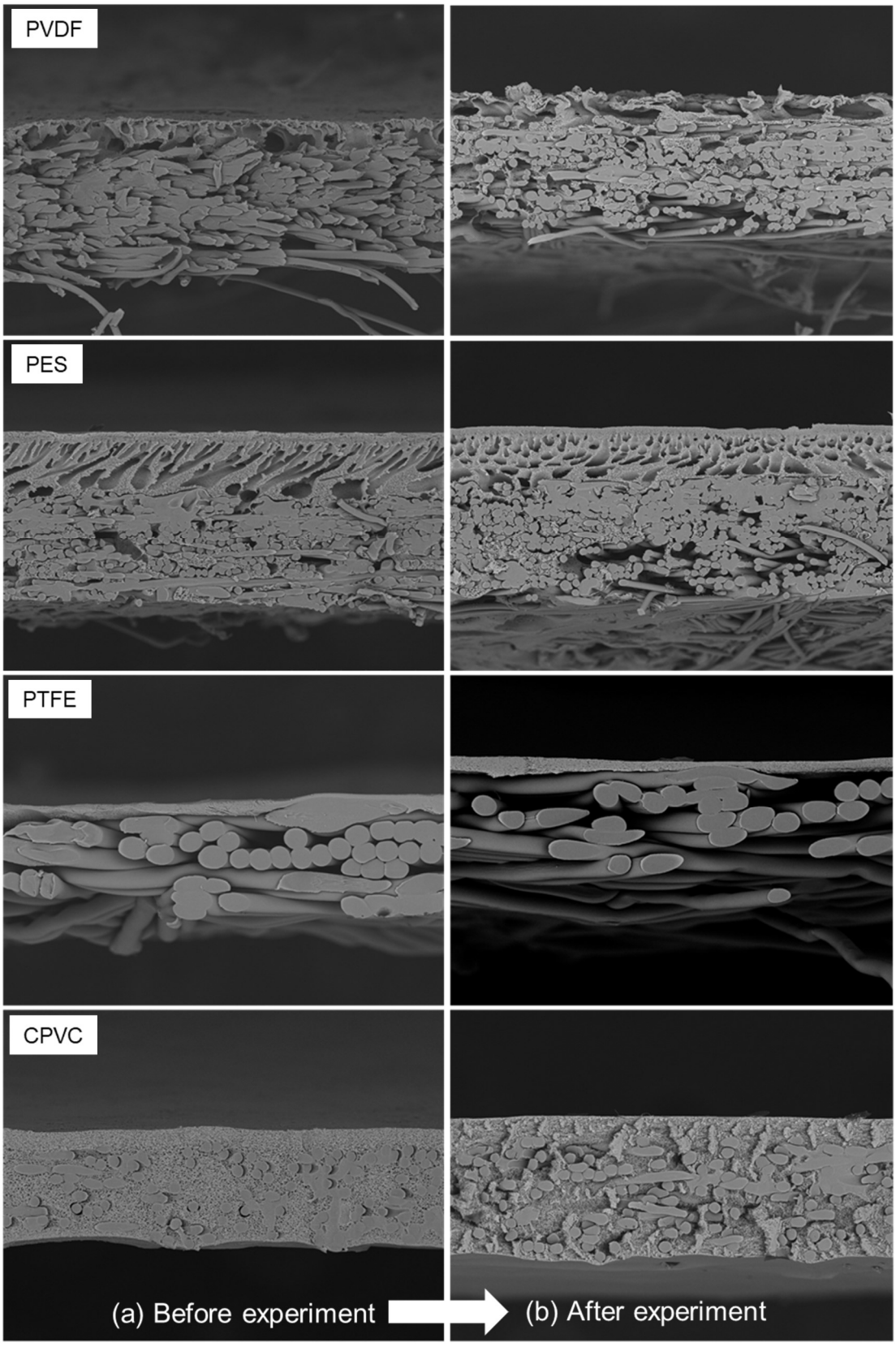

Fig. 2-5 SEM images of cross-sections of flat-sheet membranes (a) before and (b) after experiment.

Table 2-2 Contact angles of various membranes before and after experiment

	Contact angle (°)	
	Before experiment	After experiment
PVDF	55*	128
CPVC	108	111
PTFE	123	123
PES	75	77

* Membrane was subjected to hydrophilic treatment by manufacture.

the PVDF membrane changed significantly after operations, with the membrane becoming hydrophobic. This indicated that the bare supporting layer of non-woven PET increases hydrophobicity. It was believed that the shearing force generated during aeration or the physical cleaning with a sponge is responsible for the phenomenon. In order to confirm this, the effects of aeration and physical cleaning on the membrane surfaces were investigated using the following procedure. First, a fresh flat-sheet PVDF membrane was installed within a reactor and subjected to aeration at the same air flow rate (5 L/min) as that used during the earlier operations for 16 days. Next, two pieces were cut from the membrane from the same side and cleaned with 0.5% hypochlorite solution. One of these samples was physically scrubbed with a sponge, while the other sample was not. Both the samples were analyzed using SEM and their internal structures were compared. The SEM images of the conditions of membrane surfaces before and after aeration and after scrubbing are shown in Fig. 2-6. Several large pores were observed on the membrane surface after aeration, with the surface roughness also increasing. However, there was only small changes in the membrane surface after scrubbing with a sponge. Based on these results, it was concluded that the PVDF layer can be readily removed from the non-woven PET layer by the aeration process; therefore, the PVDF membrane exhibited the highest TMP in MBR/Lab in this study. This is discussed in

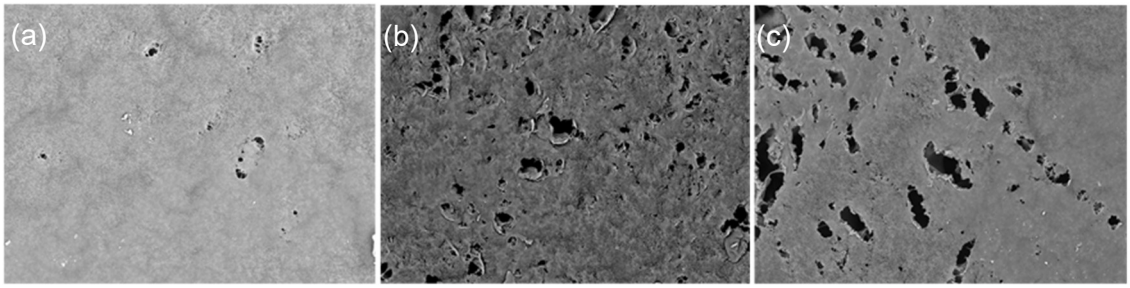

Fig. 2-6 SEM images of surface of PVDF membrane before and after aeration: (a) before aeration, (b) after aeration, and (c) after aeration and scrubbing with sponge.

detail later.

II.3.3 Comparison of characteristics of suspension liquids from laboratory-scale submerged membrane bioreactor, night-soil treatment plant with an membrane bioreactor, and sewage treatment plant with a common aeration tank

In order to explore the possibility of extrapolating the knowledge obtained in this study to actual wastewater treatment, the characteristics of the suspension liquids from MBR/Lab and those from actual wastewater treatment plants (MBR/NTP and AT/STP) were compared to elucidate their differences.

Figure 2-7 shows the particle size distributions of the matter suspended in the MBR/Lab, MBR/NTP, and AT/STP liquids. The particle size range was 0.01-1000 μm, and the sizes of most of the particles lay within a narrow range (5-1000 μm). The smallest and largest particles were observed in the samples from MBR/NTP and AT/STP, respectively. The particle size of the sample from MBR/Lab lay between those of the particles in the liquids from two other plants. It was believed that these differences are related to the differences in the length of SRT. The SRT was the highest for MBR/NTP (> 30 days), which was followed by MBR/Lab (30 days) and AT/STP (10 h). Further, the

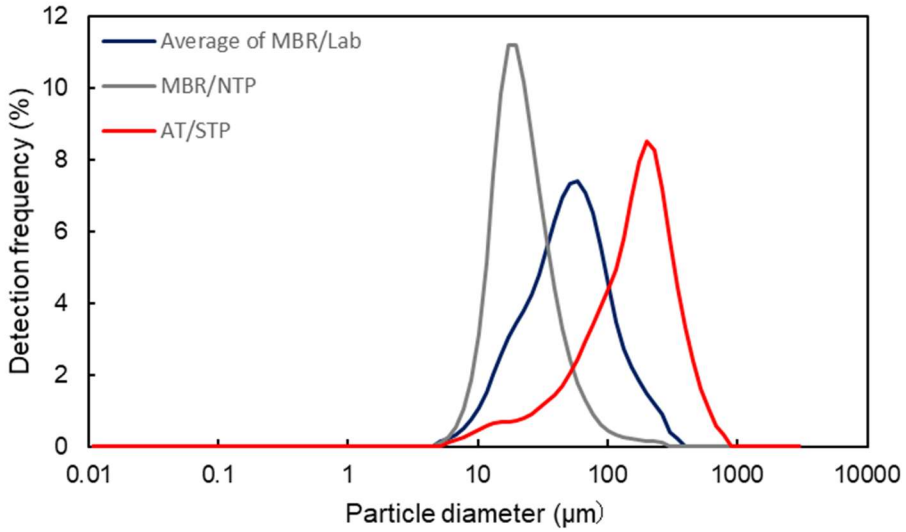

Fig. 2-7 Particle size distributions of suspended solids in MBR/Lab, MBR/NTP, and AT/STP.

aeration intensity would also affect the particle size distribution, because the aeration intensity in AT/STP was probably lower than that in the other MBRs. It was assumed that the large suspended solids (flock) can be broken into smaller ones during the operation of the MBR under the conditions, which may include high SRT and vigorous aeration. This is because the seed sludge for MBR/Lab was obtained from AT/STP. Many researchers have reported that the suspended matter probably does not contribute significantly to fouling, in contrast to dissolved compounds such as EPSs [3,43]. However, even the suspended matter must be considered when the membrane surface is broken, as was the case for the PVDF flat-sheet membrane used in this study.

Figure 2-8 shows the concentrations of carbohydrates and proteins in the supernatant (Fig. 2-8(a)), LB-EPS (Fig. 2-8(b)), TB-EPS (Fig. 2-8(c)), and suspension liquid as a whole (Fig. 2-8(d)) for the three reactors. There were no significant differences in the carbohydrate and protein concentrations of the supernatants, though the protein concentration in the MBR/NTP supernatant was slightly higher than those of the other

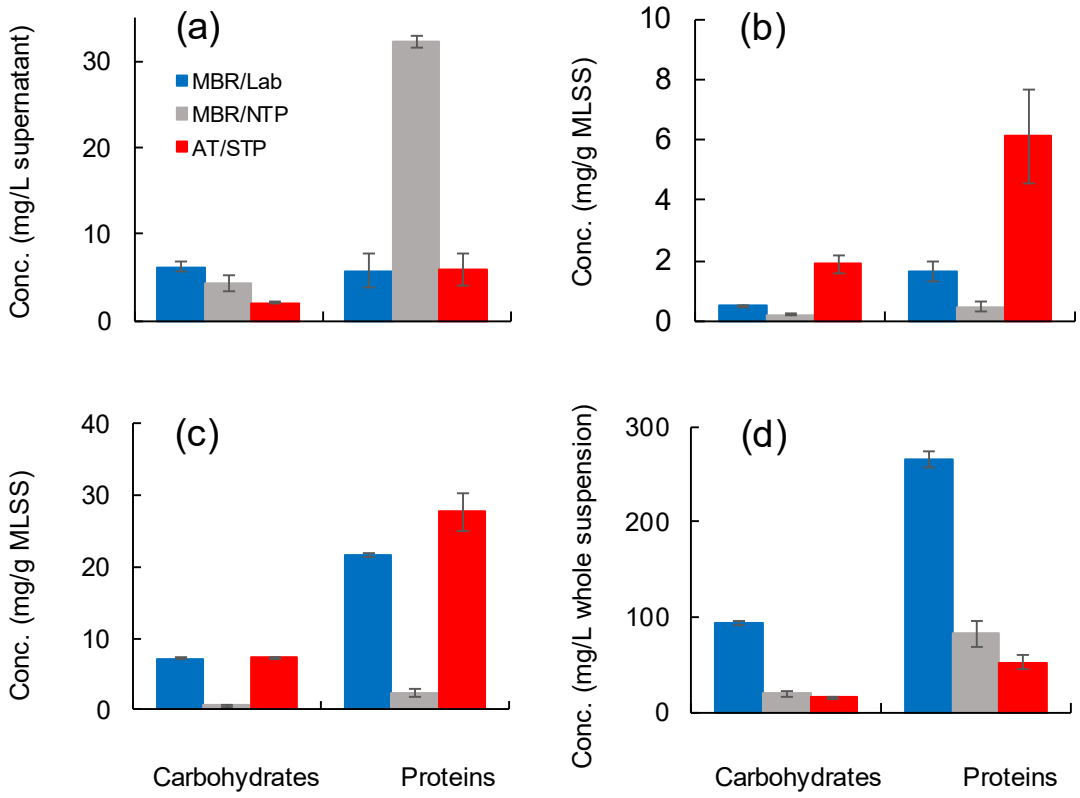

Fig. 2-8 Concentrations of carbohydrates and proteins in (a) supernatant, (b) LB-EPS samples, (c) TB-EPS samples, and (d) suspensions from various reactors.

supernatant. On the other hand, the carbohydrate and protein concentrations of the LB-EPS and TB-EPS samples from MBR/NTP were lower than those of the corresponding samples from the other reactors. These results probably mean that the EPS components were more readily released from the MLSS into the suspension liquid in MBR/NTP than was the case in the other reactors due to more vigorous aeration in the real wastewater treatment plant with MBR. The concentrations of carbohydrates and proteins were the highest in the case of the liquid from MBR/Lab (Fig. 2-8(d)) because this liquid contained MLSSs in larger quantities than did the liquid from AT/STP

Figure 2-9 shows the EEM fluorescence spectra of the supernatants from the

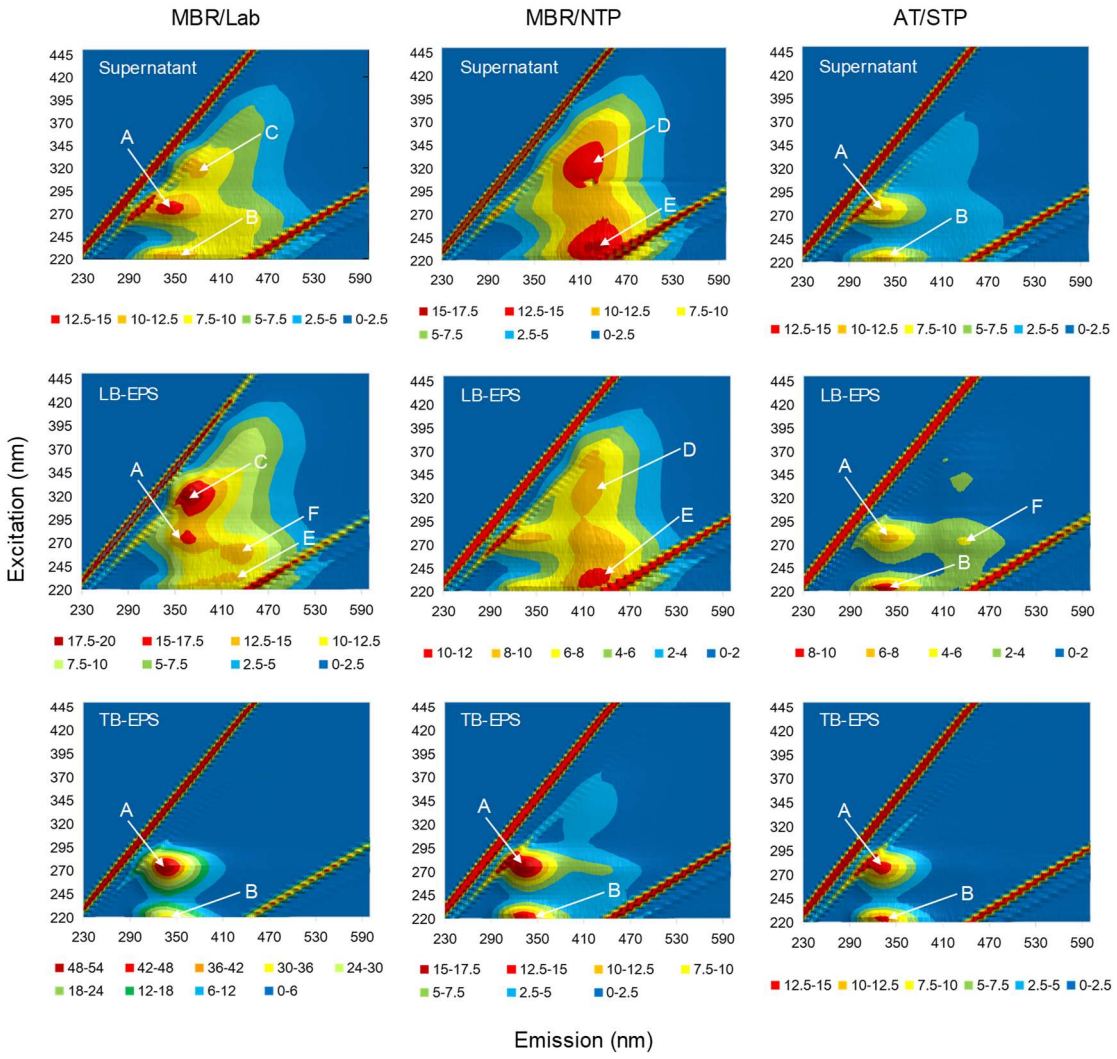

Fig. 2-9 EEM fluorescence spectra of supernatant, LB-EPS samples, and TB-EPS samples from MBR/Lab, NBR/NTP, and AT/STP.

reactors. The EEM spectra of TB-EPS for the various samples were similar and exhibited two major peaks, A and B. These peaks were probably related to protein-like compounds [44,45]. However, the shapes of the spectra of the LB-EPS samples and the supernatants of the different liquid samples were different. The shapes of the spectra of the LB-EPS and supernatant of the liquid from AT/STP were similar to those of the spectra of TB-EPS. However, the spectra of the LB-EPS samples of the liquids from MBR/Lab and

MBR/NTP contained peaks related to humic-like substances (peaks D, E, and F) [44-47]. The supernatant of the liquid from MBR/NTP also showed peaks related to humic-like compounds (peaks D and E). Overall, the EEM spectra of the various samples (supernatant, LB-EPS, and TB-EPS) from MBR/Lab and MBR/NTP were similar, indicating that the compositions of the dissolved matter related to the EPS were not that different and the possibilities of extrapolation of the knowledge obtained in the laboratory MBR operation to real treatment plant with MBR. On the other hand, the EEM spectra of the samples from AT/STP were a little different from those from the reactors. However, given that the seed sludge for MBR/Lab was obtained from the activated sludge of AT/STP, it can be assumed that the dissolved matter related to the EPS probably changes with the operating conditions of the MBR.

II.4 Discussion

In this study, I investigated the differences in fouling behaviors of membranes prepared from four different materials (PVDF, CPVC, PTFE, and PES), which were used to form membrane modules, by comparing their TMP values when used in continuous submerged MBRs with synthetic wastewater. No significant differences were observed in the TMPs of the four membranes for a membrane flux used for safe operations (0.3 $m^3/m^2 \cdot d$), even though the hydrophilicities and average pore sizes of the membranes were different. These results are in keeping with those of a previous study by Choi et al. [9], who investigated the effects of the membrane type on the TMP in submerged MBR using three types of membrane materials (phase-inversed polytetrafluoroethylene, track-etched polycarbonate, and track-etched polyester). They reported no increase in the TMP when the reactors were operated using the designed flux and concluded that there was no

relationship between the hydrophilicity of the membranes and their TMP value [9]. However, when the membrane flux was increased to 0.65 and 0.92 $m^3/m^2 \cdot d$, the TMPs of the membranes showed differences, with the PVDF membrane exhibiting the highest value. These results were unexpected and not consistent with those of previous studies [4,28] because the PVDF membrane had a larger pore size (Table 2-1) and lower filtration resistance than the other membranes. Miyoshi et al. compared the changes in the TMPs of membranes of three different polymeric materials (PVDF, polyvinyl butyral (PVB), and CAB) using a bench-scale MBR with activated sludge. They also investigated the effects of the membrane pore size on the development of fouling and found that the PVDF membrane with a pore size of 0.4 μm showed lower fouling propensity than the membranes with smaller pore size (0.02 and 0.25 μm) [28]. These results suggested that hydrophobic PVDF membranes with a pore size of approximately 0.3 μm do not undergo fouling as readily as hydrophilic CAB membranes. Yamato et al. evaluated the fouling behaviors of PVDF and polyethylene (PE) membranes in an MBR at an actual wastewater treatment plant and reported that the PVDF membrane was superior to the PE membrane in terms of the prevention of irreversible fouling [4].

On the other hand, the results of this study were only partially in agreement with commonly recognized knowledge, i.e. more hydrophilic membranes will exhibit a lower fouling propensity [3,7,11]. Jeon et al. found that, during batch filtration tests, the TMP increase more sharply in the case of hydrophobic PVDF membranes than for hydrophilic cellulose acetate membranes and that this is the case even when membranes with similar permeabilities and pore sizes are used [7]. Nittami et al. compared the changes in the TMPs of a PVDF membrane and two types of PTFE membranes, viz. a hydrophobic PTFE (Hpo) membrane and a hydrophilic PTFE (Hpi) membrane. They employed a

submerged MBR with flat-sheet membranes and used activated sludge from a laboratory reactor and a municipal wastewater treatment plant (WWTP). They found that the effects of surface hydrophilicity on the degree of membrane fouling depend on the hydrophobicity of the membrane with respect to the activated sludge. The hydrophobic PVDF membrane showed higher fouling propensity than the two PTFE membranes in the MBR with the activated sludge from the laboratory-scale reactor, which was more hydrophilic than that from an actual WTTP [11]. Both these studies had focused on the relationship between the hydrophobicity of the membranes with respect to the suspension liquid (activated sludge). However, in this study, the hydrophobic PTFE membrane showed lower fouling propensity than the hydrophilic PES membrane during the first operation. Further, during the second operation (i.e., after chemical cleaning), all the membranes (hydrophobic CPVC, hydrophilic PES and hydrophobic PTFE) except for the PVDF membrane showed fouling propensities that were similar to and lower than that of the PVDF membrane. This result is in contrast to those of the above-mentioned studies. Thus, it was believed that the hydrophobicity and pore size of the membrane material do not have as strong an effect on the membrane fouling behavior as has been reported previously [9,28,48].

On the basis of these results, it was investigated that the changes in the physical structures of the flat-sheet membranes after the operations using SEM in order to elucidate the reasons the PVDF membrane showed the highest fouling propensity. As a result, it was found that the surface of the PVDF membrane was almost completely destroyed by the aeration process, in contrast to the case for the other membranes. These results suggest that the internal structures of the various membranes were different and depended on the membrane fabrication process. The flat-sheet PVDF and PES membranes were produced

using NIPS method and had a non-woven PET layer as the supporting layer [36]. The CPVC membrane was produced by the VIPS method [37], whereas the PTFE membrane was produced by the stretching and lamination method [38]. The CPVC and PTFE membranes exhibited almost homogenous internal structures, starting from the surface of the membrane to the surface of the supporting layer (non-woven PET layer). On the other hand, the PVDF and PES membranes, which had asymmetric structures, were composed of a "dense top layer" on the surface and a "finger-like porous sublayer" at the subsurface. Moreover, while the dense top layer of the PES membrane could be seen clearly, that of the PVDF membrane was only barely visible. In this regard, the dense top layer of the PVDF membrane used in this study was found to be quite thin compared to that of the PES membrane, implying that the dense top layer of PVDF membrane was easily broken. Therefore, the near-complete breakage of the surface of the PVDF flat-sheet membrane was due to the shearing stresses generated by the aeration process and the suspended matter. The surface layer of the PVDF membrane was almost completely removed to expose its supporting layer. This allowed the fouling matter to penetrate the membrane, which led to a very high degree of fouling. In addition, the contact angle of the PVDF flat-sheet membrane changed significantly, making the membrane hydrophobic (Table 2-2). Thus, this increase in the hydrophobicity may have also contributed to the fouling development of the membrane. Together, these results suggest that, in addition to the properties of the membrane material, the structure and strength of the membranes and their supporting layers also have a determining effect on the fouling behavior of flat-sheet membranes in continuous submerged MBRs.

In this study, it was also investigated the characteristics of the suspension liquid in MBR/Lab and compared them to those of liquid samples from actual wastewater

treatment plants in order to determine whether the knowledge obtained in the laboratory study can be extrapolated to actual wastewater treatment plants. As a result, the characteristics of the suspension liquid (particle size distribution, EPSs and EEM spectra) from MBR/Lab and actual wastewater treatment plants were not that different, thus the possibility of extrapolating was suggested.

II.5 Conclusions

The fouling behaviors of flat-sheet membrane with four materials were analyzed using a continuous submerged MBR. The PVDF flat-sheet membrane showed the highest TMP because that the surface layer was separated from the supporting layer by the shearing stress of aeration, indicating that the structural vulnerability of flat-sheet membranes is quit important factor determining their fouling propensity. The characteristics of the suspension liquid from MBR/Lab and actual plants were not that different, suggesting that the results obtained from this study can be extrapolated to actual wastewater treatment plants as well.

References

[1] L. Deng, W. Guo, H.H. Ngo, H. Zhang, J. Wang, J. Li, S. Xia and Y. Wu, Biofouling and control approaches in membrane bioreactors, *Bioresour. Technol.*, 221, 656-665 (2016).

[2] V. Jegatheesan, B.K. Pramanik, J. Chen, D. Navaratna, C.Y. Chang and L. Shu, Treatment of textile wastewater with membrane bioreactor: a critical review, *Bioresour. Technol.*, 204, 202-212 (2016).

[3] F. Meng, S. Zhang, Y. Oh, Z. Zhou, H.S. Shin and S.R. Chae, Fouling in membrane

bioreactors: an updated review, *Water Res.*, 147, 393-402 (2017).

[4] N. Yamato, K. Kimura, T. Miyoshi and Y. Watanabe, Difference in membrane fouling in membrane bioreactors (MBRs) caused by membrane polymer materials, *J. Membr. Sci.*, 280, 911-919 (2006).

[5] M. Villain, I. Bourven, G. Guilbaud and B. Marrot, Impact of synthetic or real urban wastewater on membrane bioreactor (MBR) performances and membrane fouling under stable conditions, *Bioresour. Technol.*, 155, 235-244 (2014).

[6] S. Rajabzadeh, R. Sano, T. Ishigami, Y. Kakihana, Y. Ohmukai and H. Matsuyama, Preparation of hydrophilic vinyl chloride copolymer hollow fiber membranes with antifouling properties, *App. Surf. Sci.*, 324, 718-724 (2015).

[7] S. Jeon, S. Rajabzadeh, R. Okamura, T. Ishigamai, S. Hasegawa, N. Kato and H. Matsuyama, The effect of membrane material and surface pore size on the fouling properties of submerged membranes, *Water (Switzerland)*, 8, 1-11 (2016).

[8] C. Jacquin, G. Traber, W. Pronk and M. Heran, Three-dimensional excitation and emission matrix fluorescence (3DEEM) for quick and pseudo-quantitative determination of protein- and humic-like substances in full-scale membrane bioreactor (MBR). *Water Res.*, 118, 82-92 (2017).

[9] J.H. Choi and H.Y. Ng, Effect of membrane type and material on performance of a submerged membrane bioreactor, *Chemosphere*, 71, 853-859 (2008).

[10] N. Dizge, D.Y. Koseoglu-Imer, A. Karagunduz and B. Keskinler, Effect of sludge retention time on membrane bio-fouling using different type and pore size of membranes in a submerged membrane bioreactor, *Water Sci. Technol.*, 67, 604-611 (2013).

[11] T. Nittami, H. Tokunaga, A. Satoh, M. Takeda and K. Matsumoto, Influence of surface hydrophilicity on polytetrafluoroethylene flat sheet membrane fouling in a

submerged membrane bioreactor using two activated sludges with different characteristics, *J. Membr. Sci.*, 463, 183-189 (2014).

[12] A. Ding, H. Liang, G. Li, N. Derlon, I. Szivak, E. Morgenroth and W. Pronk, Impact of aeration shear stress on permeate flux and fouling layer properties in a low pressure membrane bioreactor for the treatment of grey water, *J. Membr. Sci.*, 510, 382-390 (2016).

[13] M. Higashi, J. Morita, N. Shimada and T. Kitagawa, Long-term-hydrophilic flat-sheet microfiltration membrane made from chlorinated poly (vinyl chloride), *J. Membr. Sci.*, 500, 180-189 (2016).

[14] L. Zhao, F. Wang, X. Weng, R. Li, X. Zhou, H. Lin, H. Yu and B.Q.Liao, Novel indicators for thermodynamic prediction of interfacial interactions related with adhesive fouling in a membrane bioreactor, *J. Colloid Interf. Sci.*, 487, 320-329 (2017).

[15] X. Cai, G. Yu, H. Hong, Y. He, L. Shen and H. Lin, Impacts of morphology on fouling propensity in a membrane bioreactor based on thermodynamic analyses, *J. Colloid Interf. Sci.*, 531, 282-290 (2018).

[16] S. Arabi and G. Nakhla, Impact of molecular weight distribution of soluble microbial products on fouling in membrane bioreactors, *Sep. Purif. Technol.*, 73, 391-396 (2010).

[17] M.C. Marti-Calatayud, S. Schneider, S. Yuce and M. Wessling, Interplay between physical cleaning, membrane pore size and fluid rheology during the evolution of fouling in membrane bioreactors, *Water Res.*, 147, 393-402 (2018).

[18] Y.Q. Wang, T. Wang, Y.L. Su, F.B. Peng, H. Wu and Z.Y. Jiang, Remarkable reduction of irreversible fouling and improvement of the permeation properties of poly (ether sulfone) ultrafiltration membranes by blending with pluronic F127, *Langmuir*, 21 11856-11862 (2005).

[19] W. Zhao, Y. Su, C. Li, Q. Shi, X. Ning and Z. Jiang, Fabrication of antifouling

polyethersulfone ultrafiltration membranes using Pluronic F127 as both surface modifier and pore-forming agent, *J. Membr. Sci.*, 318, 405-412 (2008).

[20] H. Choi, Y. Kwon, Y. Jung, S. Hong and T. Tak, Preparation and characterization of antifouling poly (vinylidene fluoride) blended membranes, *J. Appl. Polym. Sci.*, 123, 286-291 (2011).

[21] W. Ma, S. Rajabzadeh and H. Matsuyama, Preparation of antifouling poly (vinylidene fluoride) membranes via different coating methods using a zwitterionic copolymer, *Appl. Surf. Sci.*, 357, 1388-1395 (2015).

[22] M. Kim, B. Sankararao, S. Lee and C. Yoo, Prediction and identification of membrane fouling mechanism in a membrane bioreactor using combined mechanistic model, *Ind. Eng. Chem. Res.*, 52, 17198-17205 (2013).

[23] A.T. Besha, A.Y. Gebreyohannes, R.A. Tufa, D.N. Bekele, E. Curcio and L. Giorno, Removal of emerging micropollutants by activated sludge process and membrane bioreactors and effects of micropollutants on membrane fouling: a review, *J. Environ. Chem. Eng.*, 5, 2395-2414 (2017).

[24] L. Duan, Y. Song, H. Yu, S. Xia and S.W. Hermanowics, The effect of solids retention times on the characterization of extracellular polymeric substances and soluble microbial products in a submerged membrane bioreactor, *Bioresour. Technol.*, 163, 395-398 (2014).

[25] H. Hazrati, A.H. Moghaddam and M. Rostamizadeh, The influence of hydraulic retention time on cake layer specifications in the membrane bioreactor: Experimental and artificial neural network modeling, *J. Environ. Chem. Eng.*, 5, 3005-3013 (2017).

[26] M. Aslam, A. Charfi, G. Lesage, M. Heran and J. Kim, Membrane bioreactors for wastewater treatment: a review of mechanical cleaning by scouring agents to control membrane fouling, *Chem. Eng. J.*, 307, 897-913 (2017).

[27] Z. Cui, J. Wang, H. Zhang, H.H. Ngo, H. Jia, W. Guo, F. Gao, G. Yang and D. Kang, Investigation of backwashing effectiveness in membrane bioreactor (MBR) based on different membrane fouling stages, *Bioresour. Technol.*, 269, 355-362 (2018).

[28] T. Miyoshi, K. Yuasa, T. Ishigami, S. Rajabzadeh, E. Kamio, Y. Ohmukai, D. Saeki, J. Ni and H. Matsuyama, Effect of membrane polymeric materials on relationship between surface pore size and membrane fouling in membrane bioreactors, *Appl. Surf. Sci.*, 330, 351-357 (2015).

[29] T.C. Ng and H.Y. Ng, Characterization of initial fouling in aerobic submerged membrane bioreactors in relation to physico-chemical characteristics under different flux conditions, *Water Res.*, 44, 2336-2348 (2010).

[30] J. Teng, L. Shen, Y. He, B.Q. Liao, G. Wu and H. Lin, Novel insights into membrane fouling in a membrane bioreactor: Elucidating interfacial interactions with real membrane surface, *Chemosphere*, 210, 769-778 (2018).

[31] Z. Zhao, Y. Lou, Y. Chen, H. Lin, R. Li and G. Yu, Prediction of interfacial interactions related with membrane fouling in a membrane bioreactor based on radial basis function artificial neural network (ANN), *Bioresour. Technol.*, 282, 262-268 (2019).

[32] J. Teng, M. Zhang, K.T. Leung, J. Chen, H. Hong, H. Lin and B.Q. Liao, A unified thermodynamic mechanism underlying fouling behaviors of soluble microbial products (SMPs) in a membrane bioreactor. *Water Res.*, 149, 477-487 (2019).

[33] M. Zhang, H. Hong, H. Lin, L. Shen, H. Yu, G. Ma, J. Chen and B.Q. Liao, Mechanistic insights into alginate fouling caused by calcium ions based on terahertz time-domain spectra analyses and DFT calculations, *Water Res.*, 129, 337-346 (2018).

[34] R. Li, Y. Lou, Y. Xu, G. Ma, B.Q. Liao, L. Shen and H. Lin, Effects of surface morphology on alginate adhesion: Molecular insights into membrane fouling based on

XDLVO and DFT analysis, *Chemosphere*, 233, 373-380 (2019).

[35] Y. Chen, J. Teng, L. Shen, G. Yu, R. Li, Y. Xu, F. Wang, B.Q. Liao and H. Lin, Novel insights into membrane fouling caused by gel layer in a membrane bioreactor: effects of hydrogen bonding, *Bioresour. Technol.*, 276, 219-225 (2019).

[36] J.T. Jung, J.F. Kim, H.H. Wang, E. di Nicolo, E. Drioli and Y.M. Lee, Understanding the non-solvent induced phase separation (NIPS) effect during the fabrication of microporous PVDF membranes via thermally induced phase separation (TIPS), *J. Membr. Sci.*, 514, 250-263 (2016).

[37] V.P. Khare, A.R. Greenberg and W.B. Krantz, Vapor-induced phase separation-effect of the humid air exposure step on membrane morphology: Part I. Insights from mathematical modeling, *J. Membr. Sci.*, 258, 140-156 (2005).

[38] T. Kitamura, K. Kurumada, M. Tanigaki, M. Ohshima and S. Kanazawa, Formation mechanism of porous structure in polytetrafluoroethylene (PTFE) porous membrane through mechanical operations, *Polym. Eng. Sci.*, 39, 2256-2263 (1999).

[39] Committee on Environmental and Sanitary Engineering, Japan Society of Civil Engineering, *Laboratory Manual for Environmental Microbiotechnology* (Kankyo Biseibutsu Kogaku Kenkyuhou in Japanese), Gihodoshuppan, Tokyo (1993).

[40] APHA, *Standard Method for the Examination of Water and Wastewater*, 19th ed., American Public Health Association, Washington, D.C. (1995).

[41] X.Y. Li and S.F. Yang, Interface of loosely bound extracellular polymeric substances (EPS) on the flocculation, sedimentation and dewaterability of activated sludge, *Water Res.*, 41, 1022-1030 (2007).

[42] M. Basuvaraj, J. Fein and S.N. Liss, Protein and polysaccharide content of tightly and loosely bound extracellular polymeric substances and the development of a granular

activated sludge floc, *Water Res.*, 82, 104-117 (2015).

[43] X. Su and Z. Zhang, Structural characteristics of extracellular polymeric substances (EPS) in membrane bioreactor and their adsorptive fouling, *Water Sci. Technol.*, 77, 1537-1546 (2018).

[44] P.G. Coble, Characterization of marine and terrestrial DOM in seawater using excitation-emission matrix spectroscopy, *Marine Chem.*, 51, 325-346 (1996).

[45] C.A. Stedmon and S. Markager, Resolving the variability in dissolved organic matter fluorescence in a temperate estuary and its catchment using PARAFAC analysis, *Limnol. Oceanogra.*, 50, 686-697 (2005).

[46] E. Parlanti, L.K. Worz, L. Geoffroy and M. Lamotte, Dissolved organic matter fluorescence spectroscopy as a tool to estimate biological activity in a coastal zone submitted to anthropogenic inputs, *Org. Geochem.*, 31, 1765-1781 (2000).

[47] Z. Wang, Z. Wu and S. Tang, Characterization of dissolved organic matter in a submerged membrane bioreactor by using three-dimensional excitation and emission matrix fluorescence spectroscopy, *Water Res.*, 43, 1533-1540 (2009).

[48] J.H. Choi, S.K. Park and H.Y. Ng, Membrane fouling in a submerged membrane bioreactor using track-etched and phase-inversed porous membranes, *Sep. Purif. Technol.*, 65, 184-192 (2009).

Chapter III

Mechanical durability and fouling development of flat-sheet membranes in a submerged membrane bioreactor

---

III.1 Introduction

Microplastics, commonly defined as plastic particles smaller than 5 mm, have received great attention in recent years as substances that may have an adverse effect on ecosystems and human health [1]. Evidence also suggests that influence of microplastics on marine ecosystem is serious [2,3]. Studies looking for the sources of microplastics have been conducted; and artificial fibers from laundry washing is one such important source [4-8]. These fibers eventually reach wastewater treatment plants (WWTPs) via the sewer system [5], and while more than 90% microplastics are removed [9-12], almost 10% of microplastics slip through and flow into the environmental water [13-16]. Therefore, microplastic removal by conventional WWTPs may be insufficient.

The membrane bioreactor (MBR), is an advanced wastewater treatment technology, that has excellent microplastic removal performance [1,17,18]. Lares et al. reported that an MBR was able to remove 99.4% of microplastics [17], while Li et al. reported no microplastics in the MBR permeate [18]. This suggests that MBRs are a promising solution to marine pollution caused by microplastics. Nevertheless, most of the membranes applied in practical MBR plants are polymeric membrane, that is, they are made from plastics materials. Thus, the membranes themselves may become a pollutant if they deteriorate and break. Although it is drinking water treatment plants rather than wastewater treatment plants, Ding et al. have reported that there is a similar possibility

[19]. Furthermore, there is a possibility that a broken membrane accelerates the development of membrane fouling [20], which is a serious issue for MBR application in wastewater treatment. When membrane fouling becomes severe, membrane cleaning or replacement is needed, leading to an increase in the operation costs [21,22]. Membrane fouling is known to be influenced by various factors, including membrane characteristics [23,24], and the most important characteristic contributing to the fouling development among the membrane characteristics is considered to be membrane structure [25-30]. It is also likely that the membrane structure is affected by membrane deterioration.

Therefore, to further promote the application of MBRs to wastewater treatment technology in the future, it is necessary to consider not only the antifouling property of the membrane but also its mechanical durability. Therefore, it is expected that membranes with high mechanical durability for MBR operation would contribute to both reducing the microplastics production by themselves and removing the microplastics in wastewater.

I investigated the relationship between fouling development and membrane material using a laboratory-scale MBR with four kinds of materials in Chapter II: polyvinylidene fluoride (PVDF), polytetrafluoroethylene (PTFE), polyethersulfone (PES), and chlorinated polyvinyl chloride (CPVC); and revealed that the PVDF membrane showed the highest fouling propensity among them because of its vulnerability to the shearing stress caused by vigorous aeration in MBRs [20]. The PVDF membrane therefore breaks easily during MBR operation and hence risks becoming a microplastic source. However, the mechanical durability of the other three types of membranes has not been investigated. In addition, there have been no studies on the changes in membrane characteristics and morphology related to its mechanical durability during continuous MBR operation. Therefore, this study aimed to identify membrane characteristics

associated with mechanical durability and antifouling performance. The change in the membrane structure and properties of the pristine membranes and the membranes after the MBR operation of each membrane type (PES, CPVC, and PTFE) were compared.

III.2 Materials and methods

III.2.1 Flat-sheet membranes used in this study

The flat-sheet membranes of the three different materials; CPVC, PTFE, and PES, which are commercially available for use in actual wastewater treatment facilities worldwide, were used. Table 3-1 lists the physical and chemical characteristics of the pristine membrane material. The PES membrane structure is called “asymmetric” whereas those of the CPVC and PTFE membranes are called “symmetric,” depending on their fabrication process. The PES flat-sheet membrane module is commonly produced by a non-solvent induced phase separation (NIPS) method [31] with a non-woven polyester fabric as the support layer. The PES membrane used in this study had a finger-like structure with a skin layer (approximately 10 μm) forming only one side of the support layer. The CPVC flat-sheet membrane module is produced by the vapor-induced phase separation (VIPS) method [32] with a non-woven polyester fabric as the support layer. The CPVC membrane used had a sponge-like structure formed inside and on both sides of the support layer. In contrast, for PTFE flat-sheet membranes, a thin film of PTFE is produced in advance and stretched to induce micropores [33], then laminated with a non-woven polyester fabric [34]. Thus, the relationship between the membrane and support layer of the PTFE flat-sheet membrane is different from that of the other two membranes. The PTFE membrane used in this study had a structure with polymer nodules connected by thin fibers that were laminated on one side of the support layer. These flat-

Table 3-1 Membrane properties of the used membranes and transmembrane pressure (TMP) at the end of MBR operation in Chapter II [20]

Material		CPVC	PTFE	PES
Pore size	Nominal (μm)*	0.2	0.1	0.05
	Mean flow (μm)	0.17	0.16	< 0.04
Contact angle (°)		108	108	75
Thickness (μm)		162	132	208
Pure water permeability ($ml/cm^2 \cdot bar \cdot min$)		17.0	20.2	2.66
Intrinsic membrane resistance (R_i) (1/m)		3.96×10^{10}	2.83×10^{10}	3.00×10^{11}
Pore morphology		Symmetric	Symmetric	Asymmetric
TMP at the termination of operation (kPa)		38	36	37

* Information from manufacture

sheet membranes operated in laboratory-scale submerged MBRs using the common flux-step method [35-37] for almost two months in Chapter II [20].

III.2.2 Operation of laboratory-scale submerged membrane bioreactor experiment and membrane cleaning

In this study, the three types of membranes, which had used for the treatment experiment using MBRs in Chapter II [20], were successively used. The experiment was carried out in the lab-scale submerged MBRs for synthetic wastewater using the common flux-step method [35-37] for almost two months. The MBR had a 6.8L effective working volume. Activated sludge from a municipal wastewater treatment plant in Kumamoto City, Japan was used as a seed sludge. Synthetic wastewater was prepared with D-glucose, meat extract, polypeptone, and inorganic salts, and pH was adjusted at 7.2 ± 0.2 with 2 mol/L NaOH solution. The concentration of mixed liquor suspended solids (MLSS) was periodically measured and constantly maintained within 11000-12500 mg/L. The sludge retention time (SRT) was approximately 30 days. The trend in transmembrane pressure

(TMP), indicating membrane fouling development of the three kinds of membranes at the end of the experiment [20] is shown in Table 3-1. After the experiment, the membranes were subjected to physical and chemical cleaning. Physical cleaning involved wiping the membrane surfaces with soft sponge and flushing with tap water. Chemical cleaning was conducted by immersing the membranes in 5000 mg/L sodium hypochlorite solution and 10000 mg/L hydrochloric acid for 2 h each. The chemically cleaned membranes were rinsed with distilled water and dried at 50 °C in an oven, for analysis.

III.2.3 Analysis of membrane property

To evaluate the mechanical durability of the three types of membranes, the changes in membrane structural properties; including membrane thickness, pure water permeability, pore size, surface roughness, mechanical strength, and membrane morphology were investigated for the pristine and chemically cleaned membranes. The thickness of each membrane was measured using a digital micrometer (MDC-25MX, Mitutoyo Co., Japan). The membrane thickness was measured four times, and the average values and standard deviation were calculated. The pure water permeability was measured by filtration of distilled water as follows: the membranes were cut into small disks (diameter, 4.7 cm) and placed onto a dead-end filtration unit with a 13.8 cm^2 effective area (KP-47S, Toyo Roshi Kaisha Ltd., Japan). Distilled water was filtrated under constant pressure (0.5 bar) and temperature (25 °C), and the filtration time was measured at a filtration volume of 100 mL. The pure water permeability, L ($ml/cm^2 \cdot bar \cdot min$), was calculated using the following equation [25]:

$$L = \frac{Q}{A \times \Delta t \times \Delta P} \qquad (3-1)$$

where Q is the filtration volume (mL), A is the effective membrane area (cm^2), Δt is the filtration time (min), and ΔP is the applied TMP (bar). The measurement of pure water permeability was conducted twice; the average values and standard deviation were calculated. The pore size and distribution of membranes were measured using a capillary flow porometer (CFP-1200A, Porous Materials Inc., USA). This apparatus was used to determine the pore size diameter of the membrane by the liquid-gas displacement process. The membranes were cut into small disks with a diameter of 25 mm and were fully wetted with Galwick (Porous Materials Inc., USA) which has a low surface tension of 1.59×10^{-2} N/m. Then, the fully wetted membrane was placed in the sample chamber. The liquid was extruded from the membrane pores by gradually increasing the air pressure. The air flow rate extruded from membrane pores was measured by using a flow meter placed in the apparatus. The mean flow diameter, d expressed in μm, was calculated using following equation [38,39]:

$$d = \frac{C\gamma}{p} \qquad (3-2)$$

where C is a constant, γ is the Galwick surface tension, and p is the differential pressure when wet flow is one half of the dry flow. The surface roughness of the membranes was measured using a portable surface roughness tester (Surftest SJ-410, Mitutoyo Corp., Japan) at a contact force of 7.5×10^{-4} N, measurement speed of 0.5 mm/s with a diamond stylus tip, and a sampling length of 4 mm. The ten-point average roughness (R_z) for each membrane was calculated according to the Japanese Industrial Standard [40]. To evaluate the mechanical properties of the pristine and chemically cleaned membranes, the tensile strength and elongation break of the membranes were measured using a precision

universal testing machine (AGC-J, Shimadzu Co., Japan) in the following steps. All samples were cut into dumbbell shapes with a minimum part width of 15 mm and measured at a speed of 20 mm/min using 1000 N load cells. The membrane surface was observed using a scanning electron microscope (SEM, TM3030, Hitachi High-Technologies Co., Japan). Membrane morphology was evaluated by comparing the SEM images of the pristine and chemically cleaned membranes. The membranes were cut into small pieces so that they could be placed on the sample table and then sputtered with gold to produce electrical conductivity prior to SEM observation.

III.2.4 Filtration resistance measurement

I evaluated the fouling propensity of the three membranes by comparing their filtration resistances after MBR operation. The filtration resistance, R (1/m), was calculated using the following equation [41-43]:

$$R = \frac{\Delta P}{\mu J} \qquad (3-3)$$

where ΔP is the TMP difference (N/m^2), μ is the permeation viscosity (Ns/m^2), and J is the permeation flux (m/s). Next, the total permeation resistance, R_t, was defined as the sum of the following three components according to previous studies [44,45]:

$$R_t = R_m + R_r + R_{ir} \qquad (3-4)$$

where R_m (1/m) is the resistance of the chemically cleaned membrane after the MBR operation, R_r (1/m) is the reversible filtration resistance, and R_{ir} (1/m) is the irreversible

filtration resistance. R_r was generated by the reversible fouling development, which was caused by the cake layer formation on the membrane surface, and R_{ir} was generated by irreversible fouling caused by foulant deposition inside the membrane pores. Thus, R_r was calculated as the difference between resistance of the fouled membrane and that of the physically cleaned membrane, and R_{ir} was calculated as the difference between resistance of the physically cleaned membrane and that of the chemically cleaned membrane.

III.3 Results

IV.3.1 Changes in membrane property before and after membrane bioreactor operations

Figure 3-1 shows the membrane thickness of the pristine membrane and the chemically cleaned membranes after laboratory-scale MBR operation for almost two months. As shown in Fig.3-1, the thicknesses of the CPVC and PTFE membranes remained. However, it was judged that the membrane thickness of the PES membrane was slightly decreased after conducting the MBR operation by t-test ($p < 0.05$). Figure 3-2 shows the pure water permeabilities of the pristine and chemically cleaned membranes. The pure water permeability of the PES membrane significantly increased after MBR operation, as shown in Fig.3-2. The difference in the pure water permeabilities of the PES membrane before and after the MBR operation was 8.74 ml/cm^2・bar・min, which was more than four times the value of the pristine membranes. Whereas, the pure water permeabilities of CPVC and PTFE membranes clearly decreased 3.6 and 4.6 ml/cm^2・bar・min, respectively. These values are approximately 20% of those of the pristine membranes.

Table 3-2 shows the mean flow pore sizes of the pristine and chemically cleaned membranes. The mean flow pore size was commonly expressed as the averaged value of

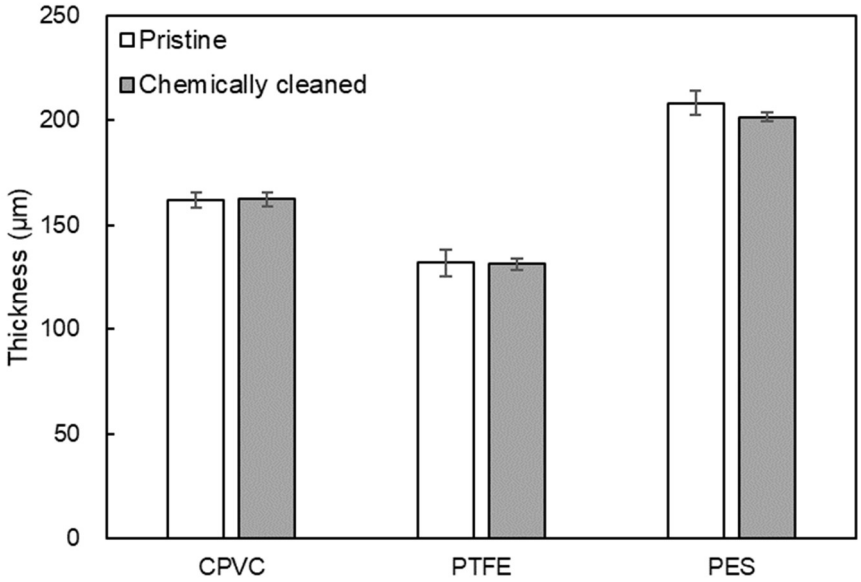

Fig. 3-1 Average values of membrane thicknesses of the pristine and chemically cleaned membranes. The bar indicates standard deviation.

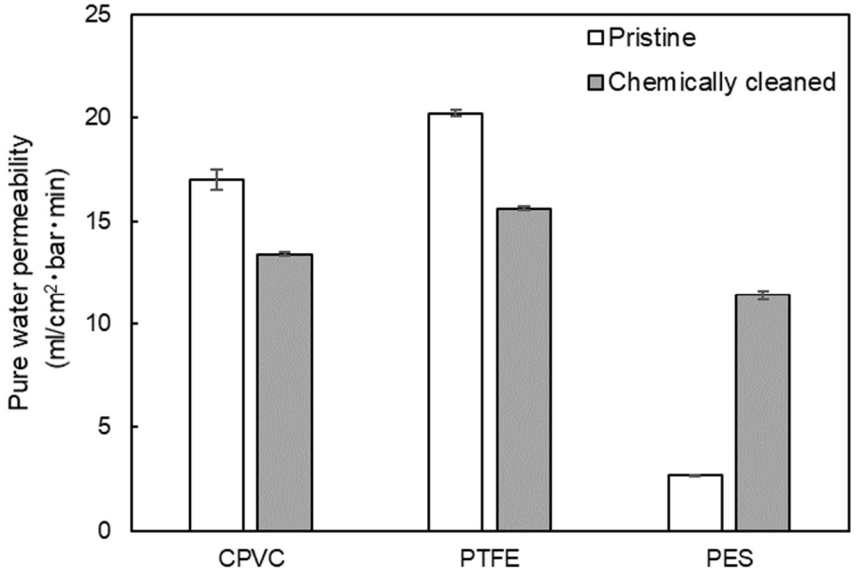

Fig. 3-2 Average values of pure water permeabilities of the pristine and chemically cleaned membranes. The bar indicates standard deviation.

Table 3-2 Pore size of the pristine and chemically cleaned membranes

Material	Mean flow pore size (μm)	
	Pristine	Chemically cleaned
CPVC	0.17 ± 0.01	0.16 ± 0.03
PTFE	0.16 ± 0.01	0.15 ± 0.01
PES	< 0.04	0.047 ± 0.002

* The average value and standard deviation are represented by two mesurements for each membrane.

the inhomogeneous pore sizes of the membrane. The membranes, except the pristine PES membrane, had a pore size distribution more than the detection limit (0.04 μm) of the capillary flow porometer used in this study. However, the pore size distribution range of the pristine PES membrane was smaller than the detection limit; therefore, the value of the pristine PES membrane was expressed as "< 0.04" in Table 3-2. The mean flow pore sizes of the pristine CPVC and PTFE membranes, which have symmetric membrane structures. were almost the same and one order of magnitude greater, respectively, than that of the PES membrane. Furthermore, CPVC and PTFE membranes showed the same mean flow pore sizes after the MBR operation. In contrast, it is likely that the mean flow pore size of PES membrane increased after the operation.

Figure 3-3 and Table 3-3 show the surface roughness line profiles and R_z values of the pristine and chemically cleaned membranes, respectively. As shown in Fig.3-3, the difference in the surface roughness between the pristine and chemically cleaned PES membranes was more pronounced than that of the other membranes. However, the surface roughness of the CPVC and PTFE membranes showed little change after MBR operation. In addition, it was revealed that CPVC membrane had the smoothest surface among the three membranes and remained even after the MBR operation resulting from R_z measurement (Table 3-3).

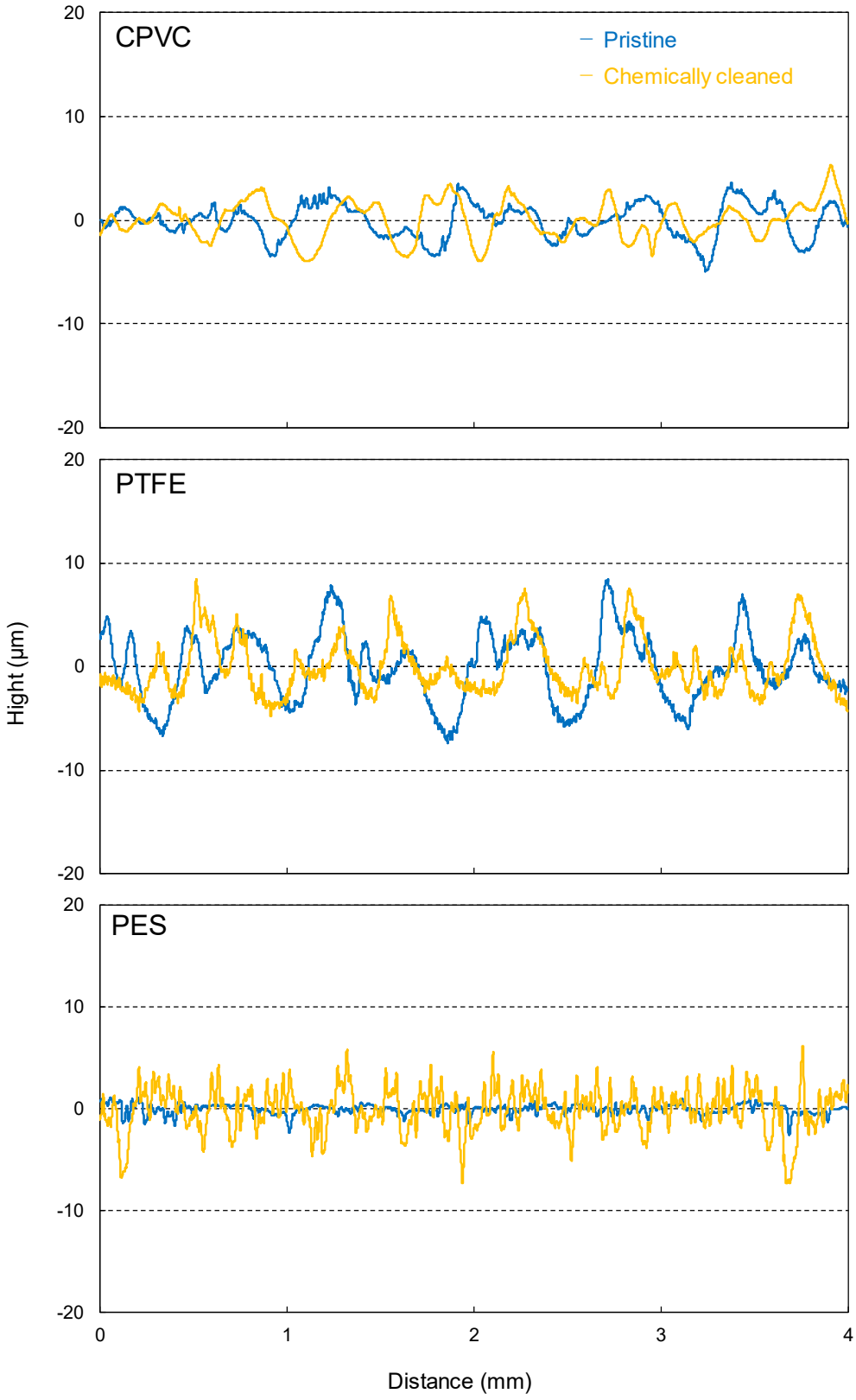

Fig. 3-3 Surface roughness line profiles of the pristine and chemically cleaned membranes.

Table 3-3 Surface roughness of the pristine and chemically cleaned membranes

Material	Rz (μm)	
	Pristine	Chemically cleaned
CPVC	5.9 ± 0.7	6.5 ± 0.7
PTFE	11.7 ± 0.8	11.9 ± 1.2
PES	2.77 ± 0.3	11.1 ± 1.2

* The average value and standard deviation are represented by the triple mesurements for each membrane.

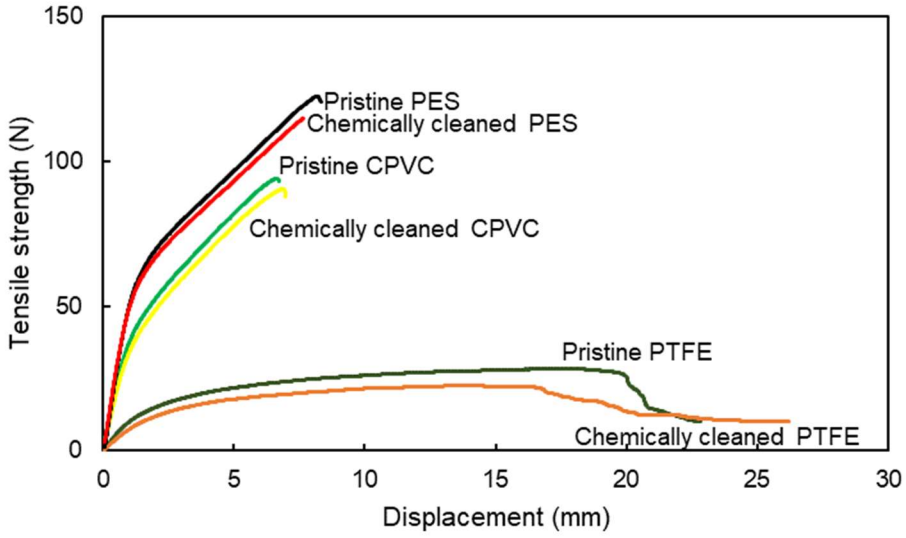

Fig. 3-4 Tensile strength curves of the pristine and chemically cleaned membranes.

Table 3-4 Mechanical properties of the pristine and chemically cleaned membranes

Material	Tensile strength at break (N/mm^2)		Elongation at break (%)	
	Pristine	Chemically cleaned	Pristine	Chemically cleaned
CPVC	42.4 ± 2.3	43.0 ± 0.01	9.6 ± 0.2	9.9 ± 0.1
PTFE	13.3 ± 1.1	10.5 ± 0.3	19.3 ± 0.7	19.8 ± 0.2
PES	40.6 ± 0.03	41.1 ± 1.3	12.6 ± 0.9	12.8 ± 0.8

* The average value and standard deviation are represented from the mesured data for each membrane shown in Fig. 3-4.

Figure 3-4 shows the tensile strength curves of the pristine and chemically cleaned membranes. The tensile strength curves of the CPVC and PES membranes

showed almost the same trend between the pristine and chemically cleaned membranes, indicating that the tensile strengths of these two membranes remained unchanged after the MBR operation. Contrarily, the tensile strength of the PTFE membrane appears to be slightly decreased by the operation. Table 3-4 shows the averaged tensile strength values and elongation at break of the pristine and chemically cleaned membranes. The tensile strength of each membrane showed the same tendency (Fig.3-4); however, the values of elongation at break were maintained for the all membranes through the MBR operation.

IV.3.2 Changes in membrane morphology before and after membrane bioreactor operations

To confirm the changes in the membrane morphology by the MBR operation, difference in membrane structure between the pristine membranes and chemically cleaned membranes was compared by SEM analysis (Fig. 3-5). As shown in Fig.3-5, there was no remarkable change in the surfaces of the PTFE and CPVC membranes. However, it was clear that the surface of the PES membrane ruptured significantly, indicating damage during MBR operation.

IV.3.3 Filtration resistances of the fouled membranes

Table 3-5 summarizes the values of filtration resistances (R_t, R_m, R_r, R_{ir}) and the ratio of each R_m, R_r, R_{ir} to R_t of the membranes after the MBR operation for two months, and Fig. 3-6 shows the intrinsic membrane resistance (R_i) and R_m. The PES membrane showed the highest R_t (28.9×10^{11} 1/m) although the difference between the PTFE membrane showing the lowest value (23.6×10^{11} 1/m) was small. The R_m ratios to R_t for all the membranes were less than 3%.

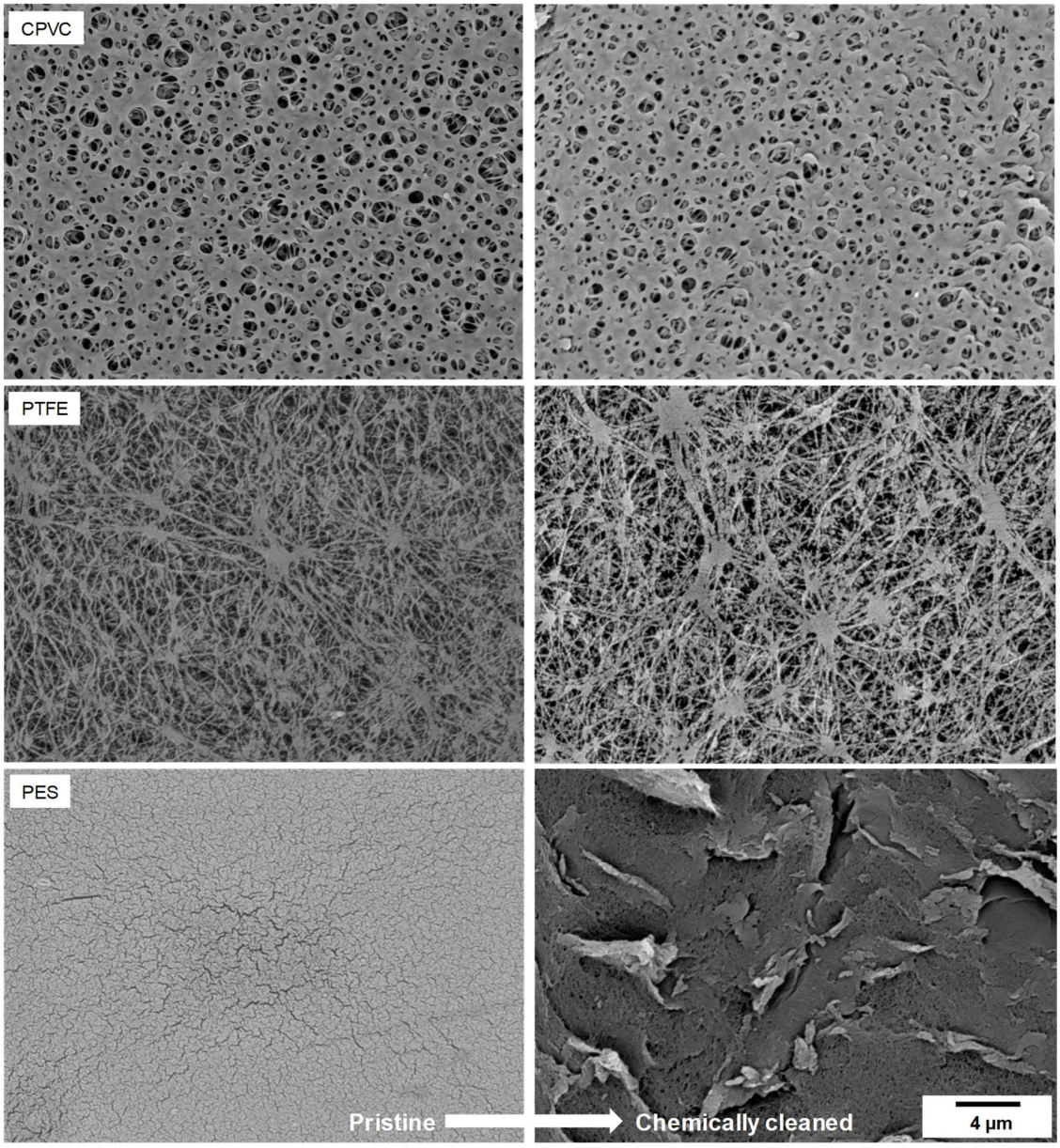

Fig. 3-5 SEM images of surface of the pristine and chemically cleaned membranes.

Table 3-5 Filtration resistance of the fouled membranes.

Material	Resitance ($\times 10^{11}$ 1/m)				Ratio (%)		
	R_t	R_m	R_r	R_{ir}	R_m/R_t	R_r/R_t	R_{ir}/R_t
CPVC	26.5	0.504	23.9	2.11	1.90	90.1	7.96
PTFE	23.6	0.435	20.2	2.95	1.84	85.6	12.5
PES	28.9	0.603	27.6	0.712	2.09	95.5	2.46

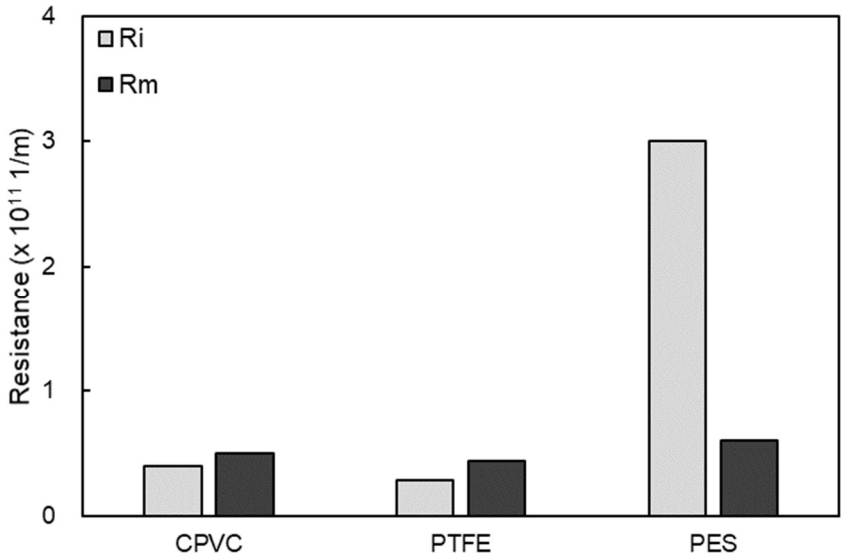

Fig. 3-6 Intrinsic membrane resistance (R_i) and the resistance of chemically cleaned membrane after the MBR operation (R_m).

The percentage of R_r in R_t was higher than that in R_m and R_{ir}, and 95.5% and 85.6% were obtained on the PES and PTFE membranes, respectively. R_r is generated by reversible fouling caused by formation of cake layer on the membrane surface. Therefore, to evaluate the membrane fouling property, comparing the R_r values of membranes would be appropriate. On the other hand, the percentage of R_{ir} in R_t was only 2.46% on the PES membrane to 12.5% on PTFE membrane, indicating contribution of R_{ir} to the membrane fouling property was not very high. R_{ir} is obviously influenced by the membrane structure because it causes pore plugging fouling inside the membrane [36]. As shown in Table 3-5, the R_{ir} value of PES (0.712×10^{11} 1/m) was obviously lower than those of CPVC (2.11×10^{11} 1/m) and PTFE (2.95×10^{11} 1/m), reflecting the difference in the membrane structure among these membranes, that is, the PES membrane has an asymmetric structure and the

other CPVC and PTFE membranes have a symmetric structure. This result may suggest that membranes with an asymmetric structure would cause less pore plugging fouling than the membrane with a symmetric structure. However, the difference between R_i and R_m of the PES membrane was the highest, as shown in Fig. 3-6.This result indicates the possibility that the change in the membrane structure of the PES membrane by the MBR operation was the most drastic among the membranes; thus, the mechanical durability of the PES membrane was lower than that of the CPVC and PTFE membranes used in this study.

III.4 DISCUSSION

In this study, with the recent concerns about environmental problems caused by microplastics, the mechanical durability of three-types and their antifouling performance were investigated. The membranes used in this study included CPVC, PTFE, and PES.

Results from Chapter II revealed that of the membranes studied, only the PVDF membrane was mechanically vulnerable to MBR operation, leading to a significant increase in measurement in TMP, which reflects antifouling capacity. The work presented here is this first study of mechanical durability in MBR operation.

SEM analysis revealed significant damage to the surface of the PES membrane during the MBR operation compared to the CPVC and PTFE membranes (Fig. 3-5). The rupture of the surface was likely caused by the shearing force with vigorous aeration for the MBR operation, as well as damage to PVDF membranes identified in Chapter II. This damage naturally caused an increase in the mean flow pore size (Table 3-2) and surface roughness (Table 3-3). The changes in these parameters indicate deterioration of membrane; however, they contribute to increase water permeability as shown in Fig. 3-2.

Therefore, the fouling development for PTFE membrane in the MBR operation could be reduced in Chapter II. In addition, the thickness and mechanical strength of the PES and the other membranes were maintained even after the MBR operation (Figs. 3-1 and 3-4), that is, it is expected that the MBR operation using the PES membrane will work well even after membrane deterioration. On the contrary, the difference between R_i and R_m of the PES membrane was significant as shown in Fig. 3-6, suggesting that the mechanical durability of the PES membrane was lower than those of CPVC and PTFE membranes. Thus, the PES membrane has the highest potential for production of microplastics and leads to environmental problems out of the three types used in this study.

The CPVC and PTFE membranes showed only a slight change in the membrane structure and membrane properties before and after MBR operation. The surface roughness of the CPVC membrane was slightly increased by the MBR operation, as indicated by the change in the R_z values (Table 3-3), although the difference between the SEM images of the pristine and chemically cleaned membranes was not clearly observed. Thus, it is a possible that the mechanical durability of CPVC is a slightly lower than that of PTFE. However, the R_z value of the chemically cleaned CPVC membrane was still much lower than that of the pristine PTFE membrane. The durability of these membranes may therefore be is slightly different. On the other hand, a slight decrease in the tensile strength of the PTFE membrane was observed (Table 3-4). This is likely due to the decrease in the adhesive strength by the slight peeling between the PTFE film and the non-woven fabric as the support layer.

The total filtration resistance for the three kinds of membranes used in this study, R_t, varied from 23.6×10^{11} 1/m of the PTFE membrane to 28.9×10^{11} 1/m of the PES membrane. The filtration resistance of every membrane was dominated by the reversible

fouling R_r caused by the cake layer formation, indicating that all membranes were of the "cake layer resistance dominant type." Fang et al. carried out a filtration test using activated sludge from a local municipal wastewater treatment plant on four types of membranes and concluded that the "cake layer resistance dominant type of membranes" would be suitable for MBRs [26]. Therefore, all three membranes used in this study seem to be appropriate for wastewater treatment by MBRs in terms of the membrane fouling. However, as mentioned above, it must be noted that membranes with low mechanical durability may have a high potential risk for generating microplastics through their deterioration in MBR operations. Therefore, the PES membrane was considered to have the highest potential risk for generating microplastics among the membranes used in this study.

III.5 CONCLUSIONS

In this study, the mechanical durability of the membrane in continuous MBR operation was investigated, as well as antifouling property, to explore the role of MBRs in the recent microplastic pollution problem in water environment. The mechanical durability of three kinds of membranes (CPVC, PTFE, PES) was evaluated by comparing the change in the membrane structure and membrane properties between their pristine membranes and the membranes after the MBR operation. Results shows substantial breakage on the surface of the PES membrane was observed by SEM analysis compared with the other CPVC and PTFE membranes, indicating that the PES membrane was more susceptible to damage by the shearing force with aeration for MBR than the other membranes. In addition, a sharp increase in the mean flow pore size and surface roughness caused by damage to the membrane was also confirmed. The PES membrane

was therefore considered to have the lowest mechanical durability of the membranes used in this study. On the other hand, the membrane structure and properties of the CPVC and PTFE membranes showed only a slight change before and after the MBR operation; the durability of these two kind membranes was therefore slightly different. All three membranes used in this study very similar antifouling performance, however the PES membrane may have a higher potential risk for generating microplastics because of a lower mechanical durability than the other membranes. To our knowledge, this is the first report of changes in the membrane characteristics and morphology related to mechanical durability and the membrane fouling problem.

REFERENCES

[1] X. Xiao, S. Liang, S. Wang, C. Chen and X. Huang, Current state and challenges of full-scale membrane bioreactor applications: a critical review, *Bioresour. Technol.*, 271, 473-481 (2019).

[2] J.R. Jambeck, R. Geyer, C. Wilcox, T.R. Siegler, M. Perryman, A. Andrady, R. Narayan and K.L. Law, Plastic waste inputs from land into the ocean, *Science*, 347, 768-771 (2015).

[3] S. Rezania, J. Park, M.F.F. Din, S.M. Taib, A. Talaiekhozani, K.K. Yadav and H. Kamyab, Microplastics pollution in different aquatic environments and biota: a review of recent studies, *Mar. Pollut. Bull.*, 133, 191-208 (2018).

[4] M.A. Browne, P. Crump, S.J. Niven, E. Teuten, A. Tonkin, T. Galloway and R. Thompson, Accumulation of microplastic on shorelines worldwide sources and sinks, *Environ. Sci. Technol.*, 45, 9175-9179 (2011).

[5] R. Dris, J. Gasperi, V. Rocher, M. Saad, N. Renault and B. Tassin, Microplastic

contamination in an urban area: a case study in Greater Paris, *Environ. Chem.*, 12, 592-599 (2015).

[6] I.E. Napper and R.C. Thomson, Release of synthetic microplastic plastic fibres from domstic washing machines: effects of fabric type and washing condition, *Mar. Pollut. Bull.*, 112, 39-45 (2016).

[7] N.L. Hartline, N.J. Bruce, S.N. Karba, E.O. Ruff, S.U. Sonar and P.A. Holden, Microfiber masses recovered from conventional machine washing of new or aged garments, *Environ. Sci. Technol.*, 50, 11532-11538 (2016).

[8] E. Hernandez, B. Nowack and D.M. Mitrano, Polyester textiles as a source of microplastics from households: a mechanistic study to understand microfiber release during washing, *Environ. Sci Technol.*, 51, 7036-7046 (2017).

[9] R.M. Blair, S. Waldron and C. Gauchotte-Lindsay, Average daily flow of microplastics through a tertiary wastewater treatment plant over a ten-month period, *Water Res.*, 163, 114909 (2019).

[10] J. Bayo, S. Olmos and J. López-Castellanos, Microplastics in an urban wastewater treatment plant: the influence of physicochemical parameters and environmental factors, *Chemosphere*, 238, 124593 (2020).

[11] C. Edo, M. González-Pleiter, F. Leganés, F. Fernández-Piñas and R. Rosal, Fate of microplastics in wastewater treatment plants and their environmental dispersion with effluent and sludge, *Environ. Pollut.*, 259, 113837 (2020).

[12] P. Masia, D. Sol, A. Ardura, A. Laca, Y.J. Borrell, E. Dopico, A. Laca, G. Machado-Schiaffino, M. Díaz and E. Garcia-Vazquez, Bioremediation as a promising strategy for microplastics removal in wastewater treatment plants, *Mar. Pollut. Bull.*, 156, 111252 (2020).

[13] S. Carr, J. Liu and A.G. Tesoro, Transport and fate of microplastic particles in wastewater treatment plants, *Water Res.*, 91, 174-182 (2016).

[14] F. Murphy, C. Ewins, F. Carbonnier and B. Quinn, Wastewater treatment works (WwTW) as a source of microplastics in the aquatic environment, *Environ. Sci. Technol.*, 50, 5800-5808 (2016).

[15] A.M. Mahon, B. O'Connell, M.G. Healy, I. O'Connor, R. Officer, R. Nash and L. Morrison, Microplastics in sewage sludge: effects of treatment, *Environ. Sci. Technol.*, 51, 810-818 (2017).

[16] A.A. Horton, A. Walton, D.J. Spurgeon, E. Lahive and C. Sevendsen, Microplastics in freshwater and terrestrial environments: evaluating the current understanding to identify the knowledge gaps and future research priorities, *Sci. Total Environ.*, 586, 127-141 (2017).

[17] M. Lares, M.C. Ncibi, M. Sillanpää and M. Silanpää, Occurrence, identification and removal of microplastic particles and fibers in conventional activated sludge process and advanced MBR technology, *Water Res.*, 133, 236-246 (2018).

[18] L. Li, D. Liu, K. Song and Y. Zhou, Performance evaluation of MBR in treating microplastics polyvinylchloride contaminated polluted surface water, *Mar. Pollut. Bull.*, 150, 110724 (2020).

[19] H. Ding, J. Zhang, H. He, Y. Zhu, D.D. Dionysiou, Z. Liu and C. Zhao, Do membrane filtration systems in drinking water treatment plants release nano/microplastics?, *Sci. Total Environ.*, 755, 142658 (2021).

[20] T. Sano, Y. Koga, H. Ito, L.V. Duc, T. Hama and Y. Kawagoshi, Effects of structural vulnerability of flat-sheet membranes on fouling development in continuous submerged membrane bioreactor, *Bioresour. Technol.*, 304, 123015 (2020).

[21] P. Le-Clech, V. Chen and T.A.G. Fane, Fouling in membrane bioreactors used in wastewater treatment, *J. Membr. Sci.*, 284, 17-53 (2006).

[22] W. Yang, N. Cicek and J. Llg, State-of-the-art of membrane bioreactors: worldwide research and commercial applications in North America, *J. Membr. Sci.*, 270, 201-211 (2006).

[23] S. Judd, The MBR Book: Principles and Applications of Membrane Bioreactors for Water and Wastewater Treatment 2nd ed., Elsevier, Oxford (2011).

[24] H. Matsuyama, T. Takahashi and M. Yasukawa, Present situation and future prospects of water treatment technology with membrane, *membrane*, 39, 209-216 (2014).

[25] J.-H. Choi, S.-K. Park and H.-Y. Ng, Membrane fouling in a submerged membrane bioreactor using track-etched and phase-inversed porous membranes, *Sep. Purif. Technol.*, 65, 184-192 (2009).

[26] H.H.P. Fang and X. Shi, Pore fouling of microfiltration membranes by activated sludge, *J. Membr. Sci.*, 264, 161-166 (2005).

[27] J.-H. Choi and H.Y. Ng, Effect of membrane type and material on performance of a submerged membrane bioreactor, *Chemosphere*, 71, 853-859 (2008).

[28] T. Miyoshi, K. Yuasa, T. Ishigami, S. Rajabzadeh, E. Kamio, Y. Ohmukai, D. Saeki, J. Ni and H. Matsuyama, Effect of membrane polymeric materials on relationship between surface pore size and membrane fouling in membrane bioreactors, *Appl. Surf. Sci.*, 330, 331-357 (2015).

[29] P. van der Marel, A. Zwijnenburg, A. Kemperman, M. Wessling, H. Tenmink, W. van der Meer, Influence of membrane properties on fouling in submerged membrane bioreactors, *J. Membr. Sci.*, 348, 66-74 (2010).

[30] L. Jin, S.L. Ong and H.Y. Ng, Comparison of foluing characteristics in different pore-

sized submerged ceramic membrane bioreactors, *Water Res.*, 44, 5907-5918 (2010).

[31] G.R. Guillen, Y. Pan, M. Li and E.M.V. Hoek, Preparation and characterization of membrane formed by nonsolvent induced phase separation: a review, *Ind. Eng. Chem. Res.*, 50, 3798-3817 (2011).

[32] T. Sano, S. Yamamoto, I. Kokubo, N. Murakami and K. Saito, Effects of Pluronic TR-702 on chlorinated poly(vinyl chloride) flat-sheet membranes prepared by water vapor induced phase separation, *membrane*, 46, 44-52 (2021).

[33] T. Kitamura, K. Kurumada, M. Tanigaki, M. Ohshima and S. Kanazawa, Formation mechanism of porous structure in polytetrafluoroethylene (PTFE) porous membrane through mechanical operations, *Polym. Eng. Sci.*, 39,2256-2263 (1999).

[34] T. Nittami, H. Tokunaga, A. Satoh, M. Takeda and M. Matsumoto, Influence of surface hydrophilicity on polytetrafluoroethylene flat sheet membrane fouling in a submerged membrane bioreactor using two activated sludges with different characteristics, *J. Membr. Sci.*, 463, 183-189 (2014).

[35] N. Shimada, J. Morita, M. Higashi, T. Kitagawa and J. Nakajima, Long term pilot MBR test for a newly development flat sheet membrane made from chlorinated polyvinyl chloride in treatment of kitchen wastewater from cafeteria, *J. Water Environ. Technol.*, 14, 329-340 (2016).

[36] M.R. Bilad, L. Marbelia, C. Laine and I.F.J. Vankelecom, A PVC-silica mixed-matrix membrane (MMM) as novel type of membrane bioreactor (MBR) membrane, *J. Membr. Sci.*, 493, 19-27 (2015).

[37] P. Le-Clech, B. Jefferson, I.S. Chang and S. Judd, Critical flux determination by the flux-step method in a submerged membrane bioreactor, *J. Membr. Sci.*, 227,82-93 (2003).

[38] A. Jena and K. Gupta, Advances in pore structure evaluation by porometry, *Chem.*

Eng. Technol., 33, 1241-1250 (2010).

[39] T. Marino, E. Blasi, S. Tornaghi, E.D. Nicolo and A. Fogoli, Polyethersulfone membranes prepared with Rhodiasolv ®Polaclean as water soluble green solvent, *J. Membr. Sci.*, 549, 192-204 (2018).

[40] Japanese industrial standards: Geometrical product specifications (GPS) – surface texture: profile method – teams, definitions and surface texture parameters, JIS B0601 (2013).

[41] I.S. Chang and C.H. Lee, Membrane filtration characteristics in membrane-coupled activated sludge system - the effect of physiological states of activated sludge on membrane fouling, *Desalination*, 120, 221-233 (1998).

[42] I. le Roux, H.M. Krieg, C.A. Yeates and J.C. Breytenbach, Use of chitosan as an antifouling agent in a membrane bioreactor, *J. Membr. Sci.*, 248, 127-136 (2005).

[43] T.-H. Bae and T.-H. Tak, Interpretation of fouling characteristics of ultrafiltration membranes during the filtration of membrane bioreactor mixed liquor, *J. Membr. Sci.*, 264, 151-160 (2005).

[44] J. Lee, W.-Y. Ahn, C.-H. Lee, Comparison of the filtration characteristics between attached and suspended growth microorganisms in submerged membrane bioreactor, *Water Res.*, 35, 2435-2445 (2001).

[45] T. Kurita, K. Kimura and Y. Watanabe, The influence of granular materials on the operation and membrane fouling characteristics of submerged MBRs, *J. Membr. Sci.*, 469, 292-299 (2014).

Chapter IV

Direct and indirect effects of membrane pore size on fouling development in a submerged membrane bioreactor with a symmetric chlorinated poly(vinyl chloride) flat-sheet membrane

---

IV.1 Introduction

Membrane bioreactors (MBRs) have been widely used for treating municipal and industrial wastewater because of their numerous advantages, including high-quality effluent, small footprint requirements, and ease of operation compared with conventional activated sludge systems, which use settling tanks [1-3]. MBRs also show high pollutant removal performance because suspended solids, including valuable microorganisms, remain inside the reactor [3]. Thus, MBRs have been widely adopted in a variety of wastewater treatment plants worldwide [4,5]. However, MBRs still have a critical issue of a decrease in water permeability caused by membrane fouling, similar to other water treatments by membranes. Membrane fouling is a phenomenon whereby suspended matter is deposited on the membrane surface and captured in membrane pores; as a result, the filtration resistance increases over time through the operation [3,6-8]. When critical membrane fouling is observed, membrane module cleaning and replacement are needed, leading to an increase in operating and maintenance costs [4,9]; therefore, the reduction of fouling development is still a major challenge for further application of MBRs in the future.

Numerous researchers have attempted to mitigate membrane fouling in MBRs, but an effective technique has not yet been established. The nature and degree of

membrane fouling are influenced by many factors, such as membrane properties [10], characteristics of feed water and activated sludge [5,11,12], and operating conditions [3,13]. The multiple effects of these factors further complicate membrane fouling phenomena [14,15]. In the case of membrane characteristics, previous studies reported that the membrane material, membrane morphology, surface hydrophilicity, surface charge, pure water permeability, pore size and distribution, surface porosity, membrane porosity, and surface roughness are important factors that influence the development of membrane fouling [16-26]. However, the relationship between the characteristics of the membrane material and fouling phenomena is still unclear. For instance, Miyoshi et al. investigated the relationship between membrane pore size and the development of membrane fouling using membranes made of different materials and a bench-scale MBR. They suggested that the optimal membrane pore size to prevent membrane fouling depends on the membrane material. For polyvinylidene fluoride (PVDF), the larger the pore size, the greater the degree of suppression, whereas the opposite result was obtained in the case of cellulose acetate butyrate (CAB) [23]. However, to date, only a few studies have investigated the relationship between membrane pore size and fouling phenomena by comparing membranes made from the same membrane material, which have similar membrane characteristics but different membrane pore sizes [20,21,26]. Jin et al. investigated the relationship between membrane pore size and membrane fouling using ceramic membranes with four different pore sizes and a laboratory-scale MBR. They found that the membrane with the smallest pore size exhibited the slowest membrane fouling, whereas the membrane with the largest pore size exhibited the fastest membrane fouling [21]. Nittani et al., however, obtained completely opposite results. They investigated the relationship between membrane pore size and membrane fouling using

symmetrical hydrophobic polytetrafluoroethylene (PTFE) membranes with different pore sizes and a laboratory-scale MBR and reported that the membrane with the smallest pore size exhibited the fastest membrane fouling [26]. These results also suggest that the relationship between membrane pore size and fouling propensity depends on the membrane material; thus, this relationship should be investigated using individual membranes made from the same material. Most membranes used in practical MBR plants are polymeric membranes prepared via the phase inversion method or stretching method [14], and membrane materials such as PVDF, PTFE, polyethersulfone (PES), chlorinated polyvinyl chloride (CPVC), and polyethylene (PE) are the most popular. In particular, flat-sheet membranes made of CPVC with non-woven polyester fabric as a support layer have been widely adopted in MBRs because of their excellent chemical and mechanical properties for MBR operation [27-31]. CPVC flat-sheet membranes are prepared via the vapor-induced phase separation (VIPS) method [24], and a symmetric pore structure is formed in and on the support layer. However, no study has investigated the relationship between the pore size of a CPVC flat-sheet membrane prepared via the VIPS method and the fouling propensity in MBRs.

Furthermore, it is considered that the membrane characteristics, including membrane pore size, not only depend on the membrane material but also interrelate with each other; for instance, a change in the membrane pore size can affect other membrane characteristics such as surface morphology and porosity, even in the same membrane material [32-36]. However, no study has examined the mutual relationships among the membrane characteristics and their effects on fouling phenomena. I believe that clarifying the relationship pore size and another characteristic of membrane and membrane fouling is necessary for establishing technique for mitigating membrane fouling.

In this study, CPVC flat-sheet membranes with four different pore sizes were prepared via the VIPS method to investigate the influence of the pore size of the CPVC membrane on membrane fouling in a laboratory-scale submerged MBR. In addition, the mutual relationship of membrane characteristics such as membrane pore size, surface porosity, and surface roughness was demonstrated by conducting batch experiments related to filtration resistance parameters, and the direct and indirect effects of membrane characteristics on fouling phenomena was examined.

IV.2 Materials and methods

IV.2.1 Materials

CPVC with a polymerization degree of approximately 800 was purchased from KANEKA Corp., Japan. Tetrahydrofuran (THF) and 2-propanol (IPA) were purchased from FUJIFILM Wako Pure Chemical Corp., Japan. Bovine serum albumin (BSA) was purchased from Jackson ImmunoReserach Laboratories Inc., USA.

IV.2.2 Membranes preparation with different pore sizes

A schematic diagram of a flat-sheet membrane preparation is shown in Fig. 4-1. The flat-sheet membrane was prepared via the VIPS method using non-woven polyester fabric as a support layer as follows. The non-woven polyester fabric was guided from an unwinding roll to a ink pan and dipped into a dope solution containing CPVC as a membrane polymer, THF as a solvent, and IPA as an additive. The dope solution was prepared with different concentrations of CPVC to create membranes with different pore sizes. The dipped non-woven fabric was exposed to water vapor atmosphere to solidify and form the membrane structure, guided to a drying furnace, and then wound using a

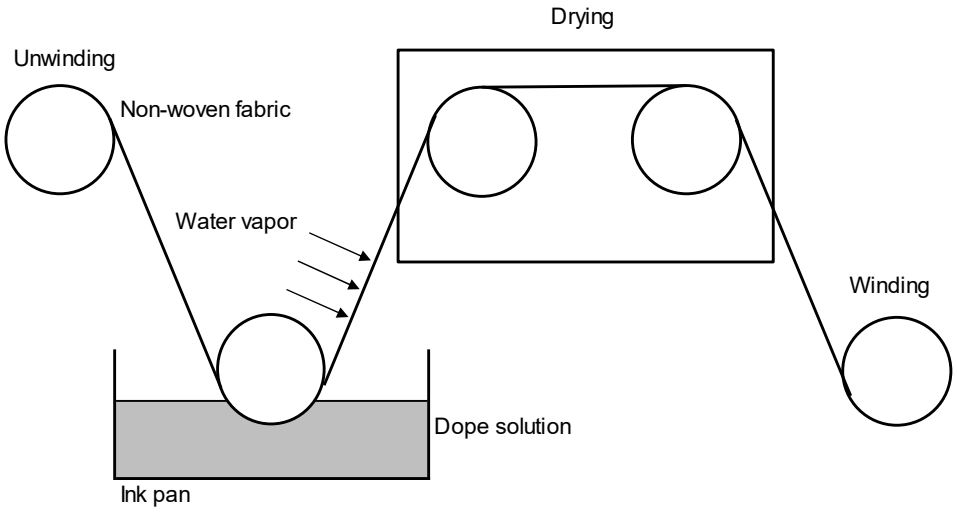

Fig. 4-1 Schematic diagram of membrane preparation via vapor induced phase separation (VIPS).

winding roll.

IV.2.3 Membrane module fabrication and setup of a laboratory-scale submerged membrane bioreactor

A membrane module was fabricated with each pore size of the CPVC flat-sheet membranes for application to MBRs. Two sheets of flat-sheet membranes were placed on both sides of a corrugated plastic plate with punched holes and fixed to a plastic frame of polyvinyl chloride by gluing the edges together. Each side of the flat-sheet membrane was separated from the corrugated plastic plate using polyester non-woven fabric spacers (Fig. 4-2). The effective filtration area of the membrane module was approximately 0.11 m^2 (0.19 m × 0.29 m × 2 sides).

The schematic of the laboratory-scale submerged MBR used in this study is shown in Fig. 4-3. The reactor was prepared for each membrane pore size. A total of four reactors were prepared in this study. All the reactors had a 6.8 L effective working volume

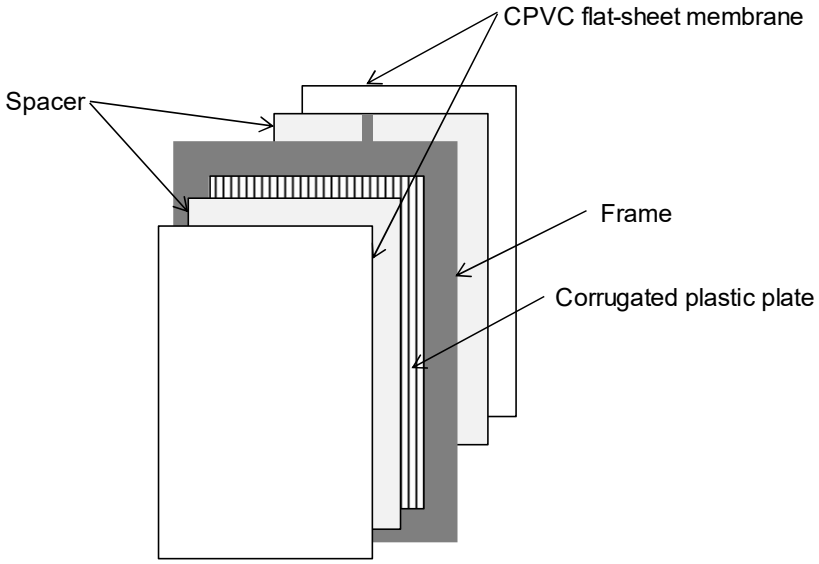

Fig. 4-2 Schematic of flat-sheet membrane module.

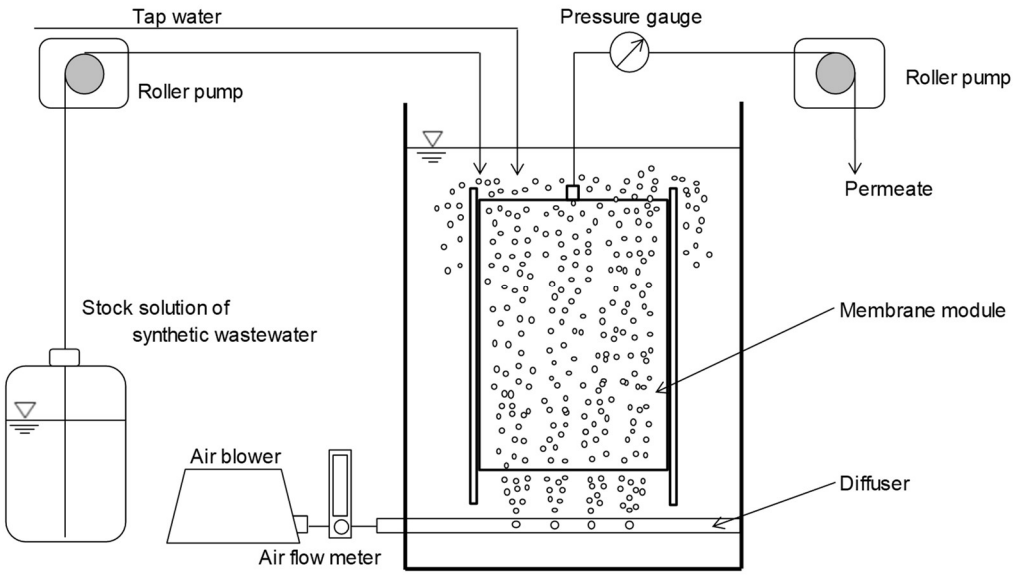

Fig. 4-3 Schematic figure of laboratory-scale submerged MBR apparatus.

and were made of clear polyvinyl chloride. A membrane module with each membrane was installed in each reactor. There were two roller pumps (MP-2000, Tokyo Rikakikai,

Co. Ltd., Japan) in the MBR. One roller pump was utilized, and the membrane filtrate was removed from the reactor. The filtration flux was constantly monitored and maintained by manually controlling the rotation speed of the roller pump. The other roller pump was utilized to feed synthetic wastewater from a stock solution vessel to the reactor. An air diffuser was installed in the reactor, and the air was supplied by an air pump with a pressure regulator (SCO-4-115L, Nippon Flow Cell Co., Japan) at 5 L/min to flow across both outside surfaces of the membrane modules. The transmembrane pressure (TMP) was periodically measured using a digital pressure gauge (GC31-174, Nagano Keiki Co. Ltd., Japan) to evaluate the degree of membrane fouling.

IV.2.4 Synthetic wastewater and membrane bioreactor operating condition

Before the operation, the dry membrane modules were immersed in ethanol for 10 min to saturate the modules with ethanol. Then, they were removed from ethanol and immersed in tap water for 30 min to replace ethanol with tap water. Activated sludge from a municipal wastewater treatment plant in Kumamoto City, Japan, was used as a seed sludge. Synthetic wastewater fed to each reactor by the roller pump. The synthetic wastewater was prepared with 250 mg/L D-glucose, 50 mg/L meat extract, 40 mg/L polypeptone, 50 mg/L K_2HPO_4, 20 mg/L $(NH_4)H_2PO_4$, 3.0 mg/L NaCl, 5.0 mg/L $MgSO_4 \cdot 7H_2O$, 2.5 mg/L $CaCl_2 \cdot 2H_2O$, and 0.5 mg/L $FeCl_3 \cdot 6H_2O$, and pH was adjusted at 7.2 ± 0.2 with 2 mol/L NaOH solution. The dissolved organic carbon (DOC) concentration in the synthetic wastewater was 120 mg/L, and the DOC removal efficiency was maintained at more than 98% in all reactors throughout the experiment. The concentration of mixed liquor suspended solids (MLSS) was measured periodically by drawing out an appropriate volume of the activated sludge (200-300 mL), in order to ensure that it

remained constant. The sludge retention time (SRT) was varied depending on the drawn volume of activated sludge, but was generally 30 days. The suspension liquids of all the reactors were removed and stirred every two days, and then returned to the reactors to equalize the MLSS concentration and characteristics of the suspension liquids in all the reactors. The operation was carried out at room temperature, the temperature in the reactors were not controlled but periodically monitored with a thermometer, and pH was manually adjusted at 7.2 with 2 mol/L NaOH solution per day.

A constant filtration flux mode was used. This mode is based on the general flux-step method to evaluate changes in the TMP [28,37,38]. In this study, MBR operation was repeated four times, and two filtration flux conditions were attempted for the all operations except the first operation, namely a basic flux of 0.3 $m^3/m^2 \cdot d$ (12.5 $L/m^2 \cdot h$), hydraulic retention time (HRT): 5 hours), which is a safety flux for common MBR operation in practical use and a higher flux of 0.5 $m^3/m^2 \cdot d$ (20.8 $L/m^2 \cdot h$, HRT: 3hours). The membrane modules were removed from the reactors at the end of each operation and cleaned using physical and chemical methods. Physical cleaning was carried out by wiping the membrane surfaces with a soft sponge and flushing with tap water. Chemical cleaning was carried out by immersing the membrane module into a 5000 mg/L sodium hypochlorite solution for 2 h. The cleaned membrane modules were returned to the reactors for subsequent operations.

IV.2.5 Analytical methods

IV.2.5.1 Characterization of prepared membranes

The pore size and distribution of membrane were determined using a capillary flow porometer (CFP-1200A, Porous Materials Inc., USA) [35,39]. The pure water

permeability through the membrane was measured by filtrating distilled water using a dead-end filtration unit with a 13.8 cm^2 effective area (KP-47S, Toyo Roshi Kaisha Ltd., Japan) and was calculated using the formula in previous literature [40,41]. The surface roughness of the membranes was measured using atomic force microscopy (AFM, AFM5100N, Hitachi High-Technologies Co., Japan) [34,42]. The measurements were conducted in the dynamic force mode using an SI-DF3P2 (spring constant = 2 N/m) cantilever with a silicon tip at room temperature in air. The scanned size was 5 μm × 5 μm. The membrane surface was observed using a scanning electron microscope (SEM, TM3030, Hitachi High-Technologies Co., Japan) to evaluate surface morphology [43,44] and the surface porosity. The surface porosity of the membranes was calculated by binarizing the SEM images. The binarized images were obtained using image processing software (Image J, National Institutes of Health, USA). The surface porosity was determined by the ratio of the open area to the total surface area of the binarized images [24].

IV.2.5.2 Characterization of suspension liquid in membrane bioreactor

The concentration of MLSS was measured with 100 mL of suspension liquid according to standard methods [45]. The concentration of DOC was measured using a total organic carbon analyzer (TOC-V, SHIMADZU Co., Japan) using the filtrated suspension liquid from a disposable membrane filter with a pore diameter of 0.45 μm (ADVANTEC Co., Japan). The rejection rate during the third and fourth operations was calculated using the following equation:

$$rejection\ rate\ (\%) = \left(1 - \frac{C_p}{C_s}\right) \times 100 \qquad (4-1)$$

where C_s and C_p are the concentrations of the DOC in the supernatant of the liquid suspension in the reactor and membrane filtrate, respectively.

The particle size distributions of the suspension liquid were measured with a laser differential scattering spectrometer (LA-950 V2-ADB, Horiba Co. Ltd, Japan).

IV.2.5.3 Measurement and evaluation of filtration resistance

The total filtration resistance R_t (1/m) of the fouled membrane from MBR operation is recognized as the sum of three types of resistances as follows:

$$R_t = R_r + R_{ir} + R_m \qquad (4-2)$$

where R_r (1/m) is the resistance as a result of reversible fouling (reversible filtration resistance), R_{ir} (1/m) is the resistance as a result of irreversible fouling (irreversible filtration resistance), and R_m (1/m) is the intrinsic membrane resistance.

Reversible fouling occurs owing to cake layer formation on the membrane surface. Here, the cake layer is mainly composed of two layers of soluble microbial products (SMP) and activated sludge. However, the SMP layer is sometimes referred to as the gel layer in some previous studies to distinguish it from the cake layer [46,47]. In this study, the reversible filtration resistance (R_r) was evaluated from only the resistance of the gel layer because the layer of the activated sludge is easily peeled from the membrane during aeration operation and taking out the reactor in the MBR. This approach does not affect the overall discussion, as the resistance of the gel layer makes up the majority of the resistance of the cake layer [48-50]. Meanwhile, irreversible fouling is commonly caused by foulant deposition inside the pores (R_{ir}) [25]. Reversible filtration resistance (R_r) was calculated as the difference between the resistance of the fouled

membrane flushed with tap water to remove the sludge layer and that of the membrane after physical cleaning which was carried out by wiping the membrane surface with a soft sponge flushing with tap water. Irreversible filtration resistance (R_{ir}) was calculated as the difference between the resistance of the pristine membrane and that of the membrane after physical cleaning.

In this study, R_r, R_{ir}, and R_m were measured using the following method, and R_t was calculated. The membranes were cut into small disks (4.7 cm in diameter) from the modules and placed on a dead-end filtration unit with an effective area of 13.8 cm^2 (KP-47S, Toyo Roshi Kaisha Ltd., Japan). Distilled water was filtrated under a constant pressure of 0.05 MPa, and the filtration flux was measured. Finally, the filtration resistance (R_r, R_{ir}, R_m) was calculated using the following equation according to Darcy's law [51-53]:

$$Filtration\ resistance\ (R_r, R_{ir}, R_m) = \frac{\Delta P}{\mu J} \qquad (4-3)$$

where ΔP is the difference in the TMP (N/m^2), μ is the filtration viscosity ($N \cdot s/m^2$), and J is the filtration flux (m/s).

In addition, the mechanism of fouling caused by pore plugging was also evaluated via dead-end batch filtration tests using BSA as a model foulant according to the following methods. BSA solutions (200 mL, 500 mg/L) were filtrated in the first and second batches, and 500 mL of the same solution was filtrated in the six subsequent batches using the membranes under a constant pressure of 0.05 MPa, and the membranes were physically cleaned after each batch. Physical cleaning was carried out by wiping the

membrane surfaces with a soft sponge flushing with tap water. The batch test was carried out eight times (total filtration volume of BSA solution: 3400 mL). The filtration resistance (R_f) was calculated from the measurement of pure water permeability after physical cleaning in each batch test. The resistance by pore plugging (R_p) was calculated using the following equation:

$$R_p = R_f - R_m \qquad (4-4)$$

IV.2.5.4 Gel layer observation

The surface appearance of fouled, physically cleaned and chemically cleaned membranes were observed using SEM. Membrane pieces were immediately placed after sampling in 4.0 % glutaraldehyde with a 0.2 M phosphate buffer solution at pH = 7.4 for 2 h at room temperature. Then, the membrane pieces were washed by immersion in the 0.2 M phosphate buffer solution at pH = 7.4 overnight at 4 °C. Afterward, the membrane pieces were dehydrated by immersion in a series of ethanol solutions of 50, 70, 80, 95, 100, 100 and 100 % concentration and dried for 30 min at room temperature. The dried membrane pieces were coated with gold prior to SEM observation.

IV.3 Results

IV.3.1 Preparation and characterization of chlorinated poly(vinyl chloride) membranes with different pore size

Table 4-1 lists the characteristics of the four CPVC membranes prepared in this study. The membranes were labelled M1, M2, M3, and M4 in ascending order of CPVC concentration in the dope solution during the preparation step. Figure 4-4 shows the pore

Table 4-1 Characteristics of the membranes prepared in this study

Sample name		M1	M2	M3	M4
Pore size	Mean flow pore size (μm)	0.08	0.31	0.57	1.70
	Bubble point pore size (μm)	0.14	0.59	0.89	3.41
	Half width $\times 10^{-2}$ (μm)	0.49	2.05	3.95	25.5
Surface roughness, RMS (nm)		12.1	39.5	82.9	137
Surface porosity (%)		11.0	30.0	39.4	43.7
Pure water permeability (ml/cm^2·bar·min)		7.14	50.3	98.4	446

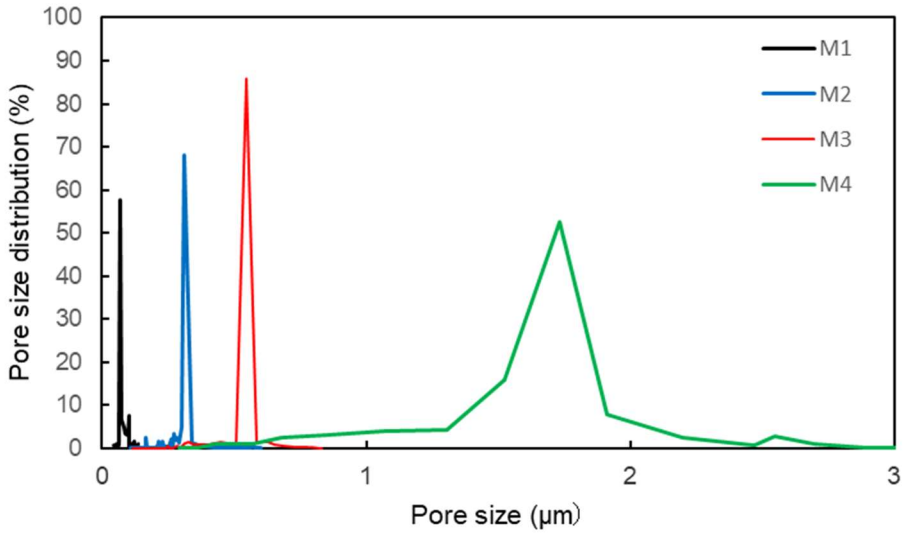

Fig. 4-4 Pore size distribution curves of prepared membranes.

size distribution curves of the membranes. In Table 4-1, the mean flow pore size is the average pore size, that is, 0.08, 0.31, 0.57, and 1.70 μm, and the bubble point pore size is the maximum pore size, that is, 0.14, 0.59, 0.89 and 3.41 μm. The half-width is half the width of the peak in the pore size distribution in Fig. 4-4. As shown in Fig.4-4, the M1, M2, and M3 membranes showed a narrow distribution range; in contrast, the M4 membrane showed a much broader distribution range than the other membranes. The difference in the pore size distribution of the membranes shown in Fig.4-4 is also quantitatively indicated in the half width presented in Table 4-1. The half widths of M1,

M2, and M3 membranes gradually increased from 0.49 $\times 10^{-2}$ μm to 3.95×10^{-2} μm, whereas that of M4 is a significantly large value of 25.5×10^{-2} μm. The pure water permeability of M4 is also a significantly large value of 446 ml/cm^2·bar·min compared with those of the other membranes. Figure 4-5 shows three-dimensional surface images of the membranes. Figure 4-6 shows the SEM images of the membranes.

As shown in Figs. 4-5 and 4-6, the M1 membrane seemed to have a smooth surface structure compared with those of the other membranes. This result was reflected by the quantitative characteristics of the membranes, such as pore size and surface roughness, and particularly the pure water permeability, as presented in Table 4-1; the difference in the characteristic values between M1 and M2 was approximately three to four times, but the difference between M2 and M3 was less than or almost two times. On the other hand, the surface porosity calculated from the SEM images showed a relatively small difference between the membranes, and increased gradually from M1 to M4 membranes. Table 4-2 shows the correlation coefficients of the membrane characteristics and pure water permeability. As shown in Table 4-2, the three parameters related to pore size (mean flow pore size, bubble point pore size and half width) naturally showed strong correlation mutually, and also had strong correlation with the pure water permeability (>0.99). In contrast, surface roughness and surface porosity showed relatively weak correlations of 0.93 and 0.72, respectively with the pure water permeability. Thus, it was considered that the pore size condition particularly influenced the pure water permeability of the membranes prepared in this study.

IV.3.2 Changes in transmembrane pressure and mixed liquor suspended solids concentrations in a laboratory-scale submerged membrane bioreactor

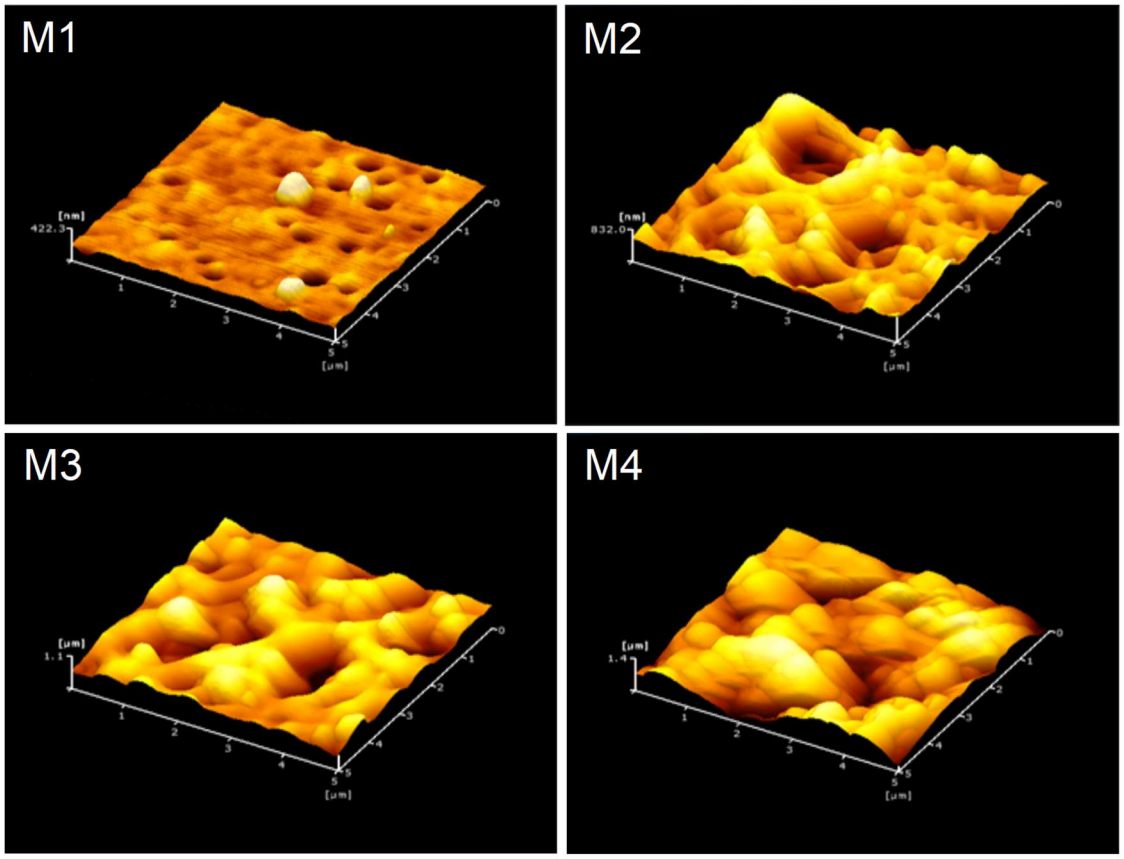

Fig. 4-5 Three-dimensional images of membrane surface of prepared membranes.

Figure 4-7 shows the changes in the TMP and MLSS concentrations over the entire experimental period. The MLSS concentration was maintained within the range of 11000-12500 mg/L, and the variation coefficient among the four reactors was within 0.25%. The particle size range of suspension liquid 5.0-500 μm. The temperature and pH of the suspension liquid were maintained at 23-25 °C and 6.9-7.1, respectively. The membrane modules were physically and chemically cleaned to restore flux at the end of each operation (after 20, 35, and 55 days).

The TMPs of the membranes, except M1 (mean flow pore size: 0.08 μm), were maintained at less than 5.0 kPa at basic flux (0.3 $m^3/m^2 \cdot d$) in all the operations. In particular, the TMP of M3 (mean flow pore size: 0.57 μm) was well maintained at less

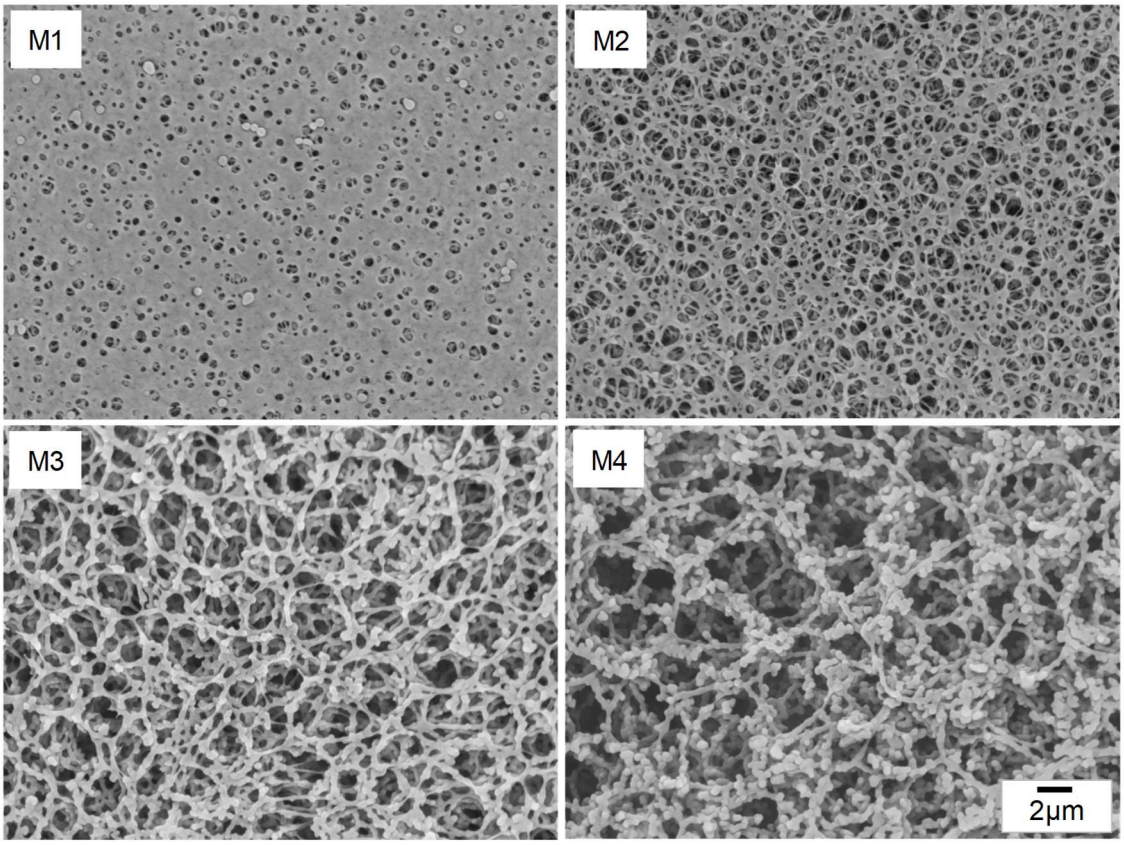

Fig. 4-6 SEM images of membrane surface of prepared membranes.

Table 4-2 Correlation coefficient of membrane characteristics and pure water permeability

	MFP	BPPS	HW	SR	SP
MFP	—				
BPPS	**0.997**	—			
HW	**0.987**	**0.995**	—		
SR	**0.960**	**0.935**	**0.903**	—	
SP	0.779	0.739	0.672	**0.904**	—
PWP	**0.995**	**0.999**	**0.998**	**0.929**	0.719

* MFP: Mean flow pore size, BPPS; Bubble point pore size, HW: Half width, SR: Surface roughness
SP: Surface porosity, PWP: Pure water permeability

than 3.0 kPa throughout the entire operation. Meanwhile, the TMP of M1 rapidly increased from the beginning and reached over 15 kPa within 10 days, and then became stable at approximately 20 kPa in each operation. For the other two membranes of M2

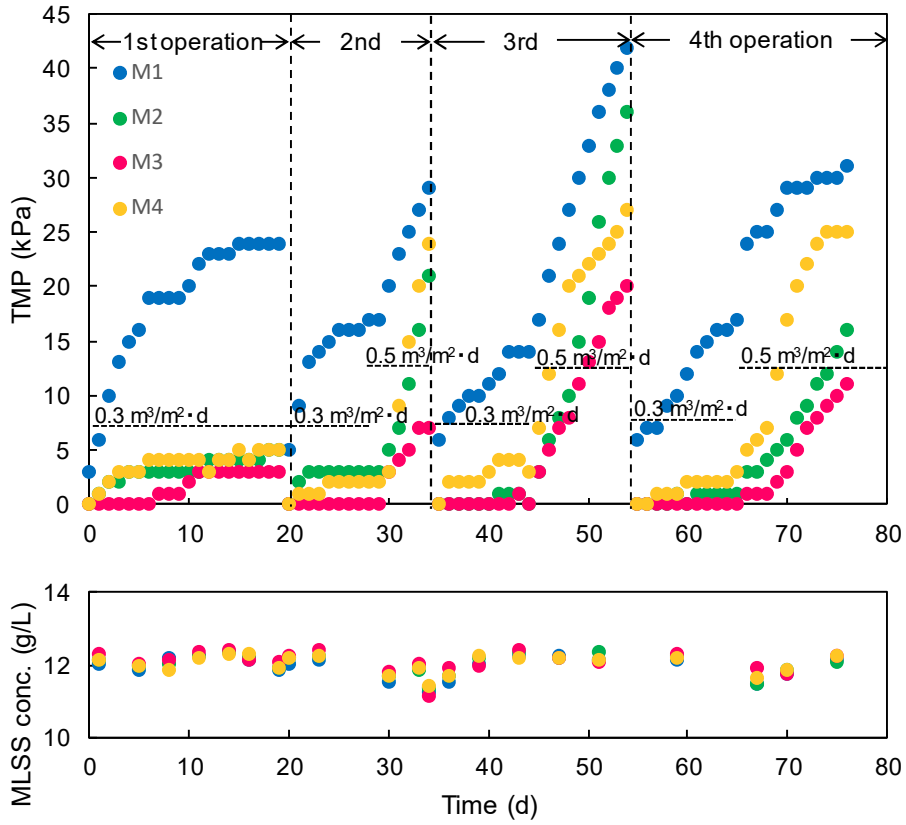

Fig. 4-7 Changes in TMP and MLSS concentrations during whole experimental period.

(mean flow pore size: 0.31 μm) and M4 (mean flow pore size: 1.7 μm), there was no significant difference in the TMP at basic flux in all the operations, although the TMPs of M4 were slightly higher than that of M2 in the first, third, and fourth operations. At a higher flux (0.5 $m^3/m^2 \cdot d$), all membranes showed an increasing trend at each operation. The TMPs of M1 and M4 drastically increased at the beginning of changing the flux and reached over 25 kPa within 4 days and 8 days, respectively, and the predetermined flux of 0.5 $m^3/m^2 \cdot d$ could not be maintained. The M2 membrane also showed a rapidly increasing trend in the second and third operations. In contrast, the M3 membrane showed a relatively gradual increasing trend compared with the other membranes, although the

TMP increased up to 20 kPa in the third operation. These results suggest that the two membranes of M1 and M4 that had the smallest and largest pore sizes, respectively were more vulnerable to fouling development compared with the other membranes (M2 and M3) that had intermediate pore sizes. In particular, it is suggested that the membrane with a pore size of less than 0.1 μm is not suitable for MBRs because of the increasing TMP trend of M1 membrane.

The DOC rejection rate was 99.6% or higher in all the membranes, indicating that there was no significant difference among the membranes. Thus, it is considered that the DOC rejection performance was almost constant regardless of the pore size for the membranes used in this study

IV.3.3 Filtration resistance of the fouled membranes

The distilled water flow rate was measured after the experiment to evaluate the deterioration of the filtration performance of the fouled membranes. Table 4-3 summarizes the parameter values related to the membrane resistance. The total filtration resistance (R_t), which is the sum of the intrinsic membrane resistance (R_m), reversible filtration resistance (R_r), and irreversible filtration resistance (R_{ir}), increased in the order of M1, M4, M2, and M3 membranes. This order coincided with the order of TMP development in the MBR, as mentioned above. The R_m values were lower than the other filtration resistances (R_r and R_{ir}), and the ratios of R_m to R_t (R_m / R_t) were less than 6% for all the membranes. As expected, the R_m / R_t ratio increased with increasing order of the membrane pore size. The R_{ir} values decreased with the increase in the pore size. In particular, the R_{ir} of the M1 membrane was much higher than those of the other membranes. In contrast, the R_r value was the highest for the M4 membrane, but the

Table 4-3 Relationship between mean flow pore size and parameters related to the filtration resistances of fouled membranes

Membrane	Mean flow pore size (μm)	Total filtration resistance (R_t) ($\times 10^{11}$ 1/m)
M1	0.08	18.2
M2	0.31	2.39
M3	0.57	2.16
M4	1.7	4.03

Membrane	Mean flow pore size (μm)	Intrinsic membrane resistance (R_m) ($\times 10^{11}$ 1/m)	Reversible filtration resistance (R_r) ($\times 10^{11}$ 1/m)	Irreversible filtration resistance (R_{ir}) ($\times 10^{11}$ 1/m)
M1	0.08	0.944	1.62	15.6
M2	0.31	0.134	1.42	0.839
M3	0.57	0.069	1.74	0.347
M4	1.7	0.015	3.92	0.093

Membrane	Mean flow pore size (μm)	Ratio of R_m to R_t (R_m/R_t) (%)	Ratio of R_r to R_t (R_r/R_t) (%)	Ratio of R_{ir} to R_t (R_{ir}/R_t) (%)
M1	0.08	5.2	8.9	85.9
M2	0.31	5.6	59.3	35.1
M3	0.57	3.2	80.7	16.1
M4	1.7	0.4	97.3	2.3

difference in the R_r value among the membranes was relatively small compared with the difference in the R_{ir} value. The ratio of R_{ir} to R_t (R_{ir} / R_t) was high for M3 and M4 membranes (80.7% and 97.3%, respectively); on the other hand, the ratio of R_{ir} to R_t (R_{ir} / R_t) was quite high for the M1 membrane. Thus, it is considered that the reversible resistance (R_r) is the dominant factor in the total resistance (R_t) of M3 and M4 membranes, which had a relatively moderate pore size; in contrast, the irreversible resistance (R_{ir}) was the dominant factor in the R_t of the M1 membrane, which had the smallest pore size.

The pore plugging resistance (R_p) of each membrane was determined through

filtration of the BSA solution to verify the relationship between R_{ir} and R_p. Figure 4-8 shows the change in the R_p value of each membrane with the filtration volume. The relative filtration volume for the horizontal axis in Fig. 4-8 is the ratio of the accumulated filtration volume of the batch test to the total filtration volume (3400 mL). As shown in Fig. 4-8, the R_p values of the M1 membrane were much higher than those of the other membranes, and clearly showed an increasing trend with the relative filtration volume. The R_p values of the M2 membrane also showed an increasing trend, but their levels were as small as those of M3 and M4 membranes. The R_p values of M3 and M4 membranes were almost the same and remained low throughout the batch test, although the value of M3 was slightly higher than that of M4. The descending order of the R_p values was M1, M2, M3, and M4, which is consistent with the results of the R_{ir} values. In addition, it was confirmed that the R_p value was close to that of R_{ir} for each membrane.

IV.3.4 Gel layer observation on the membrane surface

Figure 4-9 shows the surface appearance of the membranes at the end of the experiment (fouled), after physical cleaning (physically cleaned), and chemical cleaning (chemically cleaned) by SEM observation. As shown in the Fig. 4-9, the surfaces of the fouled membranes of M2, M3, and M4 were completely covered with a gel layer. However, the gel layer could not be observed in the M1 membrane. The gel layer-like layers on the surfaces of the M2-M4 membranes were confirmed visually and by touching. The gel layers were removed by physical cleaning of the M2 and M3 membranes, but not for M4. However, the gel layers of all the membranes, including M4, were finally removed by chemical cleaning; thus, it is considered that the fouling components developing the gel layer were almost completely removed by physical and

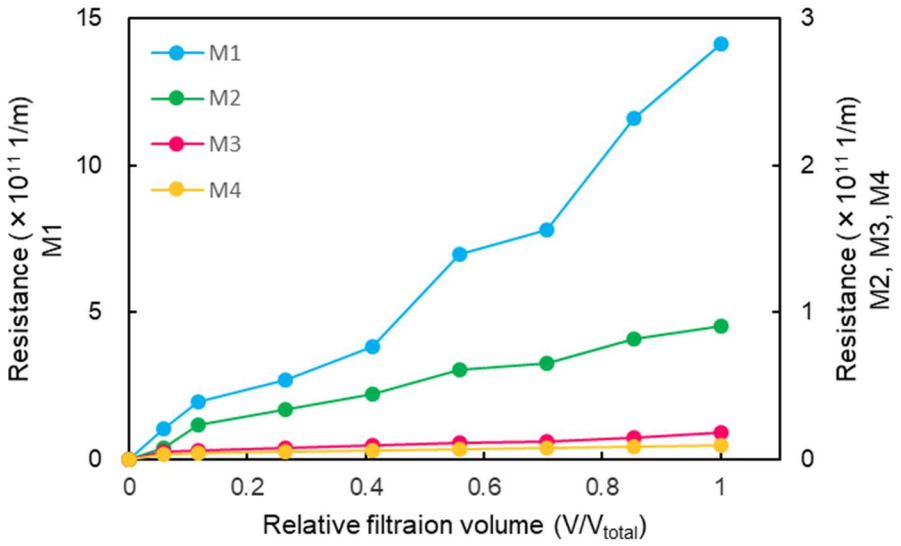

Fig. 4-8 Change in pore plugging fouling resistances with relative filtration volume of BSA solution.

chemical cleaning.

IV.4 Discussion

The principal objective of this study is to investigate the influence of the pore size of a membrane on fouling development in the operation of a submerged MBR using a CPVC flat-sheet membrane as a membrane material. However, it is easy to imagine that the change in the membrane pore size affects other membrane properties such as surface porosity and membrane roughness. For instance, increasing the pore size may simultaneously increase the surface roughness and surface porosity, and pure water permeability [20,33,54,55]. Furthermore, one of the membrane properties may not only be related to other membrane properties but may also affect the fouling phenomena indirectly; for instance, an increase in surface roughness may lead to more adhesion with the foulant in a liquid suspension and promote cake layer formation on the membrane surface. Therefore, in this study, original CPVC flat-sheet membranes with different pore

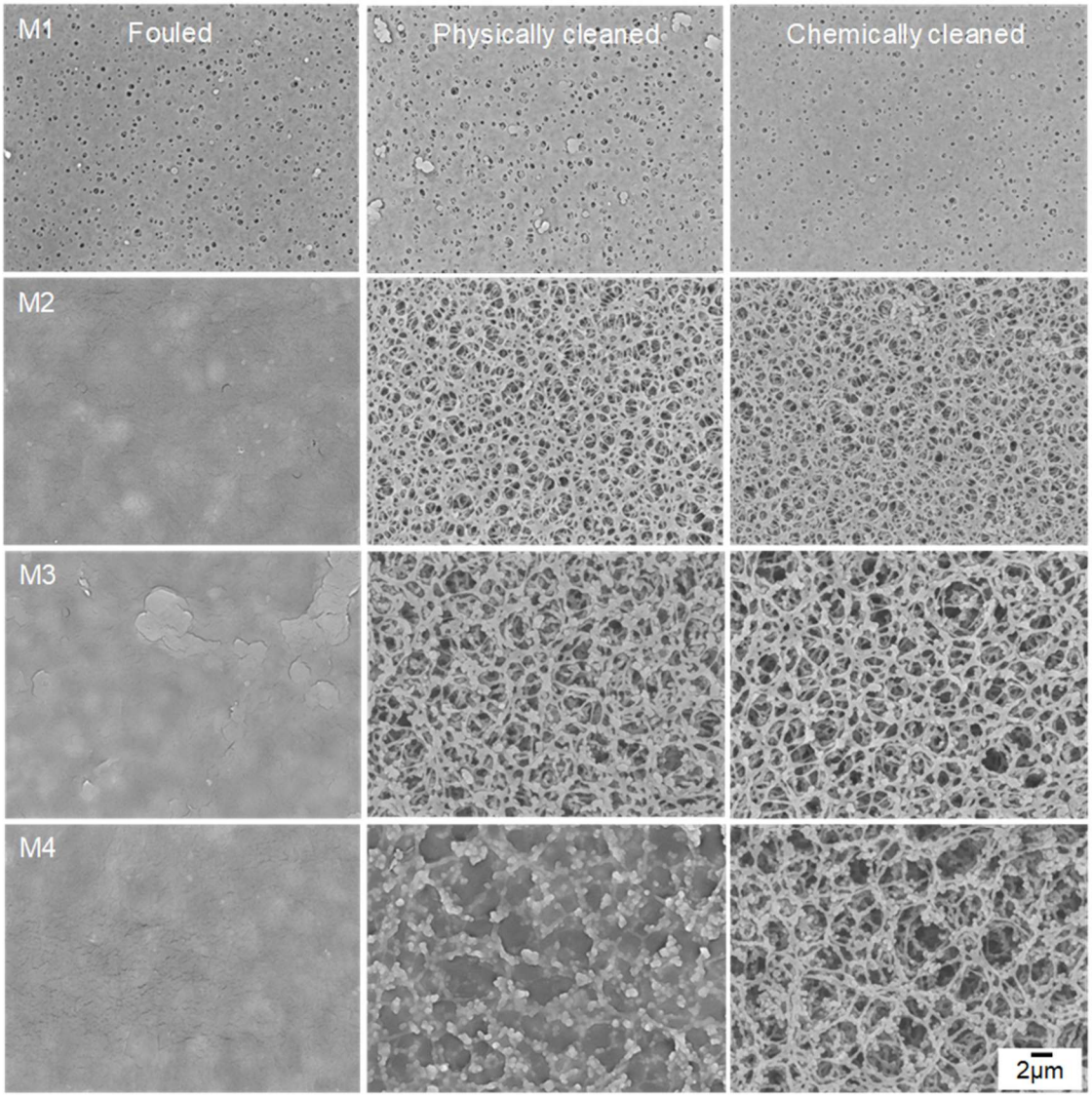

Fig. 4-9 SEM images of surfaces of fouled, physically cleaned and chemically cleaned membranes.

sizes were prepared using the VIPS method, and the effect of membrane pore size on fouling development was investigated. At the same time, the other membrane properties, namely surface roughness, surface porosity, and pure water permeability of prepared membranes, were measured to analyze their mutual relationship related to fouling phenomena based on batch tests in order to evaluate the reversible filtration resistance (R_r) and irreversible filtration resistance (R_{ir}) with the fouled membranes after the MBR

operation.

On the other hand, it is difficult to appropriately investigate and discuss the multiple effects of membrane properties on fouling phenomena because of the complexity and limitations of experiments. It is well-known that the membrane material [18], pure water permeability [56], surface porosity [20], surface roughness [19,21,25,57], and surface hydrophilicity [22,58,59] have significant effects on membrane fouling in MBRs. Choi et al. explained the effect of pure water permeability on fouling phenomena using a membrane with the same pore size; however, the effects of other membrane properties were ambiguous because other properties such as the membrane material and surface hydrophilicity were not unified [51]. Yamato et al. reported the effect of the membrane material on fouling development in an MBR and discussed the main contributing factor of fouling phenomena; however, their conclusion lacks appropriate explanation because they provided minimal description of the membrane properties other than the membrane material [18].

In this study, however, reversible filtration resistance (R_r) and irreversible filtration resistance (R_{ir}) were investigated using the fouled membranes through an MBR operation to determine the effect of membrane pore size on fouling phenomena in a complex way. That is, R_r is mainly caused by the formation of gel and cake layers related to membrane surface conditions such as surface roughness, and R_{ir} is as a result of pore plugging due to the adhesion of the foulant inside the membrane related to the membrane internal conditions such as pure water permeability. Thus, a combined analysis of membrane pore size, other membrane properties, R_r, R_{ir}, reduction in the performance of organic matter (DOC) by filtration, gel layer formation, and their effects on fouling phenomena would be very important to elucidate fouling phenomena.

First, R_{ir} value decreased as the membrane pore size increased, as presented in Table 4-3 and this result is consistent with the results of pore plugging resistance in the batch test using BSA as the model foulant, as shown in Fig. 4-8. Therefore, it was considered that the membrane pore size would directly affect irreversible fouling and R_{ir} value due to pore plugging phenomena inside membrane. Many studies have investigated the relationship between protein and membrane fouling in MBRs, and it was suggested that protein plays an important role in fouling development [23,60-65]. Miyoshi et al. conducted a batch filtration test using the supernatant of a mixed liquor suspension of activated sludge with hydrophobic PVDF membranes to confirm the major foulant [23]. They reported that the main mechanism of membrane fouling can be explained by pore plugging fouling caused by protein adherence to the internal pores of the membrane, and suggested that the smaller the membrane pore size, the easier it is for membrane fouling to occur because the size of protein is much smaller than that of a common membrane pore. These results are similar to the relationship between R_{ir} and membrane pore size obtained in this study. However, the results of TMPs in the MBR, which indicates fouling development, demonstrated a different tendency (Fig. 4-7), that is, the membranes with relatively intermediate pore sizes (0.31 μm and 0.57 μm) had a lower fouling propensity than those with smaller (0.08 μm) and larger (1.7 μm) pore sizes. Thus, it is clear that protein and protein-like compounds are the most contributors to irreversible fouling in MBRs.

Second, the reversible filtration resistance (R_r) increased with the pore size in the three membranes, except for the membrane with the smallest pore size (M1 membrane; 0.08 μm pore size), as presented in Table4-3. Meanwhile, Fig. 4-9 shows that the gel layer significantly covered the membrane surface of the fouled membranes, except M1. In

particular, the gel layer seems to remain a little for the M4 membrane even after physical cleaning, and this explains the change in the TMP, as shown in Fig. 4-7; that is, the increasing tendency of the TMP of M4 became much more remarkable in the 2nd to 4th operations after physical cleaning. From these results, it is considered that R_r reflects gel layer formation on the membrane surface. In addition, it is strongly suggested that gel layer formation is closely related to the surface roughness of the membrane, as demonstrated by the results in Table 4-1, indicating that the surface roughness is significantly high for M4. The morphological appearance may also support this conclusion. Several researchers have reported that membranes with smooth surfaces are desirable for mitigating membrane fouling [19,21,25,66]. Thus, the results in previous studies are considered to mainly highlight reversible membrane fouling on the membrane surface. In the meantime, surface roughness was obviously affected by membrane pore size. As shown in Table 4-2, the surface roughness showed relatively strong correlation with the parameters related to membrane pore size (>0.90). Therefore, it is considered that the membrane pore size would indirectly affect on reversible fouling and R_r value through the change of the surface roughness. After all, it was indicated that the membrane pore size affected both the reversible and irreversible fouling through the mutual relationship with other membrane characteristics such as the surface roughness.

This study demonstrated that reversible fouling exhibited an increasing trend, and irreversible fouling exhibited a decreasing trend with an increase in the membrane pore size. Meanwhile, it was indicated that the optimal pore size for suppressing membrane fouling would be in the range of 0.31-0.57 μm. Incidentally, considering the practical operation of MBRs for actual facilities treating real and various types of wastewater, irreversible or reversible fouling as well as total fouling development,

including both of them, are the most important issues. In other words, the optimal pore size (or range) for suppressing fouling development in MBRs and its mechanism are the most valuable pieces of information that need to be determined. Several studies have investigated the optimal pore size for suppressing fouling development in MBRs using membranes a symmetric structure, similar to the CPVC membrane used in this study [20,26]. van der Marel et al. investigated the influence of membrane pore size on membrane fouling in a pilot-scale MBR using four symmetric mixed cellulose ester (MCE) flat-sheet membranes [20]. They reported that membranes with pore sizes of 0.8 μm had superior performance in terms of fouling suppression compared with membranes with pore sizes of 0.1, 1.8, and 2.7 μm. Nittami et al. also investigated the influence of the pore size of membranes on fouling phenomena in a lab-scale MBR using symmetric PTFE flat-sheet membranes with three different pore sizes [26]. They reported that the optimum pore size of symmetrical flat-sheet membranes for suppressing fouling development is in the range of 0.5-1.0 μm. The results of these studies seem to agree with the results in this study; thus, it is assumed that the optimal range of membrane pore size for suppressing fouling development in an MBR seems to be similar when using symmetric structure membranes. However, it is still unclear why there is an optimum pore size or range. This can be considered to be well explained by the relationship between irreversible fouling, reversible fouling, and total fouling development, which is represented as irreversible filtration resistance, reversible filtration resistance, and total filtration resistance (or the apparent TMP in an MBR operation). For instance, in this study, the membrane with a pore size of 0.57 μm had the lowest TMP and total filtration resistance (R_t), as presented in Table 4-3. Here, the R_t value was obtained and added to the reversible filtration resistance (R_r), which mostly occurs on the membrane surface and

irreversible filtration resistance (R_{ir}), which mostly occurs inside the membrane; that is, the total fouling development and TMP in the MBR are exposed to a combination of fouling phenomena depending on R_r and R_{ir}. Further, the R_r value of the M2 membrane was smaller than that of M3, but the R_{ir} value was higher and R_t increased. In contrast, the R_{ir} value of M4 was much smaller than that of M3, but the R_r value was higher; furthermore, the R_{ir} values were much smaller than R_r, and the R_t value of M4 was almost double that of M3. As a result, the order of TMP development in the MBR shown in Fig. 4-7 is clearly demonstrated. To the authors' knowledge, this is the first report that explained the reason for the optimal pore size for suppressing fouling development in MBRs.

In the meantime, the above results and findings are all obtained from studies on symmetric structure membranes; therefore, they may not be applicable to asymmetric structure membranes because of the possibility that their membrane pore morphologies are different [20]. In addition, most of the polymeric membranes used in MBR plants have a pore size of 0.4 μm or less because a membrane with a large pore size has a poor solid–liquid separation performance [14]. However, the removal performances of DOC were not much different for membranes with pore sizes in the range of 0.08-1.7 μm, and hence, this does not raise significant concern. It is considered that the reason for this result is that the cake layer and gel layer on the membrane surface function as a dynamic membrane, as noted in previous studies [5,56,67-69].

IV.5 Conclusions

The influence of membrane pore size on fouling development was investigated using symmetric CPVC membranes with different pore sizes in submerged MBR. The

optimal pore size for suppressing fouling development was estimated to be in the range of 0.31-0.57 μm under the conditions in this study. It was strongly suggested that the irreversible fouling was caused by the capture of protein-like compounds inside the membrane; in contrast, reversible fouling was caused by gel and cake layers formed on the membrane surface. It was also indicated that the membrane pore size affected reversible and irreversible fouling through the mutual relationship with other membrane characteristics such as the surface roughness. Finally, the optimal membrane pore size for suppressing fouling development in MBRs is determined by the total filtration resistance caused by both irreversible and reversible fouling phenomena.

References

[1] L. Deng, W. Guo, H.H. Ngo, H. Zhang, J. Wang, J. Li, S. Xia and Y. Wu, Biofouling and control approaches in membrane bioreactors, *Bioresour. Technol.*, 221, 656-665 (2016).

[2] V. Jegatheesan, B.K. Pramanik, J. Chen, D. Navaratna, C.Y. Chang and L. Shu, Treatment of textile wastewater with membrane bioreactor: a critical review, *Bioresour. Technol.*, 204, 202-212 (2016).

[3] F. Meng, S. Zhang, Y. Oh, Z. Zhou, H.S. Shin and S.R. Chae, Fouling in membrane bioreactors: an updated review, *Water Res.*, 147, 393-402 (2017).

[4] P. Le-Clech, V. Chen and T.A.G. Fane, Fouling in membrane bioreactors used in wastewater treatment, *J. Membr. Sci.*, 284, 17-53 (2006).

[5] F. Meng, S.-R. Chae, A. Drews, M. Kraume, H.-S. Shin and F. Yang, Recent advances in membrane bioreactors (MBRs): membrane fouling and membrane material, *Water Res.*, 43, 1489-1512 (2009).

[6] Y. Long, G. Yu, L. Dong, Y. Xu, H. Lin, Y. Deng, X. You, L. Yang and B.-Q. Liao, Synergistic fouling behaviors and mechanisms of calcium ions and polyaluminum chloride associated with alginate solution in coagulation-ultrafiltration (UF) process, *Water Res.*, 189, 116665 (2021).

[7] M. Wu, Y. Chen, H. Lin, L. Zhao, L. Shen, R. Li, Y. Xu, H. Hong and Y. He, Membrane bioreactor caused by biological foams in a submerged membrane bioreactor: mechanism insights, *Water Res.*, 181, 115932 (2020).

[8] J. Teng, M. Zhang, K.-T. Leung, J. Chen, H. Hong, H. Lin and B.-Q. Liao, A unified thermodynamic mechanism underlying fouling behaviors of soluble microbial products (SMPs) in a membrane bioreactor, *Water Res.*, 149, 477-487 (2019).

[9] W. Yang, N. Cicek and J. Ilg, State-of-the-art of membrane bioreactors: worldwide research and commercial applications in North America, *J. Membr. Sci.*, 270, 201-211 (2006).

[10] I.S. Chang, P.L. Clech, B. Jefferson and S. Judd, Membrane fouling in membrane bioreactors for wastewater treatment, *J. Environ. Eng.*, 128, 1018-1029 (2002).

[11] Z. Wang, J. Ma, C.Y. Tang, K. Kimura, Q. Wang and X. Han, Membrane cleaning in membrane bioreactors: A review, *J. Membr. Sci.*, 468, 276-307 (2014).

[12] L.-G. Shen, Q. Lei, J.-R. Chen, H.-C. Hong, Y.-M. He and H.-J. Lin, Membrane fouling in a submerged membrane bioreactor: impacts of floc size, *Chem. Eng. J.*, 269 328-334 (2015).

[13] A. Ding, H. Liang, G. Li, N. Derlon, I. Szivak, E. Morgenroth and W. Pronk, Impact of aeration shear stress on permeate flux and fouling layer properties in a low pressure membrane bioreactor for the treatment of grey water, *J. Membr. Sci.*, 510, 382-390 (2016).

[14] S. Judd, The MBR Book: Principles and Applications of Membrane Bioreactors for

Water and Wastewater Treatment, second edition, Elservier, Oxford, 2011.

[15] H. Matsuyama, T. Takahashi and M. Yasukawa, Present situation and future prospects of water treatment technology with membrane, *membrane*, 39, 209-216 (2014).

[16] C.-C. Ho and A.L. Zydney, Effect of membrane morphology on the initial rate of protein fouling during microfiltration, *J. Membr. Sci.*, 155, 261-275 (1999).

[17] H.H.P. Fang and X. Shi, Pore fouling of microfiltration membranes by activated sludge, *J. Membr. Sci.*, 264, 161-166 (2005).

[18] N. Yamato, K. Kimura, T. Miyoshi and Y. Watanabe, Difference in membrane fouling in membrane bioreactors (MBRs) caused by membrane polymer materials, *J. Membr. Sci.*, 280, 911-919 (2006).

[19] J.-H. Choi and H.Y. Ng, Effect of membrane type and material on performance of a submerged membrane bioreactor, *Chemosphere*, 71, 853-859 (2008).

[20] P. van der Marel, A. Zwijnenburg, A. Kemperman, M. Wessling, H. Tenmink and W. van der Meer, Influnece of membrane properties on fouling in submerged membrane bioreactors, *J. Membr. Sci.*, 348, 66-74 (2010).

[21] L. Jin, S.L. Ong and H.Y. Ng, Comparison of foluing characteristics in different pore-sized submergd ceramic membrane bioreactors, *Water Res.*, 44, 5907-5918 (2010).

[22] T. Nittami, H. Tokunaga, A. Satoh, M. Takeda and K. Matsumoto, Influence of surface hydrophilicity on polytetrafluoroethylene flat sheet membrane fouling in a submerged membrane bioreactor using two activated sludges with different characteristics, *J. Membr. Sci.*, 463, 183-189 (2014).

[23] T. Miyoshi, K. Yuasa, T. Ishigami, S. Rajabzadeh, E. Kamio, Y. Ohmukai, D. Saeki, J. Ni and H. Matsuyama, Effect of membrane polymeric materials on relationship between surface pore size and membrane fouling in membrane bioreactors, *Appl. Surf.*

Sci., 330, 331-357 (2015).

[24] M. Higashi, J. Morita, N. Shimada and T. Kitagawa, Long-term-hydrophilic flat-sheet microfiltration membrane made from chlorinated poly (vinyl chloride), *J. Membr. Sci.*, 500, 180-189 (2016).

[25] T. Tsuyuhara, Y. Hanamoto, T. Miyoshi, K. Kimura and Y. Watanabe, Influence of membrane properties on physically reversible and irreversible fouling in membrane bioreactors, *Water Sci. Technol.*, 61, 2235-2240 (2010).

[26] T. Nittami, T. Hitomi, K. Matsumoto, K. Nakamura, T. Ikeda, Y. Setoguchi and M. Motoori, Comparison of polytetrafluoroethylene flat-sheet membranes with different pore size in application to submerged membrane bioreactor, *membranes*, 2, 228-236 (2012).

[27] M. Tokushima, Development for energy-saving MBR technology, *membrane*, 37, 235-239 (2012).

[28] N. Shimada, J. Morita, M. Higashi, T. Kitagawa and J. Nakajima, Long term pilot MBR test for a newly development flat sheet membrane made from chlorinated polyvinyl chloride in treatment of kitchen wastewater from a cafeteria, *J. Water Environ. Technol.*, 14, 329-340 (2016).

[29] T. Uesaka, Membrane separation: MBR, *Kagakukougaku*, 73, 79-82 (2009).

[30] D.S. Kim, J.S. Kang and Y.M. Lee, The influence of membrane surface porosities on fouling in a membrane bioreactor for wastewater treatment, *Sep. Sci. Technol.*, 39, 833-854 (2005).

[31] T. Sano, Y. Koga, H. Ito, L. Van Duc, T. Hama and Y. Kawagoshi, Effects of structural vulnerability of flat-sheet membranes on fouling development in continuous submerged membrane bioreactors, *Bioresour. Technol.*, 304, 123015 (2020).

[32] J.S. Kang, K. Kim and Y.M. Lee, Preparation of microporous chlorinated poly(vinyl chloride) membrane in fabric and the characterization of their pore sizes and pore-size distributions, *J. Appl. Polym. Sci.*, 86, 1195-1202 (2002).

[33] M.-H. Xu, R. Xie, X.-J. Ju, W. Wang, Z. Liu and L.-Y. Chu, Antifouling membranes with bi-continuous porous structures and high fluxes prepared by vapor-induced phase separation, *J. Membr. Sci.*, 611, 118256 (2020).

[34] Q, Zhao, R. Xie, F. Luo, Y. Faraj, Z. Liu, X.-J. Ju, W. Wang and L.-Y. Chu, Preparation of high strength poly(vinylidene fluoride) porous membranes with cellular structure via vapor-induced phase separation, *J. Membr. Sci.*, 549, 151-164 (2018).

[35] T. Marino, E. Blasi, S. Tornaghi, E.D. Nicolo and A. Figoli, Polyethersulfone membranes prepared with Rhodiasolv® Polarclean as water soluble green solvent, *J. Membr. Sci.*, 549, 192-204 (2018).

[36] T. Sano, S. Yamamoto, I. Kokubo, N. Murakami and K. Saito, Effects of Pluronic TR-702 on chlorinated poly(vinyl chloride) flat-sheet membranes prepared by water vapor induced phase separation, *membrane*, 46, 44-52 (2021).

[37] L. Marbelia, M.R. Bilad, A. Piassecka, P.S. Jishna, P.V. Nailk and I.F.J. Vankelecom, Study of PVDF asymmetric membranes in a high-throughput membrane bioreactor (HT-MBR): influence of phase inversion parameters and filtration performance, *Sep. Purif. Technol.*, 162, 6-13 (2016).

[38] P. Le-Clech, B. Jefferson, I.S. Chang and S.J. Judd, Critical flux determination by the flux-step method in a submerged membrane bioreactor, *J. Membr. Sci.*, 227, 81-93 (2003).

[39] A. Jena and K. Gupta, Advances in pore structure evaluation by porometry, *Chem. Eng. Technol.*, 33, 1241-1250 (2010).

[40] C.H. Loh, R. Wang, L. Shi and A.F. Fang, Fabrication of high performance polyehersulfone UF hollow fiber membranes using amphiphilic Pluronic block copolymers as pore-forming additives, *J. Membr. Sci.*, 380, 114-123 (2011).

[41] J. Wu, M. Xia, Z. Li, L. Shen, R. Li, M. Zhang, Y. Jiao, Y. Xu and H. Lin, Facile preparation of polyvinylidene fluoride substrate supported thin film composite polyamide nanofiltration: effect of substrate pore size, *J. Membr. Sci.*, 638, 119699 (2021).

[42] B. Liu, C. Chen, W. Zhang, J. Crittenden and Y. Chen, Low-cost antifouling PVC ultrafiltration membrane fabrication with Pluronic F127: effect of additives on properties and performance, *Desalination*, 307, 26-33 (2012).

[43] S. Xu, Q. Gao, C. Zhou, J. Li, L. Shen and H. Lin, Improved thermal stability and heat-aging resistance of silicone rubber via incorporation of UiO-66-NH_2, *Mater. Chem. Phys.*, 274, 125182 (2021).

[44] B. Chen, H. Xie, L. Shen, Y. Xu, M. Zhang, H. Yu, R. Li and H. Lin, Electroless Ni-Sn-P plating to fabricate nickel alloy coated polypropylene membrane with enhanced performance, *J. Membr. Sci.*, 640, 119820 (2021).

[45] APHA, *Standard Method for the Examination of Water and Wastewater*, 20th ed., American Public Health Association, Washington, DC, 1998.

[46] Z. Wang, Z. Wu, X. Yin and L. Tian, Membrane fouling in a submerged membrane bioreactor (MBR) under sub-critical flux operation: membrane foulant and gel layer characterization, *J. Membr. Sci.*, 325, 238-244 (2008).

[47] D. Okamura, Y. Mori, T. Hashimoto and K. Hori, Identification of biofoulant of membrane bioreactors in soluble microbial products, *Water Res.*, 43, 4356-4362 (2009).

[48] H. Nagaoka, S. Ueda and A. Miya, Influence of bacterial extracellular polymers on the membrane separation activated sludge process, *Water Sci. Technol.*, 34, 165-172

(1996).

[49] M. Zhang, W. Peng, J. Chen, Y. He, L. Ding, A. Wang, H. Lin, H. Hong, Y. Zhang and H. Yu, A new insight into membrane fouling mechanism in submerged membrane bioreactor: osmotic pressure during cake layer filtration, *Water Res.*, 47, 2777-2786 (2013).

[50] M. Zhang, H. Lin, L. Shen, B.-Q. Liao, X. Wu and R. Li, Effect of calcium ions on fouling properties of alginate solution and its mechanisms, *J. Membr. Sci.*, 525, 320-329 (2017).

[51] I.S. Chang and C.H. Lee, Membrane filtration characteristics in membrane-coupled activated sludge system: the effect of physiological states of activated sludge on membrane fouling, *Desalination*, 120, 221-233 (1998).

[52] I. le Roux, H.M. Krieg, C.A. Yeates and J.C. Breytenbach, Use of chitosan as an antifouling agent in a membrane bioreactor, *J. Membr. Sci.*, 248, 127-136 (2005).

[53] T.-H. Bae and T.-H. Tak, Interpretation of fouling characteristics of ultrafiltration membranes during the filtration of membrane bioreactor mixed liquor, *J. Membr. Sci.*, 264, 151-160 (2005).

[54] H. Rabiee, S.M.S. Shahabadi, A. Mokhtare, H. Rabiei and N. Alvandifar, Enhancement in permeation and antifouling properties of PVC ultrafiltration membranes with addition of hydrophilic surfactant additives: Tween-20 and Tween-80, *J. Environ. Chem. Eng.*, 4, 4050-4061 (2016).

[55] F. Russo, R. Castro- Muñoz, F. Galiano and A. Fogoli, Unprecedented preparation of porous Matrimid® 5218 membranes, *J. Membr. Sci.*, 585, 166-174 (2019).

[56] J.-H. Choi, S.-K. Park and H.-Y. Ng, Membrane fouling in a submerged membrane bioreactor using track-etched and phase-inversed porous membranes. *Sep. Purif. Technol.*,

65, 184-192 (2009).

[57] M. Zhang, B.-q. Liao, X. Zhou, Y. He, H. Hong, H. Lin and J. Chen, Effects of hydrophilicity/hydrophobicity of membrane on membrane fouling in a submerged membrane bioreactor, *Bioresour. Technol.*, 175 59-67 (2015).

[58] I.-S. Chang, S.-O. Bag and C.-H. Lee, Effects of membrane fouling on solute rejection during membrane filtration of activated sludge, *Process Biochem.*, 36, 855-860 (2001).

[59] N. Maximous, G. Nakhla and W. Wan, Comparative assessment of hydrophobic and hydrophilic membrane fouling in wastewater applications, *J. Membr. Sci.*, 339, 93-99 (2009).

[60] K. Kimura, T. Miyoshi, T. Narse, N. Yamato, R. Ogyu and Y. Watanabe, The difference in characteristics of foulants in submerged MBRs caused by the difference in the membrane flux, *Desalination*, 231, 268-275 (2008).

[61] T. Miyoshi, T. Tsuyuhara, R. Ogyu, K. Kimura and Y. Watanabe, Seasonal variation in membrane fouling in membrane bioreactors (MBRs) treating municipal wastewater, *Water Res.*, 43, 5109-5118 (2009).

[62] S. Tang, Z. Wang, Z. Wu and Q. Zhou, Role of dissolved organic matters (DOM) in membrane fouling of membrane bioreactors for municipal wastewater treatment, *J. Hazard. Mater.*, 178, 377-384 (2010).

[63] Y. Tian, L. Chen, S. Zhang and S. Zhang, A systematic study of soluble microbial products and their fouling impacts in membrane bioreactors, *Chem. Eng. J.*, 168, 1093-1102 (2011).

[64] Y.-T. Huang, T.-H. Huang, J.-H. Yang and R.A. Damodar, Identifications and characterizations of proteins from fouled membrane surfaces of different materials, *Int.*

Biodeter. Biodegr., 66, 47-52 (2012).

[65] T. Miyoshi, T. Aizawa, K. Kimura and Y. Watanabe, Identification of proteins involved in membrane fouling in membrane bioreactors (MBRs) treating municipal wastewater, *Int. Biodeter. Biodegr.*, 75, 15-22 (2012).

[66] S. Kang, E.M.V. Hoek, H. Choi and H. Shin, Effect of membrane surface properties during the fast evaluation of cell attachment, *Sep. Purif. Technol.*, 41, 1475-1487 (2006).

[67] T. Kurita, K. Kimura and Y. Watanabe, The influence of granular materials on the operation and membrane fouling characteristics of submerged MBRs, *J. Membr. Sci.*, 469, 292-299 (2014).

[68] C. Visvanathan, R. Ben Aim and K. Parameshwaran, Membrane separation bioreactors for wastewater treatment, *Crit. Rev. Environ. Sci. Technol.*, 30, 1-48 (2000).

[69] Y. He, P. Xu, C. Li and B. Zhang, High-concentration food wastewater treatment by an anaerobic membrane bioreactor, *Water Res.*, 39, 4110-4411 (2005).

Chapter V

Effect of surface hydrophilicity of symmetric polytetrafluoroethylene flat-sheet membranes on membrane fouling in a submerged membrane bioreactor

---

V.1 Introduction

A membrane bioreactor (MBR) is a newer wastewater treatment technique in which the solid-liquid separation process is conducted by a membrane instead of a settling tank. An MBR keeps most of the suspended solids, including microorganisms, in the reactor by membrane microfiltration, allowing it to produce clearer treated water compared to a conventional settling tank. Because of this advantage, MBRs have been recently applied to various wastewater treatment plants [1,2]. In contrast, it is known that MBR has an issue on the reduction in water permeability, which is caused by membrane fouling. Membrane fouling is a phenomenon where suspended matter is deposited on the membrane surface and captured in membrane pores, resulting in an increase in filtration resistance over time [3]. When membrane fouling becomes severe, membrane module cleaning or replacement is needed. They lead to an increase in operating and maintenance costs [1,4]. Therefore, the reduction of fouling development is a major issue for the further application of MBRs in the future.

There have been many studies on the reduction of membrane fouling in MBRs; however, a significantly effective technology has not yet been established. Membrane fouling is affected by many factors, such as the kind of the wastewater, the properties of the activated sludge, operating conditions, and membrane characteristics. These factors

and their combined effects complicate the membrane fouling phenomena [5,6]. As for the membrane characteristics, the following factors have been studied; pore morphology, hydrophilicity, surface charge, and surface roughness [2,7,8]. Among them, I focused on the membrane hydrophilicity among the above membrane characteristics because the membrane hydrophilicity has been famously considered as one of the important factors contributing to the membrane fouling and there have been a lot of related studies.

It is generally considered that a hydrophobic membrane has a higher development of membrane fouling than hydrophilic membrane on account of hydrophobic interactions between foulants, like extracellular polymeric substances (EPS) secreted from activated sludge, in the suspension liquid and membrane surface [1,2,8-11]. For this reason, many studies have focused on the hydrophilicity of membrane surfaces in the development of antifouling membranes [12-15]. In contrast, many contradictory results have been reported. For example, Miyoshi et al. reported that the fouling rate increased in the order of cellulose acetate butyrate (CAB) > polyvinylidene fluoride (PVDF) > polyvinyl butyral (PVB) membranes although PVDF was extremely hydrophobic among them [16]. Chen et al. reported that the flux diminishing rate showed in the order of cellulose acetate (CA) > PVDF > polyether sulfone (PES) membranes although CA was the most hydrophilic among them [17] and similar results have also been reported by other researchers [18,19]. Here it should be noted that the above studies [9-11,16-19] used the membrane with not only different hydrophilicity but also different other membrane characteristics for the experiments. That is, there is possibility that the effect of membrane hydrophilicity on the membrane fouling was much smaller than other membrane characteristics such as pore size and surface roughness, which led to misinterpretation of the results. Therefore, I considered that it is necessary to carry out

comparative experiments using membranes which have similar characteristics except only hydrophilicity in order to confirm the effect of the hydrophilicity on the membrane fouling as only a few previous similar kinds of studies [20]. With the above background, this study aimed to demonstrate the effect of membrane hydrophilicity on the fouling development through a comparative experiment in a laboratory-scale submerged MBR when polytetrafluoroethylene (PTFE) flat-sheet membranes with the same membrane characteristics except surface hydrophilicity was used. I also paid attention to the concentration of protein and carbohydrate, which are considered to be the main components of EPS, in mixed liquor and membrane permeate, and used them for this verification.

V.2 Materials and methods

V.2.1 Membranes and module fabrication

This study utilized hydrophilic and hydrophobic PTFE flat-sheet membranes with similar pore sizes of 0.1 μm, provided by a membrane supplier (Membrane Solutions, USA), to compare the development of membrane fouling between hydrophilic and hydrophobic membranes. The hydrophilic PTFE flat-sheet membrane was purchased from a commercially available product for MBR applications. This hydrophilic membrane was prepared by hydrophilizing the hydrophobic membrane by a membrane supplier. Therefore, I obtained the hydrophobic membrane before hydrophilizing treatment from the supplier. As a preprocess, the flat-sheet membranes were prepared by a stretching method and laminated with non-woven polyester fabric as a support layer by the supplier.

For application to MBR, a membrane module was fabricated with each of the

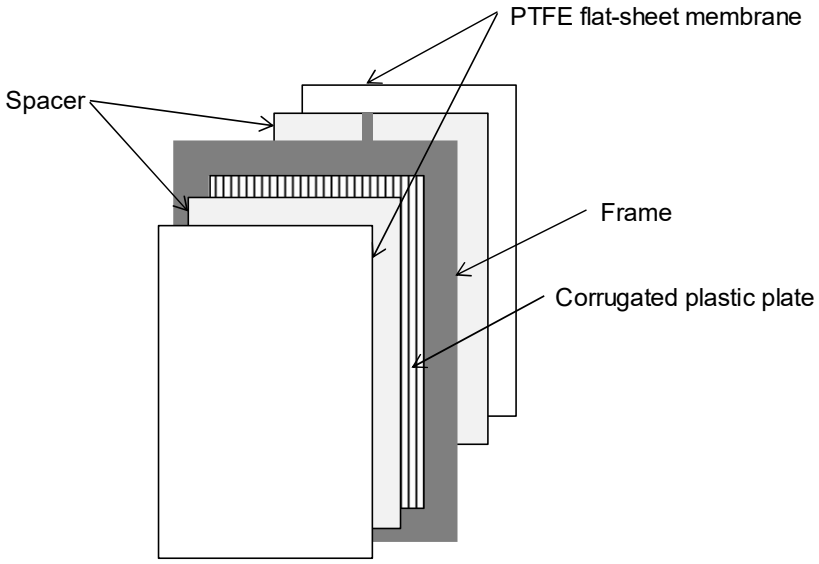

Fig. 5-1 Schematic of flat-sheet membrane module.

hydrophilic and hydrophobic PTFE flat-sheet membranes [21]. Two sheets of the flat-sheet membranes were placed on both sides of a corrugated plastic plate with punched holes and fixed to a plastic frame of polyvinyl chloride by gluing the edges together. Each side of the flat-sheet membrane was separated by polyester non-woven fabric spacers from the corrugated plastic plate (Fig. 5-1). The effective filtration area of the membrane module was approximately 0.11 m^2 (0.19 m × 0.29 m × 2 sides).

V.2.2 Setup of laboratory-scale submerged membrane bioreactor

A schematic of the laboratory-scale submerged MBR used in this study is shown in Fig. 5-2. A reactor was prepared for each of the hydrophilic and hydrophobic membranes. In total, two reactors were prepared for this study. Both reactors had a 6.8 L effective working volume and were made of clear polyvinyl chloride. A membrane module with each of the hydrophilic and hydrophobic membranes was installed in each reactor. There were two roller pumps (MP-2000, Tokyo Rikakikai, Co. Ltd., Japan) in the

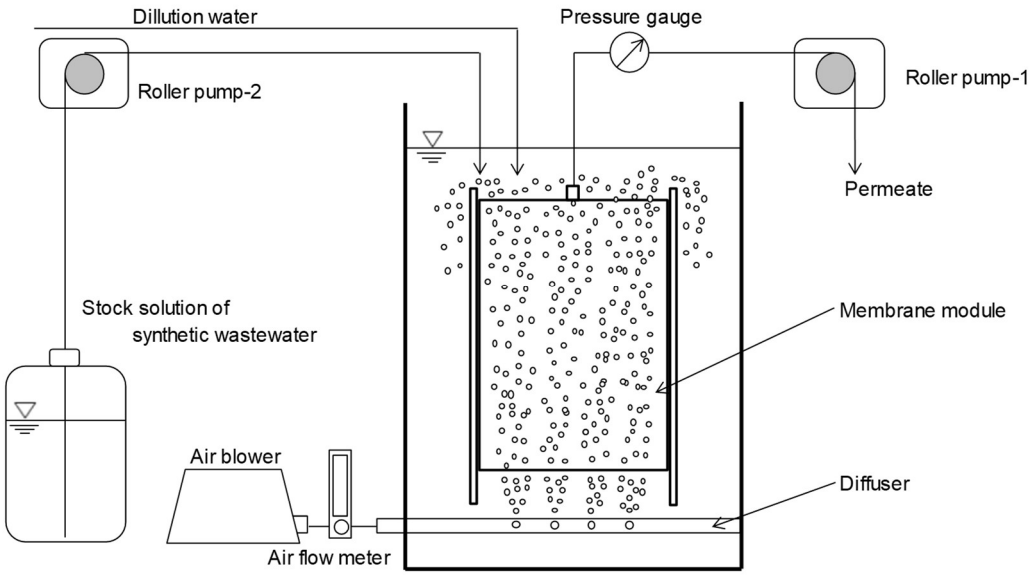

Fig. 5-2 Schematic figure of laboratory-scale submerged MBR apparatus.

MBR. Roller pump-1 was utilized, and the membrane filtrate was removed from the reactor. The filtration flux was constantly monitored and maintained by manually controlling the rotation speed of the roller pump-1. Roller pump-2 was utilized to feed synthetic wastewater from a stock solution vessel to the reactor. An air diffuser with six holes of 1.5 mm diameter each was installed in the reactor, and the air was supplied by an air pump with a pressure regulator (SCO-4-115L, Nippon Flow Cell Co., Japan) at 5 L/min to flow across both outside surfaces of the membrane module. The transmembrane pressure (TMP) was periodically measured to evaluate the degree of membrane fouling development using a digital pressure gauge (GC31-174, Nagano Keiki Co. Ltd., Japan)

V.2.3 Synthetic wastewater and operating condition

Before the operation, the dry membrane modules were immersed in ethanol for 10 min to saturate the modules with ethanol. Then, they were removed from ethanol and

immersed in tap water for 30 min to replace ethanol with tap water. Activated sludge from a municipal wastewater treatment plant in Kumamoto City, Japan, was used as a seed sludge. Synthetic wastewater fed to each reactor by the roller pump-2. The synthetic wastewater was prepared with 250 mg/L D-glucose, 50 mg/L meat extract (Kyokuto Pharmaceutical Industrial Co., Ltd., Japan), 40 mg/L polypeptone (FUJIFILM Wako Pure Chemical Corp., Japan), 50 mg/L K_2HPO_4, 20 mg/L $(NH_4)H_2PO_4$, 3.0 mg/L NaCl, 5.0 mg/L $MgSO_4 \cdot 7H_2O$, 2.5 mg/L $CaCl_2 \cdot 2H_2O$, and 0.5 mg/L $FeCl_3 \cdot 6H_2O$, and pH was adjusted at 7.2 ± 0.2 with 2 mol/L NaOH solution. The concentration of total organic carbon (TOC) in the synthetic wastewater was 120 mg/L. The concentration of mixed liquor suspended solids (MLSS) was periodically measured and constantly maintained by determining the appropriate volume of the sludge. The sludge retention time (SRT) was approximately 30 days. The suspension liquids of both reactors were removed and stirred every two days, and then returned to the reactors to equalize the MLSS concentration and characteristics of the suspension liquid in both reactors. The operation was carried out at room temperature (maintained at around 25 °C), the temperature in the reactors were not controlled but periodically monitored with a thermometer, and pH was manually adjusted at 7.2 with 2 mol/L NaOH solution per day.

A constant filtration flux mode was carried out. This mode was based on the general flux-step method to evaluate changes in TMP [22,23]. The filtration flux was fixed at 0.3 $m^3/m^2 \cdot d$ (12.5 $L/m^2 \cdot h$) for the first run, 0.5 $m^3/m^2 \cdot d$ (20.8 $L/m^2 \cdot h$) for the second run and 0.7 $m^3/m^2 \cdot d$ (29.2 $L/m^2 \cdot h$) for the third run. These three runs were repeated twice as the first and second operations, respectively. The membrane modules were removed from the reactors once after the first operation, and then cleaned by physical and chemical methods. Physical cleaning was carried out by wiping the

membrane surfaces with a soft sponge and flushing with tap water. Chemical cleaning was carried out by immersing the membrane modules into a 5000 mg/L sodium hypochlorite solution for 2 h. The cleaned membrane modules were returned to the reactors. Then, the second operation was conducted with the cleaned membrane modules.

V.2.4 Analytical methods

The contact angle was measured using a contact angle goniometer (DMs-401, Kyowa Interface Science Co., Japan) at room temperature using the sessile drop technique [24]. The pore size and distribution of the membranes were measured using a capillary flow porometer (CFP-1200A, Porous Materials Inc., USA) [25]. The microstructures of the pristine membranes were observed by a scanning electron microscope (SEM) (TM3030, Hitachi High-Technologies Co., Japan). The surface porosity of the membranes was calculated by binarizing the SEM images of the membrane surface. The binarized images were obtained using image processing software (Image J, National Institutes of Health, USA), and the surface porosity was determined by the ratio of open area to the total surface area on the binarized images. The surface roughness of the membranes was analyzed by an atomic force microscope (AFM) (AFM5100N, Hitachi High-Technologies Co., Japan). The measurements were obtained in a dynamic force mode using an SI-DF3P2 (spring constant = 2 N/m) cantilever with a silicon tip at room temperature in air. The scanned size was 5 μm × 5 μm. MLSS concentration was measured using standard methods [26]. The concentrations of carbohydrates and proteins, which are both major components of EPS, were measured using the phenol-sulfuric acid method by Dubois et al. [27], with glucose used as a standard and bicinchonimic acid (BCA) assay [28,29] (TaKaRa BCA Protein Assay kit, Takara-bio Inc., Japan) with bovine serum

albumin used as a standard, respectively. Samples for the measurement were the supernatant of the mixed liquor and membrane filtrate. The amount of proteins and carbohydrates captured inside the membranes through membrane filtration were compared. The reduced amounts of proteins and carbohydrates in the membranes as a rejection percentage (*RP*), calculated using the following equation:

$$RP\ (\%) = \left(1 - \frac{C_p}{C_s}\right) \times 100 \qquad (5-1)$$

where C_s and C_p are the concentrations of protein or carbohydrate in the supernatant of the mixed liquor, and in the membrane permeate, respectively. The three-dimension excitation-emission matrix (EEM) was observed from 220-500 nm excitation at 5 nm intervals, and 230-550 nm emission at 2 nm intervals, using a fluorescence spectrometer (F-2700, Hitachi High-Tech Science Co., Japan) for the identification of polymeric compounds as candidates for foulants. The samples for measurement were taken once from the point of 0.3 $m^3/m^2 \cdot d$ near the design flux [30-32] (approximately 0.3-0.5 $m^3/m^2 \cdot d$) in MBR using a flat-sheet membrane.

V.2.5 Membrane resistance measurement

The membrane modules were removed from the reactors after the second operation. The membranes were cut into small disks with a diameter of 4.7 cm from the modules and placed onto a dead-end filtration unit having an effective area of 13.8 cm^2 (KP-47S, Toyo Roshi Kaisha Ltd., Japan). Distilled water was filtrated under a constant pressure of 0.05 MPa, and the flow rate was measured. Filtration resistance R (1/m) was

calculated using the following equation according to Darcy's law [33,34]:

$$R = \frac{\Delta P}{\mu J} \qquad (5-2)$$

where ΔP is the transmembrane pressure difference (N/m^2), μ is the filtration viscosity (Ns/m^2), and J is the filtration flux (m/s). The total filtration resistance (R_t) was calculated as the sum of three components [19,35]:

$$R_t = R_m + R_p + R_c \qquad (5-3)$$

where Rm is the intrinsic membrane resistance, R_p is the pore fouling resistance, and R_c is the cake layer resistance. R_p is caused by foulant deposition inside the membrane pores and calculated from the difference between the resistance of the pristine membrane and that of the membrane after physical cleaning. R_c is caused by the formation of a sludge-cake layer and is measured by the difference between the resistance of the membrane fouled by the experiment and that of the membrane after physical cleaning. According to Kimura et al., the pore fouling resistance was defined as irreversible fouling resistance and cake layer resistance was defined as the reversible fouling resistance, and they were measured by the same method conducted in this study. This definition was used in the following results and discussion sections [36-38].

V.3 Results

V.3.1 Membrane characterization

Table 5-1 shows the characteristics of the hydrophilic and hydrophobic PTFE

Table 5-1 Characteristics of PTFE flat-sheet membranes used in this study

Parameter	Hydrophilic	Hydrophobic
Nominal pore size (supplier data, μm)*	0.1	0.1
Contact angle (°)**,***	66 ± 7	125 ± 2
Mean flow pore size (μm)**	0.16 ± 0.1	0.16 ± 0.1
Surface porosity (%)**	37.6 ± 0.8	38.4 ± 0.9
Surface roughness (RMS, nm)**	38.1 ± 11.5	39.3 ± 6.1

Data are expressed as mean ± standard deviation
* analyzed by membrane supplier
** analyzed in this study
*** supplemental data (Fig. S-1)

flat-sheet membranes. It was clear that the characteristics of both membranes were similar except for the contact angles. The contact angle is an indication of the surface hydrophilicity to evaluate the difference among the membranes; the smaller the contact angle, the more hydrophilic the material is. As shown in Table 5-1, the contact angle of the hydrophilic PTFE membrane was much smaller than that of the hydrophobic one. Figure 5-3 shows SEM images and the three-dimensional surface images of the feed side surface of the membranes. As shown in Fig. 5-3 (a) and (b), both membranes had similar surface structures of polymer nodules connected by fibers and surface porosity.

V.3.2 Changes in transmembrane pressure during continuous operation of laboratory-scale submerged membrane bioreactor

Figure 5-4 shows the changes in the TMP and MLSS concentration through the whole experimental period, respectively. The MLSS concentrations were well maintained within the range of 11000 to 12000 mg/L, and the variation was within 0.2% of the variation coefficient in each reactor. The values of pH and temperature in the reactors were maintained within the range of 6.9-7.1 and 20-23 °C, respectively. The removal

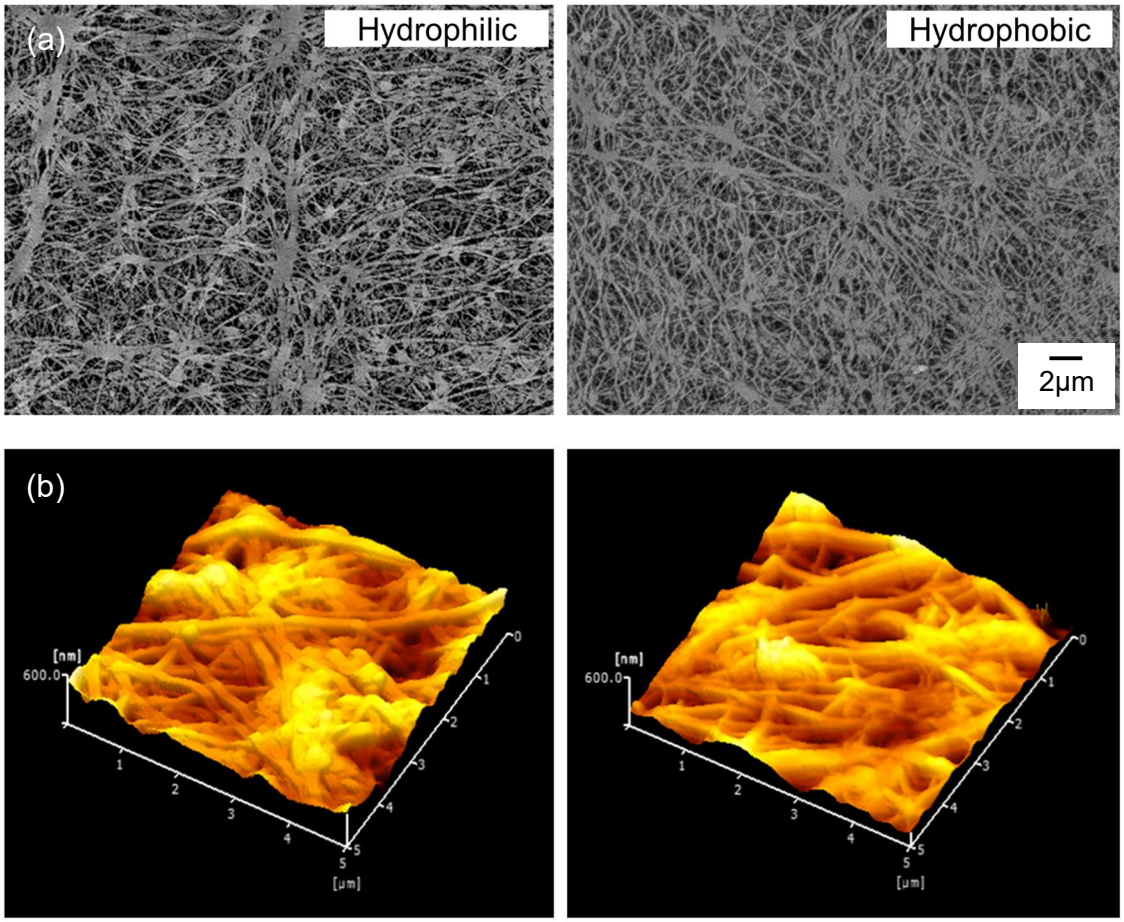

Fig. 5-3 SEM images (a) and three-dimensional surface images (b) of the PTFE flat-sheet membranes.

efficiency of TOC was maintained at more than 98% in both reactors throughout the experiment. I also confirmed that hydrophilicity was well maintained through the experiment by measuring the contact angle.

The TMPs were maintained at low values less than 1.0 kPa at a flux of 0.3 $m^3/m^2 \cdot d$, which is the safety flux in practical use, in both the first and second operations. With the flux of 0.3 $m^3/m^2 \cdot d$, it was continued for 8 days in operation 1 and for 12 days in operation 2. However, when the flux was raised to 0.5 $m^3/m^2 \cdot d$, the TMPs rapidly increased in both operations. It is considered that this rapid increases in TMP were caused by the flux of exceeding the critical flux [39,40]. In addition, the tendency of increases

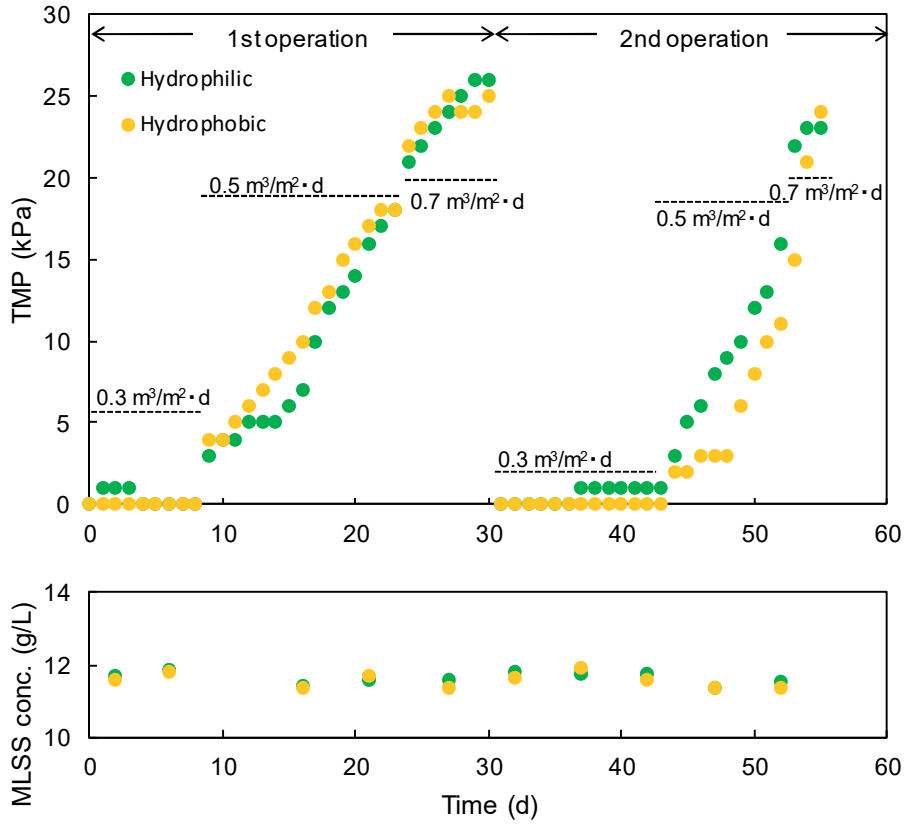

Fig. 5-4 Changes in TMP and MLSS concentration over the course of the experiment.

in TMP were not significantly different between hydrophilic and hydrophobic membranes. Finally, at 0.7 $m^3/m^2 \cdot d$, the TMPs of hydrophilic and hydrophobic membranes reached 26 kPa and 25 kPa over 6 days in first operation, and 23 kPa and 24 kPa over only two days in second operation, respectively. Thus, the TMP values were almost same even if the surface hydrophilicity of the membranes was different. This suggested that changing behavior in the TMPs of both hydrophilic and hydrophobic PTFE membranes was not that different.

V.3.3 Membrane resistance of hydrophilic and hydrophobic membranes

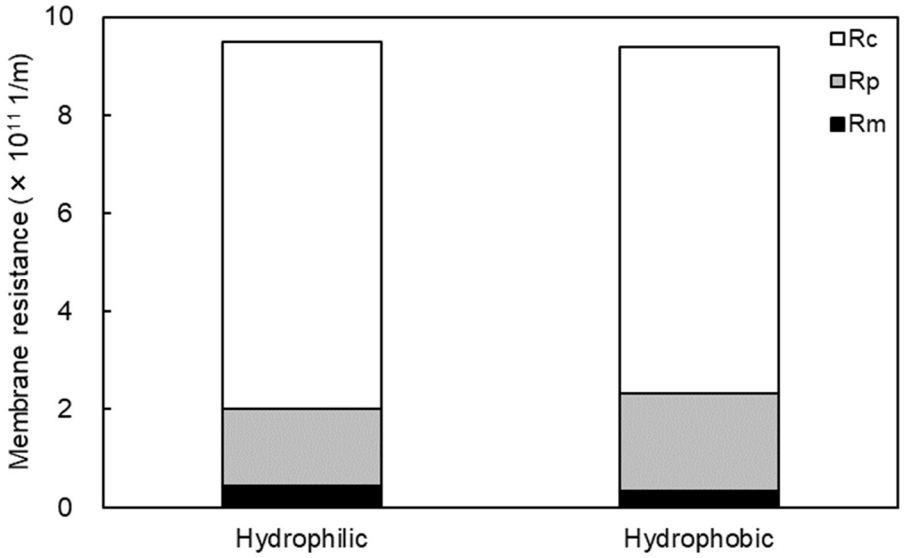

Fig. 5-5 Membrane resistance of fouled PTFE flat-sheet membranes after experiment.

Figure 5-5 shows the filtration resistances (R_m, R_p, R_c) of the membranes after all experiments. The total filtration resistances of the hydrophilic and hydrophobic membranes were 9.5×10^{11} and 9.4×10^{11} 1/m, respectively. As shown in Fig. 5-5, R_m was quite small, which contributed only 4-5% to the total filtration resistance in both membranes and the R_m value showed no change over the course of the experiment. Therefore, it was considered that the intrinsic membrane resistance (R_m) did not contribute to the fouling phenomena. In contrast, the R_p value of the hydrophilic membrane was slightly lower than that of the hydrophobic one. This suggests the possibility that the high hydrophilicity contributed to the prevention of irreversible fouling. Nevertheless, the R_p value was much smaller than the R_c value; thus, the dominant factor of membrane fouling was the cake layer resistance (R_c) for both PTFE membranes. In addition, the difference in R_c values between the membranes was small, which suggests that there was no remarkable effect of membrane hydrophilicity on the value of total filtration resistances (R_t).

It is commonly understood that the irreversible fouling was caused by EPS components, which were protein and carbohydrate. Therefore, the amount and characteristics of proteins and carbohydrates captured inside the membranes through membrane filtration were compared. Table 5-2 shows the concentrations of protein and carbohydrate (average value) in supernatant of the mixed liquor and membrane permeate, and Fig. 5-6 shows the reduced amounts of proteins and carbohydrates in the membranes as a *RP*. As shown in Fig. 5-6, the *RP* values of carbohydrates in both membranes were approximately the same, but the *RP* value of protein for the hydrophobic membrane was slightly higher than that of the hydrophilic membrane, which suggests that more proteins were captured inside the hydrophobic membrane. These results might indicate that the difference in pore fouling resistance between the membranes was affected by protein adsorption on the membrane surfaces. However, it should be noted that there is possibility that proteins and carbohydrates may also be removed by the cake layer as well as the membrane.

Figure 5-7 shows EEM fluorescence spectra for the dissolved components of the supernatant of liquid suspension and the membrane filtrate in two laboratory-scale MBRs with hydrophilic and hydrophobic PTFE flat-sheet membranes. The EEM spectra for all samples were similar and showed two major peaks of A at excitation/emission wavelengths (Ex/Em): 275/340 nm and B at Ex/Em: 225/340 nm. The two peaks were both assumed to be protein-like compounds based on the previous literature [41-47]. In addition, the fluorescence intensities of these two major peaks in the membrane filtrates were significantly less than that of the peaks in the supernatant; thus, protein-like compounds in the supernatant were adsorbed on the membrane surface and/or pore wall as mentioned above.

Table 5-2 Protein and carbohydrate concentration in supernatant and membrane permeate

Component		Hydrophilic	Hydrophobic
Protein (mg/L)	Supernatant	12.8	12.4
	Membrane permeate	9.0	7.8
Carbohydrate (mg/L)	Supernatant	9.1	11.8
	Membrane permeate	1.4	1.7

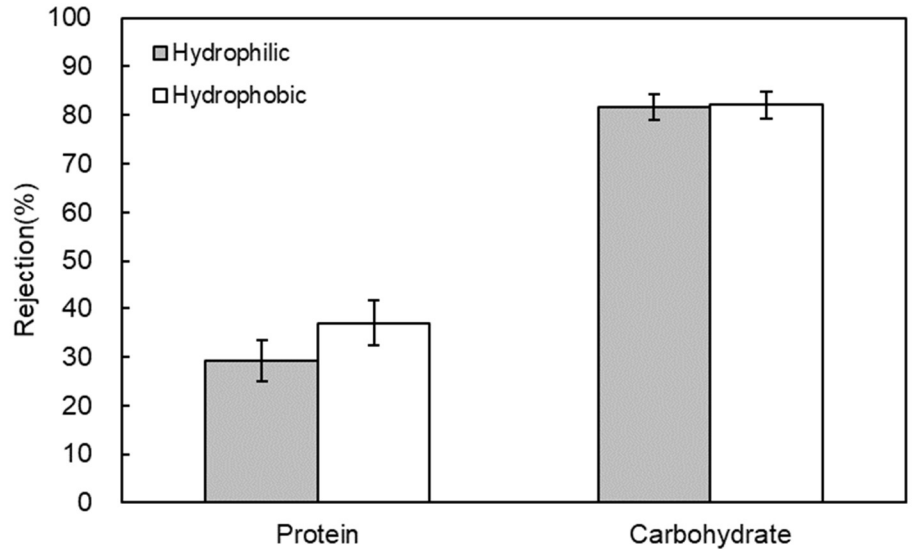

Fig. 5-6 Rejection of protein and carbohydrate on hydrophilic and hydrophobic PTFE membranes. Error bar means standard deviation.

V.4 Discussion

In this study, we investigated the difference in the membrane fouling behaviors of two types of PTFE flat-sheet membranes, which differed only in their hydrophilicities, by using continuous laboratory-scale submerged MBRs with synthetic wastewater. Therefore, there was no remarkable difference in TMPs between the membranes, regardless of the membrane flux in the continuous operations. This result was not always consistent with some previous studies conducted using membranes with similar

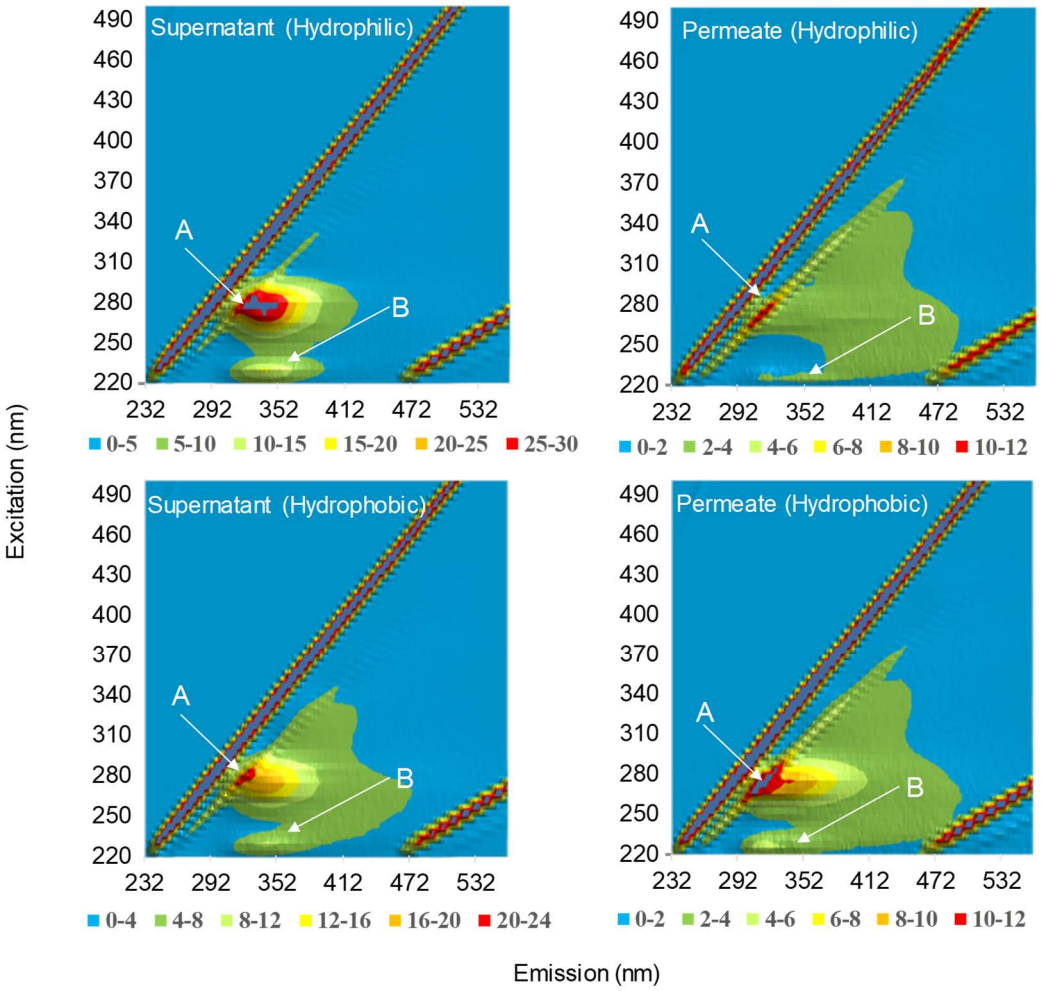

Fig. 5-7 EEM fluorescence spectra of supernatant and effluent in laboratory-scale MBR with PTFE flat-sheet membranes

characteristics, except for hydrophilicity [9,20]. Marel et al. reported that the critical flux for a hydrophobic membrane was half that of a hydrophilic membrane using asymmetrical PVDF membranes with activated sludge [9]. Nittami et al. also reported that hydrophilic membranes required longer periods to reach a certain TMP value than a hydrophobic membrane in a comparison study using symmetrical PTFE membranes [20]. However, the opposite results have also been reported. Chen et al. reported that the flux decline rate of CA membrane with the lowest contact angle was more rapid than that of PVDF and

PES membranes with higher contact angles [17]. Choo et al. also reported similar results using PVDF, CA, and polysulfone (PSf) membranes [18]. In contrast, there have been several studies that concluded that there was no clear relationship between the membrane hydrophilicity and the development of membrane fouling [35,48,49], which was consistent with the results of this study. Zhang et al. reported that the membrane surface hydrophilicity was not directly correlated with membrane fouling and suggested that membrane fouling was influenced by the zeta potential and the surface roughness of the membranes [49].

The R_p caused by irreversible fouling (pore plugging) for the hydrophilic membrane was slightly lower than that of the hydrophobic membrane. In contrast, the protein rejection when filtrating using the hydrophilic membrane was relatively lower than that of the hydrophobic membrane, although the carbohydrate rejection of both membranes was approximately the same. Furthermore, significant removal of protein was confirmed in both membranes using EEM analysis. Therefore, it was clear that the slight difference in R_p between the hydrophilic and hydrophobic membranes was caused by the protein. As mentioned in the results section, there is possibility that proteins and carbohydrates were also removed in the cake layer. However, since the resistance of the cake layers of the both membranes was almost the same, thus it is considered that the influence on the difference in the rejection percentage between the membranes is negligible. These results may indicate that the hydrophilicity of the membrane surface contributed to the prevention of irreversible fouling caused by the protein. Masimous et al. reported that pore plugging for the hydrophobic membrane was more severe than that for the hydrophilic membrane and showed that the protein rejection with filtration using a hydrophilic membrane was quite low [10]. Chang et al. also reported that the

hydrophobic membrane (PES) demonstrated more solute rejection than the hydrophilic membrane (regenerated cellulose) [11]. Thus, the results obtained in this study agree with those of previous studies.

V.5 Conclusions

This study investigated the influence of membrane hydrophilicity on membrane fouling by using laboratory-scale submerged MBRs with hydrophilic and hydrophobic PTFE flat-sheet membranes and continuously supplied synthetic wastewater. There was no remarkable difference in the changes in TMP between the two types of membranes. In addition, the total filtration resistances of the both membranes were almost the same. In conclusion, the membrane hydrophilicity had little influence on the prevention of membrane fouling development. From the detailed breakdown of resistance, it was suggested that irreversible fouling was mainly caused by protein adsorption, not carbohydrate. In contrast, reversible fouling was caused by cake layer formation on the membrane surface. The cake layer resistance was the dominant factor in the total filtration resistance.

Supplemental data

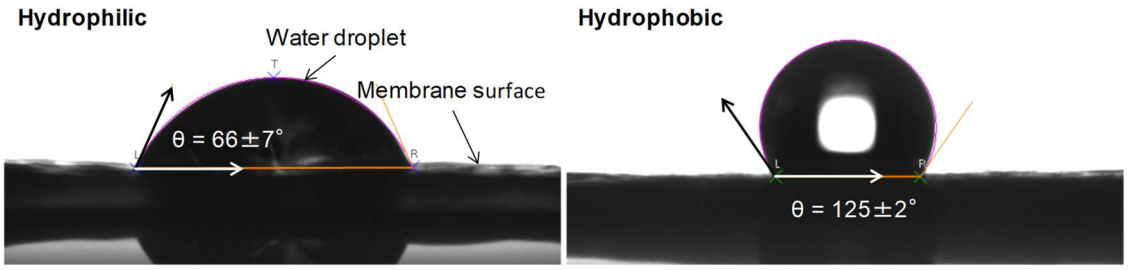

Fig. S-1 Comparison of the contact angle of water drops on the membrane surface

References

[1] P. Le-Clech, V. Chen and T.A.G. Fane, Fouling in membrane bioreactors used in wastewater treatment, *J. Membr. Sci.*, 284, 17-53 (2006).

[2] F. Meng, S.-R. Chae, A. Drews, M. Kraume, H.-S. Shin and F. Yang, Recent advances in membrane bioreactors (MBRs): Membrane fouling and membrane material, *Water Res.*, 43, 1489-1512 (2009).

[3] F. Meng, S. Zhang, Y. Oh, A. Zhou, H. Shin, S. Chae, Fouling in membrane bioreactors: An updated review, *Water res.*, 114, 151-180 (2017).

[4] W. Yang, N. Cicek and J. Llg, State-of-the-art of membrane bioreactors: worldwide research and commercial applications in North America, *J. Membr. Sci.*, 270, 201-211 (2006).

[5] S. Judd, The MBR Book: Principles and Applications of Membrane Bioreactors for Water and Wastewater Treatment 2nd ed., Oxford, Elservier, 2011.

[6] H. Matsuyama, T. Takahashi and M. Yasukawa, Present situation and future prospects of water treatment technology with membrane, *Membrane*, 39, 209-216 (2014).

[7] A. Drews, Membrane fouling in membrane bioreactors-characterization, contradictions, cause and cures, *J. Membr. Sci.*, 363, 1-28 (2010)

[8] O.T. Iorhemen, R.A. Hamza and J.H. Tay, Membrane bioreactor (MBR) technology for wastewater treatment and reclamation: Membrane fouling, *membranes*, 6, 33 (2016).

[9] P. van der Marel, A. Zwijnenburg, A. Kemperman, M. Wessling, H. Tenmink and W. van der Meer, Influnece of membrane properties on fouling in submerged membrane bioreactors, *J. Membr. Sci.*, 348, 66-74 (2010).

[10] N. Maximous, G. Nakhla and W. Wan, Comparative assessment of hydrophobic and hydrophilic membrane fouling in wastewater applications, *J. Membr. Sci.*, 339, 93-99

(2009).

[11] I.-S. Chang, S.-O. Bag and C.-H. Lee, Effects of membrane fouling on solute rejection during membrane filtration of activated sludge, *Process Biochem.*, 36, 855-860 (2001).

[12] M. Higashi, J. Morita, N. Shimada and T. Kitagawa, Long-term-hydrophilic flat-sheet microfiltration membrane made from chlorinated poly (vinyl chloride), *J. Membr. Sci.*, 500, 180-189 (2016).

[13] H.-Y. Yu, M.-X. Hu, Z.-K. Xu, J.-L. Wang and S.-Y. Wang, Surface modification of polypropylene microporous membranes to improve their antifouling property in MBR: NH_3 plasma treatment, *Sep. Purif. Technol.*, 45, 8-15 (2005).

[14] L. Liu, B. Shao, F. Yang, Polydopamine coating - Surface modification of polyester filter and fouling reduction, *Sep. Purif. Technol.*, 118, 226-233 (2013).

[15] H. Minehara, K. Dan, Y. Ito, H. Takabatake and M. Henmi, Quantitative evaluation of fouling resistance of PVDF/PMMA-g-PEO polymer blend membranes for membrane bioreactor, *J. Membr. Sci.*, 466, 211-219 (2014).

[16] T. Miyoshi, K. Yuasa, T. Ishigami, S. Rajabzadeh, E. Kamio, Y. Ohmukai, D. Saeki, J. Ni and H. Matsuyama, Effect of membrane polymeric materials on relationship between surface pore size and membrane fouling in membrane bioreactors, *Appl. Surf. Sci.*, 330, 331-357 (2015).

[17] L. Chen, Y. Tian, C.-q. Cao, J. Zhang and Z.-n. Li, Interaction energy evaluation of soluble microbial products (SMP) on different membrane surfaces: Role of the reconstructed membrane topology, *Water Res.*, 46, 2693-2704 (2012).

[18] K.H. Choo and C.H. Lee, Effect of anaerobic digestion broth composition on membrane permeability, *Water Sci. Technol.*, 34, 173-179 (1996).

[19] H.H.P. Fang and X. Shi, Pore fouling of microfiltration membranes by activated sludge, *J. Membr. Sci.*, 264, 161-166 (2005).

[20] T. Nittami, H. Tokunaga, A. Satoh, M. Takeda and K. Matsumoto, Influence of surface hydrophilicity on polytetrafluoroethylene flat sheet membrane fouling in a submerged membrane bioreactor using two activated sludges with different characteristics, *J. Membr. Sci.*, 463, 183-189 (2014).

[21] T. Sano, Y. Koga, H. Ito, L.V. Duc, T. Hama and Y. Kawagoshi, Effects of structural vulnerability of flat-sheet membranes on fouling development in continuous submerged membrane bioreactors, *Bioresour. Technol.*, 304, 123015 (2020).

[22] M.R. Bilad, L. Marbelia, C. Laine and I.F.J. Vankelecom, A PVC-silica mixed-matrix membrane (MMM) as novel type of membrane bioreactor (MBR) membrane, *J. Membr. Sci.*, 493, 19-27 (2015).

[23] N. Shimada, J. Morita, M. Higashi, T. Kitagawa and J. Nakajima, Long term pilot MBR test for a newly developed flat sheet membrane made from chlorinated polyvinyl chloride in treatment of kitchen wastewater from a cafeteria, *J. Water Environ. Technol.*, 14,329-340 (2016).

[24] S. Rajabzadeh, R. Sano, T. Ishigami, Y. Kakihana, Y. Ohmukai, H. Matsuyama, Preparation of hydrophilic vinyl chloride copolymer hollow fiber membranes with antifouling properties, *Appl. Surf. Sci.*, 324, 718-724 (2015).

[25] T. Marino, E. Blasi, S. Tornaghi, E.D. Nicolo, A. Figoli, Polyethersulfone membranes prepared with Rhodiasolv Polarclean as water soluble green solvent. *J. Membr. Sci.*, 549, 192-204 (2018).

[26] APHA, *Standard Method for the Examination of Water and Wastewater*, 20th ed., American Public Health Association, Washington, DC, 1998.

[27] M. Dubois, K.A. Gillesm J.K. Hamilton, P.A. Rebers and F. Smith, Colorimetric determination of sugars and related substances, *Anal. Chem.*, 28, 350-356 (1956).

[28] P.K. Smith, R.I. Krohn, G.T. Hermanson, A.K. Mallia, F.H. Gartner, M.D. Provenzano, E.K. Fujimoto, N.M. Goeke, B.J. Olson, D.C. Klenk, Measurement of protein using Bicinchoninic acid, *Anal. Biochem.*, 150, 76-85 (1985).

[29] E.A. Agustí, A.B. Piá, J.A.M. Roca, J.L.M. Molina, Influence of extraction methods on proteins and crabohydrates analysis from MBR activated sludge flocs in view of improving EPS determination, *Sep. Purif. Technol.*, 112, 1-10 (2013).

[30] G. Pearce, Manufacture' comparison: part 1, *Filtration & Separation*, 45, 28-31 (2008).

[31] Q.V. Bach, V.T. Le, Y.S. Yoon, X.T. Bui, W. Chung, S.W. Chang, H.H. Ngo, W. Guo, D.D. Nguyen, A new hybrid sewage treatment system combining a rolled pipe system and membrane bioreactor to improve the biological nitrogen removal efficiency: a pilot study, *J. Clean. Prod.*, 178, 937-946 (2018).

[32] P.K. Hosseini, F.P. Shariati, H.D. Amrei, A. Heydarinasab, The influence of various orifice diameters on cake resistance and pore blocking resistance of a hybrid membrane photobioreactor (HMPBR), *Sep. Purif. Technol.*, 235, 116187 (2020).

[33] I.S. Chang and C.H. Lee, Membrane filtration characteristics in membrane-coupled activated sludge system – the effect of physiological states of activated sludge on membrane fouling, *Desalination*, 120, 221-233 (1998).

[34] T.-H. Bae and T.-H. Tak, Interpretation of fouling characteristics of ultrafiltration membranes during the filtration of membrane bioreactor mixed liquor, *J. Membr. Sci.*, 264, 151-160 (2005).

[35] J.-H. Choi and H.Y. Ng, Effect of membrane type and material on performance of a

submerged membrane bioreactor, *Chemosphere*, 71, 853-859 (2008).

[36] K. Kimura, Y. Hane, Y. Watanabe, G. Amy, N. Ohkuma, Irreversible membrane fouling during ultrafiltration of surface water, *Water Res.*, 38, 3431-3441 (2004).

[37] T. Tsuyuhara, Y. Hamamoto, T. Miyoshi, K. Kimura and Y. Watanabe, Influence of membrane properties on physically reversible and irreversible fouling in membrane bioreactors, *Water Sci. Technol.*, 61, 2235-2240 (2010).

[38] T. Kurita, K. Kimura and Y. Watanabe, The influence of granular materials on the operation and membrane characteristics of submerged MBRs, *J. Membr. Sci.*, 469, 292-299 (2014).

[39] R.W. Field, D. Wu, J.A. Howell, B.B. Gupta, Critical flux concept for microfiltration fouling, *J. Membr. Sci.*, 100, 259-272 (1995).

[40] P. Le-Clech, B. Jefferson, I.S. Chang and S. Judd, Critical flux determination by the flux-step method in a submerged membrane bioreactor, *J. Membr. Sci.*, 227, 82-93 (2003).

[41] C.A. Stedmon and S. Markager, Resolving the variability in dissolved organic matter fluorescence in a temperate estuary and its catchment using PARAFAC analysis, *Limonol. Oceanogr.*, 50, 686-697 (2005).

[42] P. Kowalczuk, M.J. Durako, H. Yong, A.E. Kahn, W.J. Cooper and M. Gonsior, Characterization of dissolved organic matter fluorescence in the South Atlantic Bight with use of PARAFAC model: Interannual variability, *Mar. Chem.*, 113, 182-196 (2009).

[43] C.A. Stedmon, S. Markager and R. Bro, Tracing dissolved organic matter in aquatic environments using a new approach to fluorescence spectroscopy, *Mar. Chem.*, 82, 239-254 (2003).

[44] W. Guo, J. Xu, J. Wang, Y. Wen, J. Zhuo and Y. Yan, Characterization of dissolved organic matter in urban sewage using excitation emission matrix fluorescence

spectroscopy and parallelfactor analysis, *J. Environ. Sci.*, 22, 1728-1734 (2010).

[45] M. Villain, I. Bourven, G. Guibaud and B. Marrot, Impact of synthetic or real urban wastewater on membrane bioreactor (MBR) performances and membrane fouling under stable conditions, *Bioresour. Technol.*, 155, 235-244 (2014).

[46] G.-P. Sheng and H.-Q. Yu, Characterization of extracellular polymeric substances of aerobic and anaerobic sludge using three-dimensional excitation and emission matrix fluorescence spectroscopy, *Water Res.*, 40, 1233-1239 (2006).

[47] Y. Kawaguchi and R. Kojima, Analysis of the chromophoic dissolved organic matter in process water by EEMs and PARAFAC, *HORIBA Technical Reports*, 43, 38-42 (2014).

[48] J.-H. Choi, S.-K. Park and H.-Y. Ng, Membrane fouling in a submerged membrane bioreactor using track-etched and phase-inversed porous membranes, *Sep. Purif. Technol.*, 65, 184-192 (2009).

[49] H. Zhang, B. Wang, H. Yu, L. Zhang, S. Song, Relation between sludge properties and filterability in MBR: Under infinite SRT, *Membr. Water Treat.*, 6, 501-512 (2015).

Chapter VI

Effects of Pluronic TR-702 on chlorinated poly(vinyl chloride) flat-sheet membranes prepared by water vapor induced phase separation

---

VI.1 introduction

Membrane bioreactors (MBRs) are a wastewater treatment process that combines a solid-liquid separation process using membranes and a biological degradation process using activated sludge. In MBRs, compared with conventional activated sludge processes, suspension solids including microorganisms mostly remain in the reactor and reasonably clear water is produced by membrane filtration. Thus, MBRs have been widely applied for a variety of wastewater treatments [1]. However, similar to other water treatment processes that use membranes, MBRs are limited by permeation flux decline caused by membrane fouling. When serious membrane fouling occurs, membrane cleaning or replacement is necessary, which leads to an increase in operating and maintenance costs [1,2]. Therefore, the mitigation of membrane fouling remains an important issue for the future application of MBRs.

Many studies have focused on mitigating membrane fouling in MBRs [3-6], but a definite effective technique has not yet been established. Membrane fouling is influenced by various factors such as the characteristics of feed water, the characteristics of activated sludge, operating conditions, and membrane properties. These interrelated factors complicate the membrane fouling phenomena [7,8]. In the case of membrane properties, membrane fouling is influenced by membrane properties such as surface

hydrophilicity, pure water permeability, pore size and distribution, surface porosity, and surface roughness. van der Marel et al. investigated the influence of membrane pore size, surface porosity, pore morphology, and hydrophilicity on membrane fouling using polymeric flat-sheet membranes with activated sludge from a pilot-scale MBR [9]. They reported that increasing the pore size and surface porosity mitigated membrane fouling by reducing the local flux through the pores and the retention of feed water components. In other studies, membranes with higher pure water permeability exhibited lower fouling propensity [10,11]. Thus, controlling membrane properties has been shown to contribute to the reduction of fouling development. On the other hand, many studies have modified membrane properties by blending amphiphilic polymers such as Pluronic F127 and Tween-80 to fabricate membranes with hydrophilicity and antifouling properties [12-17]. These studies reported that amphiphilic polymers not only provided hydrophilicity and antifouling properties to the membrane surface, but also played a role in changing membrane properties such as pore size and pure water permeability. Zhao et al. reported that the pore size of the skin layer on polyethersulfone (PES) ultrafiltration membranes blended with Pluronic F127 was enlarged with an increase in surfactant content [12]. Loh et al. reported that the pure water permeability of PES ultrafiltration membranes was increased by blending with an adequate amount of Pluronic F127 [14]. Rabiee et al. reported that the porosity of polyvinyl chloride (PVC) ultrafiltration membranes blended with Tween 80 increased with an increase in additive content [15]. These results indicated that amphiphilic polymers are a key material in the development of low-fouling membranes in MBRs.

The majority of membranes applied in MBRs are polymeric membranes prepared by the phase inversion method or stretching method. Polyvinylidene fluoride

(PVDF), polytetrafluoroethylene (PTFE), chlorinated polyvinyl chloride (CPVC), polyethylene (PE), and PES are popular materials for polymeric membranes [18-25]. Among these materials, CPVC has been widely applied in MBRs because of its excellent chemical and mechanical properties [26-29]. The CPVC membranes applied in MBRs have been flat-sheet microfiltration membranes with symmetrical structures prepared by water vapor induced phase separation using polyester non-woven fabrics as a support layer [30,31]. However, the majority of studies including those described above [12-17] have reported the blending of amphiphilic polymers to ultrafiltration membranes with asymmetric structures prepared by non-solvent induced phase separation [32-35]. On the other hand, few studies have reported the application of amphiphilic polymers for microfiltration membranes with symmetric structures prepared by water vapor induced phase separation [36,37]. Therefore, establishing a technique for controlling membrane properties such as pore size and pure water permeability by blending amphiphilic polymers with CPVC membranes with symmetric structures is necessary for the future development of MBRs.

On the other hand, some studies reported that the properties of membranes that contained polymeric additives such as pure water permeability changed after the membrane was treated with sodium hypochlorite solution [38-41]. Qin et al. reported that polyvinylpyrrolidone (PVP) contents in a PES/PVP blended membrane were partially removed with hypochlorite [39]. Arahman et al. also reported that hypochlorite treatment caused partial decomposition and leaching of Tetronic 1307 components from a PES/Tetronic 1307 blended membrane [40]. In practical MBRs, the surfactant additive in the membrane is removed during operation because the membrane is periodically exposed to a chemical cleaning solution (i.e., sodium hypochlorite solution) [42]. Furthermore,

polyethylene oxide (PEO) chains in non-ionic surfactants such as Pluronic and Tetronic is selectively degraded by microorganisms [43]. Therefore, it is hypothesized that polymeric additives such as Pluronic and Tetronic do not remain in the membrane matrix during long-term operation of the MBR. Thus, in the development of a membrane for applications in MBRs, it is necessary to evaluate membranes without polymeric additives. However, prior reports on blended membranes with amphiphilic polymers have focused on hydrophilicity and antifouling properties. As such, no studies have evaluated the membrane properties of blended membranes without amphiphilic polymers. Pluronic TR-702 is an amphiphilic polymer that is commercially available and has a structure similar to that of Tetronic 1307. This study aimed to establish a technique for preparing membranes with properties appropriate for MBRs by adding Pluronic TR-702 to a symmetrical CPVC membrane.

In this study, CPVC flat-sheet membranes blended with Pluronic TR-702 as an amphiphilic polymer additive were prepared by water vapor induced phase separation, which revealed the influence of Pluronic TR-702 on the membrane properties after the Pluronic TR-702 was removed.

VI.2 Materials and methods

VI.2.1 Materials

CPVC with a polymerization degree of approximately 800 was purchased from KANEKA Corp., Japan and used to form a membrane. Tetrahydrofuran (THF) and 2-propanol (IPA) were purchased from FUJIFILM Wako Pure Chemical Corp., Japan and used as the solvent and non-solvent, respectively. Pluronic TR-702 (ethylenediamine polyethylene oxide-polypropylene oxide-polyethylene oxide triblock copolymer) which

was kindly provided by Adeka Corp., Japan was used as the additive polymer. The chemical structure of Pluronic TR-702 is shown in Fig. 6-1.

VI.2.2 Membrane preparation

Membranes were prepared from dope solutions containing CPVC, THF, IPA, and Pluronic TR-702 according to the compositions listed in Table 6-1. The procedure for preparing the dope solution is as follows. CPVC was dissolved in THF and stirred at 40 °C for 8 h in a water bath to obtain a homogeneous solution. The solution was brought to 25 °C, then IPA and Pluronic TR-702 were added and stirred for over 24 h until they dissolved completely.

The membranes were prepared via water vapor induced phase separation in a room with constant temperature and humidity. Non-woven polyester fabric which have a density of 0.55 g/cm^3 and a thickness of 130 μm was dipped into a vessel containing the dope solution as a support layer, then removed through a clearance gap between two stainless steel rolls that were adjusted to a constant distance. The temperature and humidity were maintained at approximately 30 °C and 70% in the room, respectively. The non-woven polyester fabric impregnated with the dope solution was kept in the room for over 2 h to dry completely and solidify the membrane structure.

Before evaluating the membranes, it was confirmed that Pluronic TR-702 was easily and completely soluble in ethanol. Therefore, in this study, prior to the measurements, Pluronic TR-702 was removed from the prepared membranes by soaking in ethanol. From the results of energy dispersive X-ray spectroscopy analysis, it was confirmed that membranes had no Pluronic TR-702 after soaking. The procedure was as follows. The dry prepared membranes were soaked in ethanol for 10 min, then removed

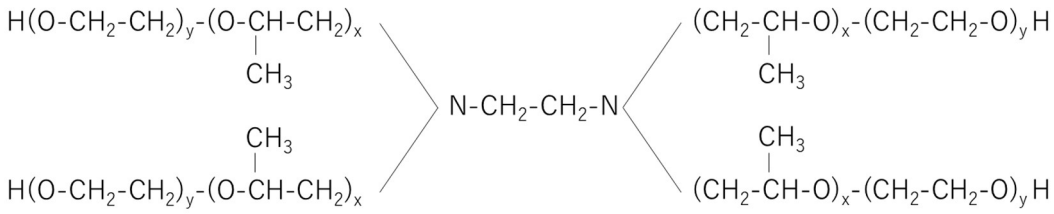

Fig. 6-1 Chemical structure of Pluronic TR-702.

Table 6-1 Composition of dope solution for preparation of CPVC/Pluronic TR-702 membranes

CPVC (g)	THF (g)	IPA (g)	TR-702 (g)	TR-702/CPVC wt/wt (%)
20	125	55	0	0
20	125	55	5	25
20	125	55	10	50
20	125	55	20	100

from the ethanol and soaked in distilled water for 30 min to replace the ethanol with distilled water. The membranes from which Pluronic TR-702 was removed were used for all evaluations. These membranes were used as prepared for measurements of pure water permeability, but when other membrane properties were measured, they were completely dried at 40 °C for 2 h before use.

The turbidity of the dope solutions was measured using a laboratory turbidimeter (2100N, Hach Co., USA). The measurements were carried out at a constant temperature of 25 °C.

VI.2.3 Membrane characterization

VI.2.3.1 Membrane thickness

The thickness of the prepared membranes was measured by using a digital

micrometer (MDC-25MX, Mitutoyo Co., Japan). For each membrane, six measurements at different locations in the membranes were taken, and the average was calculated.

VI.2.3.2 Pure water permeability

The pure water permeability through the membranes was measured by filtrating distilled water using the wetted membranes. The prepared membranes were cut into small disks with a diameter of 4.7 cm and placed onto a dead-end filtration unit with a 13.8 cm^2 effective area (KP-47S, Toyo Roshi Kaisha Ltd., Japan). Distilled water was filtrated under a constant pressure of 0.5 bar and temperature of 25 °C, and the filtration time was measured at a permeate volume of 100 mL. The pure water permeability, L ($ml/cm^2 \cdot bar \cdot min$), was calculated using the following equation [44]:

$$L = \frac{Q}{A \times \Delta t \times \Delta P} \qquad (6-1)$$

where Q is the permeate volume (mL), A is the effective membrane area (cm^2), Δt is the filtration time (min), and ΔP is the applied transmembrane pressure (bar). For each membrane, the pure water permeability was measured three times due to minimize the experimental errors and the average was calculated.

VI.2.3.3 Pore size and distribution

The pore size and distribution of the prepared membranes were measured using a capillary flow porometer (CFP-1200A, Porous Materials Inc., USA). This apparatus was used to determine the pore diameter of the membrane by the liquid-gas displacement process. The prepared membranes were cut into small disks with a diameter of 25 mm and were fully wetted with Galwick (Porous Materials Inc., USA) which has a low surface tension of 1.59×10^{-2} N/m. Then, the fully wetted membrane was placed in the sample

chamber. The liquid was extruded from the membrane pores by gradually increasing the air pressure. The air flow rate extruded from the membrane pores was measured using a flow meter placed in the apparatus. The mean flow pore diameter, *d*, was calculated using the following equation [45,46]:

$$d = \frac{C\gamma}{p} \qquad (6-2)$$

where *C* is a constant, γ is Galwick surface tension and *p* is differential pressure when wet flow was one half the dry flow.

VI.2.3.4 Membrane morphology and porosity

The surface and cross-section morphologies of the prepared membranes were observed using a scanning electron microscope (SEM; TM3030, Hitachi High-Technologies Co., Japan). The prepared membranes were cut into small pieces so that they could be placed on the sample table and then sputtered with gold to produce electrical conductivity prior to the SEM measurements. The surface porosity of the membranes was calculated by binarizing the SEM images of the membrane surface. The binarized images were obtained using image processing software (Image J, National Institutes of Health, USA). The binarized images had their open areas designated as black and closed areas designated as white, and the surface porosity was determined by the ratio between the open areas and the total surface area [30].

VI.3 Results

VI.3.1 Turbidity of the dope solutions

Table 6-2 shows the turbidity of the dope solutions consisting of CPVC, THF,

Table 6-2 Turbidity of the dope solutions

TR-702/CPVC (wt/wt%)	0	25	50	100
Turbidity (NTU)	8	16	40	1847

IPA, and Pluronic TR-702. The turbidity of the dope solutions gradually increased when the concentration of Pluronic TR-702 increased from 0 to 50 wt/wt%. However, the turbidity of the dope solution dramatically increased and reached 1847 NTU when the concentration of Pluronic TR-702 was 100 wt/wt%. Further, it was visually confirmed that the dope solution was cloudy at this concentration.

VI.3.2 Effect of Pluronic TR-702 concentration on the thickness of the prepared membranes

Table 6-3 shows the effect of the concentration of Pluronic TR-702 on the thickness of the prepared membranes. The thickness of the membranes continuously increased with the increase in Pluronic TR-702 concentration in the dope solution. All the membranes were removed from the clearance gap between two rolls adjusted to the same distances regardless of the concentration of Pluronic TR-702. Therefore, the larger the concentration of Pluronic TR-702, the thicker the membrane after removal from the clearance gap between the rolls

VI.3.3 Effect of Pluronic TR-702 concentration on the pure water permeability of the prepared membranes

Table 6-3 shows the effect of the concentration of Pluronic TR-702 on the pure water permeability of the prepared membranes. The pure water permeability of the

Table 6-3 Membrane properties of the prepared membranes

TR-702/CPVC (wt/wt%)		0	25	50	100
Thickness (μm)		143	150	156	164
Pure water permeability (ml/cm^2·bar·min)		49.4	67.9	90.0	435
Pore size	Mean flow pore size (μm)	0.32	0.46	0.65	2.1
	Bubble point pore size (μm)	0.91	1.3	2.1	5.8
	Half width ×10^{-2} (μm)	1.9	2.4	3.0	55
Surface porosity (%)		52.4	48.5	45.7	62.5

prepared membranes continuously increased with the increase in Pluronic TR-702 concentration in the dope solution. The pure water permeability gradually increased approximately two-fold from 49.4 to 90.0 ml/cm^2·bar·min when the concentration of Pluronic TR-702 increased from 0 to 50 wt/wt%. However, the pure water permeability dramatically increased approximately five-fold from 90.0 to 435 ml/cm^2·bar·min when the concentration of Pluronic TR-702 increased from 50 to 100 wt/wt%. An increase in the pure water permeability indicated a decrease in the filtration resistance of the membrane. If all the prepared membranes had the same membrane porosity, the resistance of the membranes should have increased as the thickness of the membrane increased due to the increasing distance for filtration. However, the opposite result was obtained. Thus, it was concluded that the membrane porosity was increased by the addition of Pluronic TR-702.

VI.3.4 Effect of Pluronic TR-702 concentration on the pore size and distribution of the prepared membranes

Table 6-3 shows the effect of the concentration of Pluronic TR-702 on the mean flow pore size and bubble point pore size of the prepared membranes. The mean flow pore size and bubble point pore size of the prepared membranes continuously increased

with the increase in Pluronic TR-702 concentration in the dope solution. In general, the mean flow pore size is the average pore size and the bubble point pore size is the maximum pore size. Similar to the pure water permeability, the mean flow pore size and bubble point pore size both gradually increased when the concentration of Pluronic TR-702 increased from 0 to 50 wt/wt% and dramatically increased when the concentration increased from 50 to 100 wt/wt%. The pore size distribution curves of the prepared membranes are shown in Fig. 6-2. It was clear that the membranes with a concentration of Pluronic TR-702 from 0 to 50 wt/wt% exhibited a sharper size distribution, while the membranes with concentrations of 100 wt/wt% exhibited a broader size distribution. The narrowness of the pore size distribution peak was quantified as the half width of the distribution peak. The mean flow and bubble point pore sizes together with the half widths of their peaks are listed in Table 6-3. The half width of a peak also increased with the mean flow pore size and bubble point pore size depending on the concentration of Pluronic TR-702.

VI.3.5 Effect of Pluronic TR-702 concentration on the morphology of the prepared membranes

Figure 6-3 shows the surface and cross-section morphologies of the prepared membranes with non-woven fabric polyester. The SEM photographs exhibited a porous structure on the membrane surface for all prepared membranes. It was clear that the surface pore size on the membrane expanded to an extent that differed from that of other contents when the concentration of Pluronic TR-702 was 100 wt/wt%. Furthermore, except when the concentration of Pluronic TR-702 was 100 wt/wt%, as Pluronic TR-702 concentration increased, the widths of the polymers surrounding the open pore of the

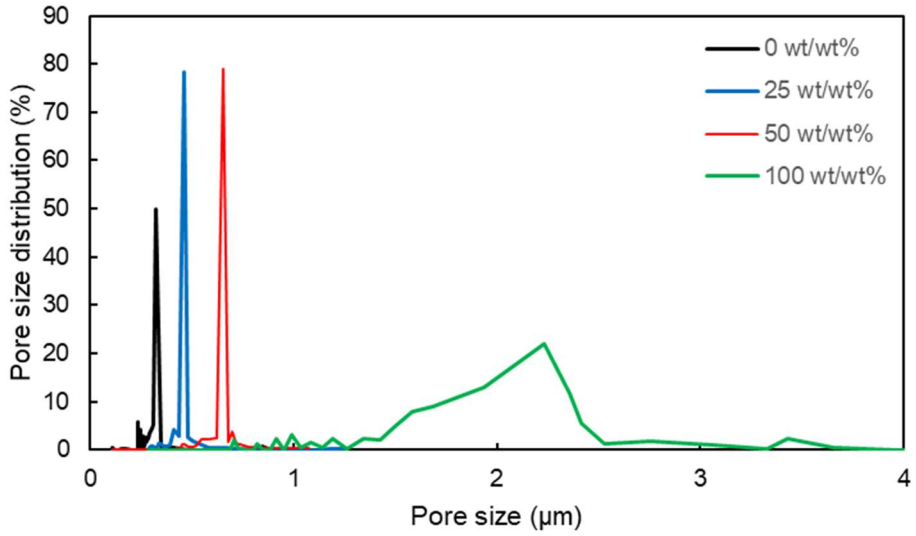

Fig. 6-2 Pore size distribution curves as a function of pore size for the membranes from CPVC solutions with different ratios of Pluronic TR-702/CPVC (wt/wt%).

membrane surfaces became thicker. However, when the concentration of Pluronic TR-702 was 100 wt/wt%, the width of the polymers seemed to be thinner than when the concentration was 50 wt/wt%. The surface porosities of the prepared membranes calculated using the binary images are shown in Table 6-3. When the concentration of Pluronic TR-702 increased from 0 to 50 wt/wt%, the surface porosity of the membranes decreased. On the other hand, the surface porosity of the membranes increased when the concentration of Pluronic TR-702 was 100 wt/wt%. The area occupied by the open pores of the membrane surface decreased or increased, respectively, as the widths of the polymers surrounding the open pore increased or decreased. The cross-section morphologies of the prepared membranes appeared to become more porous as the concentration of Pluronic TR-702 increased. In particular, when the concentration of Pluronic TR-702 was 100 wt/wt%, the membrane was significantly more porous compared to the other concentrations.

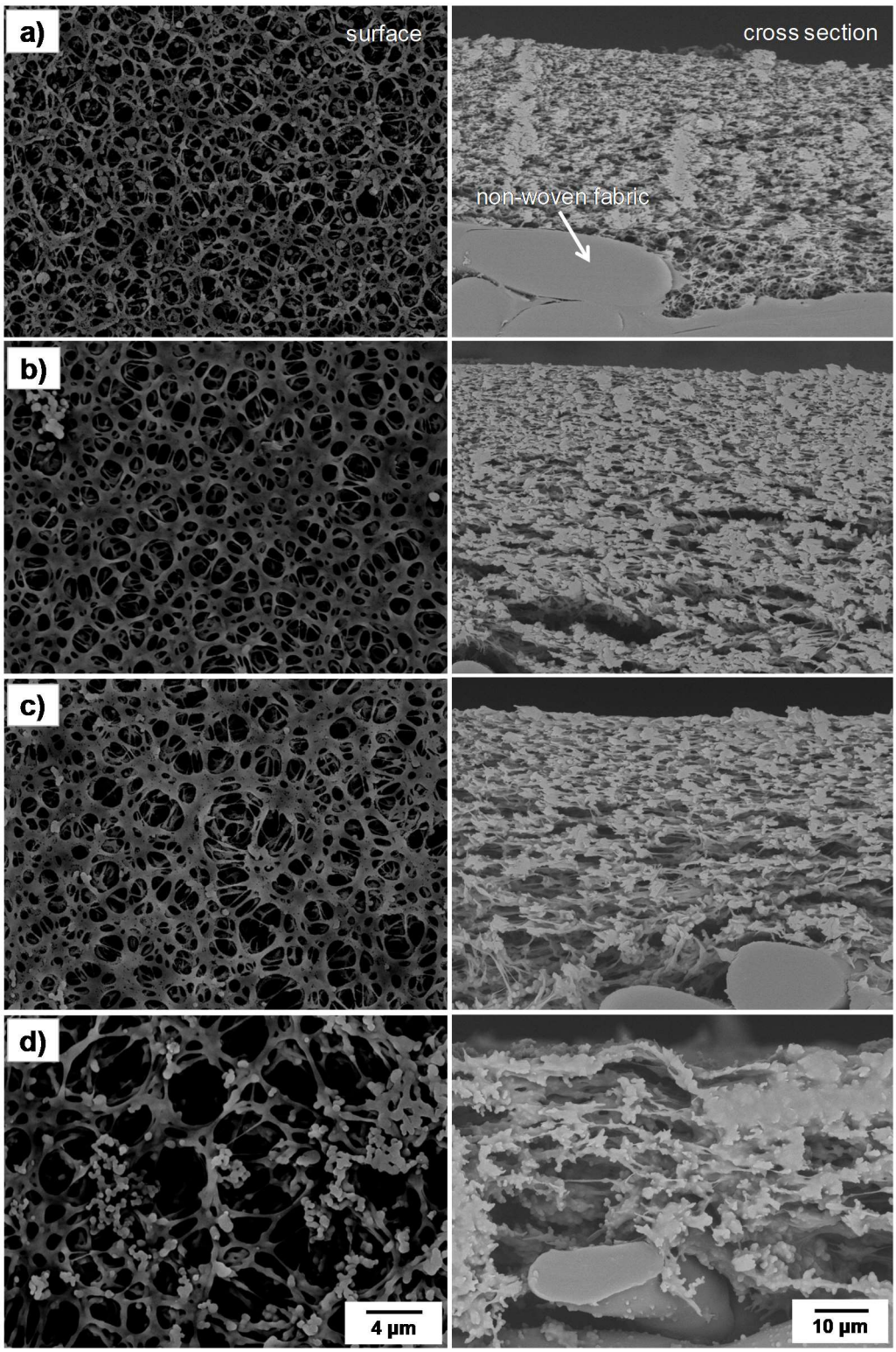

Fig. 6-3 SEM images of the surfaces and cross-sections of the prepared membranes with different concentrations of Pluronic TR-702 at a) 0 wt/wt%, b) 25 wt/wt%, c) 50 wt/wt%, and d) 100 wt/wt%.

VI.4 Discussion

The drastic increases in pore size and porosity were observed in the membrane with a Pluronic TR-702 concentration of 100 wt/wt% compared to other concentrations. As the reason for this result, it was inferred that the porosity of the membrane with a Pluronic TR-702 concentration of 100 wt/wt% increased significantly, which led to an enhanced pure water permeability of the membrane. The significant increase in porosity of the membrane with a Pluronic TR-702 concentration of 100 wt/wt% could be explained by the change in turbidity of the dope solution. When the concentration of Pluronic TR-702 was 100 wt/wt%, the turbidity of the dope solution was surprisingly high compared to that of the dope solutions with other concentrations. This phenomenon indicated that a part of the Pluronic TR-702 added to the dope solution was not dissolved and was present as particles in the dope solution. PES membranes prepared from a homogenous dope solution with added Pluronic F127 tend to have PEO units located in the external layers and polypropylene oxide (PPO) units located in the membrane matrix, as reported by Zhao et al. and Loh et al. [12,14]. In this study, the dope solution with a Pluronic TR-702 concentration of 100 wt/wt% was a heterogeneous solution in which undissolved Pluronic TR-702 particles remained. It was hypothesized that these particles remained in the internal pores of the membrane as independent particles without being incorporated into the membrane matrix when the membrane structure was prepared by phase separation. Therefore, it was probable that these particles leached out of the membrane when the membranes were immersed in ethanol and the particle sites became larger pores. Several reports have stated that microfiltration membranes with symmetric structures have an optimal pore size for suppressing fouling in MBRs [9,47]. van der Marel et al. investigated the influence of the pore size of membranes on membrane fouling in a pilot-

scale MBR using four different pore sizes of symmetric mixed cellulose ester (MCE) flat-sheet membranes [9]. They reported that the membrane with a pore size of 0.8 μm exhibited superior performance compared to the membranes with pore sizes of 0.1, 1.8, and 2.7 μm. Nittami et al. investigated the influence of membrane pore size on membrane fouling in a lab-scale MBR using three different pore sizes of symmetric PTFE flat-sheet membranes [47]. They reported that the optimal pore size of symmetric flat-sheet membranes for mitigating membrane fouling in MBRs was 0.5-1.0 μm. These results suggested that the optimal pore size of symmetric flat-sheet membranes for MBRs was slightly less than 1.0 μm. The structure of the CPVC membranes prepared in this study was also symmetric. In this study, it was concluded that the membrane with a Pluronic TR-702 concentration of 100 wt/wt% was not appropriate for MBRs because its pore size was 2.1 μm, which was much larger than 1.0 μm. In other words, it was assumed that membrane fouling was more likely to develop.

It was clear that the pure water permeability and pore size of the prepared membranes continuously and gradually increased with increasing Pluronic TR-702 concentration from 0 to 50 wt/wt% as shown in Table 6-3. When the concentration of Pluronic TR-702 was 50 wt/wt%, the membrane with the pore size of 0.65 μm, which was within the range of suitable pore size for the use in MBR (0.5-1.0 μm) in previous studies, was prepared. Several reports have shown that the pure water permeability and pore size of blended membranes typically increased with an increase in the additive polymer content in dope solutions [12,16,32,48-50]. Our results with respect to the pure water permeability and pore size are in good agreement with these previous reports. As shown in Table 7-3, the pure water permeabilities were correlated with the pore size. Therefore, the enhanced pure water permeabilities in this study were attributed to the

increased pore size of the prepared membranes. Kang et al. investigated the effect of hydrophilic PVP as an additive on the pore size and distribution of the membrane surface in the preparation of CPVC membranes by water vapor induced phase separation [36]. They reported that PVP in the dope solution promoted the incorporation of atmospheric water vapor into the dope solution resulting in an increase in the pore size because of spontaneous phase separation. Based on their discussion, it was concluded that the introduction of Pluronic TR-702 with hydrophilic PEO units in the dope solution accelerated the incorporation of atmospheric water vapor into the dope solution with non-woven polyester fabric as a support layer. As a result, the pore size and distribution increased due to the introduction of a large amount of water vapor into the dope solution. Simultaneously, an increased amount of incorporated water vapor caused an increase in membrane thickness [51]. Furthermore, in their investigation, although not shown as numerical data, it was obvious from SEM photographs that the surface porosity decreased with an increase in the amount of PVP added. This tendency was consistent with the changes in the surface porosity of the membranes prepared with a concentration of Pluronic TR-702 in the range of 0 to 50 wt/wt%. Tsai et al. investigated the influence of exposure time on the pore structure in the preparation of polysulfone (PSf) membranes by water vapor induced phase separation [52]. They reported that longer exposure times to water vapor resulted in evolution from a lacy structure to cell-like pores due to the coarsening of the polymer-rich phase. A similar tendency was also observed in the work of Su et al. [53]. I compared the SEM photographs in their results with those of this study. Consequently, I concluded that the phenomenon of the increased width of polymers surrounding the open pores in this study was the same phenomenon as the evolution of the pore structure due to the coarsening of the polymer-rich phase in the previous studies.

Although the reason for this was unknown, it is possible that all these phenomena were caused by an increase in the amount of water vapor incorporated into the dope solution. Tsai et al. also suggested that coarsening and coalescence of the polymer-rich phase could lead to the formation of a dense layer [52]. I also considered this phenomenon to be observed in this study. Therefore, it was determined that Pluronic TR-702 added to the dope solution played an important role in forming a membrane with a more porous structure and denser surface.

VI.5 Conclusions

The excessive addition of Pluronic TR-702 to the dope solution could lead to the preparation of membranes with large pore sizes that were unsuitable for applications in MBRs. On the other hand, with the addition of an appropriate amount of Pluronic TR-702 to the dope solution, it was found that the pore size and thickness of the membranes increased with an increase in the concentration of Pluronic TR-702 and the porosity of the membranes decreased with an increase in the concentration of Pluronic TR-702. In particular, the increase in pore size and thickness of the membranes led to an increased porosity of the membrane structure. Therefore, this method of adding Pluronic TR-702 was demonstrated to be appropriate for controlling the pore structure of the membrane. This improved technique for the preparation of CPVC flat-sheet membranes may contribute to the further development of MBRs due to its resulting antifouling properties.

References

[1] P. Le-Clech, V. Chen and T.A.G. Fane, Fouling in membrane bioreactors used in wastewater treatment, *J. Membr. Sci.*, 284, 17-53 (2006).

[2] W. Yang, N. Cicek and J. Llg, State-of-the-art of membrane bioreactors: worldwide research and commercial applications in North America, *J. Membr. Sci.*, 270, 201-211 (2006).

[3] N. Yamato, K. Kimura, T. Miyoshi and Y. Watanabe, Difference in membrane fouling in membrane bioreactors (MBRs) caused by membrane polymer materials, *J. Membr. Sci.*, 280, 911-919 (2006).

[4] A. Kola, Y. Ye, P. Le-Clech and V. Chen, Transverse vibration as novel membrane fouling mitigation strategy in anaerobic membrane bioreactor applications, *J. Membr. Sci.*, 455, 320-329 (2014).

[5] T. Kurita, K. Kimura and Y. Watanabe, The influence of granular materials on the operation and membrane characteristics of submerged MBRs, *J. Membr. Sci.*, 469, 292-299 (2014).

[6] C. Niu, Y. Pan, X. Lu, S. Wang, Z. Zhang, C. Zheng, Y. Tan, G. Zhen, Y. Zhao and Y.-Y. Li, Mesophilic anaerobic digestion of thermally hydrolyzed sludge in anaerobic membrane bioreactor: Long-term performance, microbial community dynamics and membrane fouling mitigation, *J. Membr. Sci.*, 612, 118264 (2020).

[7] S. Judd, The MBR Book: Principles and Applications of Membrane Bioreactors for Water and Wastewater Treatment 2nd ed., Oxford, Elservier, 2011.

[8] H. Matsuyama, T. Takahashi and M. Yasukawa, Present situation and future prospects of water treatment technology with membrane, *Membrane*, 39, 209-216 (2014).

[9] P. van der Marel, A. Zwijnenburg, A. Kemperman, M. Wessling, H. Tenmink and W. van der Meer, Influnece of membrane properties on fouling in submerged membrane bioreactors, *J. Membr. Sci.*, 348, 66-74 (2010).

[10] J.-H. Choi and H.Y. Ng, Effect of membrane type and material on performance of a

submerged membrane bioreactor, *Chemosphere*, 71, 853-859 (2008).

[11] T. Tsuyuhara, Y. Hamamoto, T. Miyoshi, K. Kimura and Y. Watanabe, Influence of membrane properties on physically reversible and irreversible fouling in membrane bioreactors, *Water Sci. Technol.*, 61, 2235-2240 (2010).

[12] W. Zhao, Y. Su, C. Li, Q. Shi, X. Ning and Z. Jiang, Fabrication of antifouling polyethersulfone ultrafiltration membranes using Pluronic F127 as both surface modifier and pore-forming agent, *J. Membr. Sci.*, 318, 405-412 (2008).

[13] E. Saljoughi, M. Amirilargani and T. Mohammdai T, Effect of poly(vinyl pyrrolidone) concentration and coagulation bath temperature on the morphology, permeability, and thermal stability of asymmetric cellulose acetate membranes, *J. Appl. Polym. Sci.*, 111, 2537-2544 (2020)

[14] C.H. Loh, R. Wang, L. Shi and A.G. Fane, Fabrication of high performance polyethersulfone UF hollow fiber membranes using amphiphilic Pluronic block copolymers as pore-forming additives, *J. Membr. Sci.*, 380, 114-123 (2011).

[15] H. Rabiee, S.M.S. Shahabadi, A. Mokhtare, H. Rabiei and N. Alvandifar, Enhancement in permeation and antifouling properties of PVC ultrafiltration membranes with addition of hydrophilic surfactant additives: Tween-20 and Tween-80, *J. Environ. Chem. Eng.*, 4, 4050-4061 (2016).

[16] J. Liu, Y. Su, J. Peng, X. Zhao, Y. Zhang, Y. Dong and Z. Jiang, Preparation and performance of antifouling PVC/CPVC blend ultrafiltration membranes, *Ind. Eng. Chem. Res.*, 51, 8308-8314 (2012).

[17] J. Wang, M. Qiu and C. He, A zwitterionic polymer/PES membrane for enhanced antifouling performance and promoting hemocompatibility, *J. Membr. Sci.*, 606, 118119 (2020).

[18] T. Miyoshi, T. Tsuyuhara, R. Ogyu, K. Kimura and Y. Watanabe, Seasonal variation in membrane fouling in membrane bioreactors (MBRs) treating municipal wastewater, *Water Res.*, 43, 5109-5118 (2009).

[19] L. Vanysacker, P. Declerck, M.R. Bilad and I.F.J. Vankelecom, Biofouling on microfiltration membranes in MBRs: role of membrane type and microbial community, *J. Membr. Sci.*, 453, 394-401 (2014).

[20] T. Nittami, H. Tokunaga, A. Satoh, M. Takeda and K. Matsumoto, Influence of surface hydrophilicity on polytetrafluoroethylene flat sheet membrane fouling in a submerged membrane bioreactor using two activated sludges with different characteristics, *J. Membr. Sci.*, 463, 183-189 (2014).

[21] J. Morita, N. Shimada, M. Higashi and T. Kitagawa, A pilot-plant test of a membrane bioreactor with a novel membrane made from chlorinated poly (vinyl chloride) (CPVC) and hydroxy-propyl cellulose, *J. Membr. Sep. Technol.*, 4, 74-88 (2015).

[22] H.H. Chu and X.-y. Li, Membrane fouling in a membrane bioreactor (MBR): sludge cake formation and fouling characteristics, *Biotechnol. Bioeng.*, 90, 323-331 (2005).

[23] K. Kimura, N. Yamato, H. Yamamura and Y. Watanabe, Membrane fouling in pilot-scale membrane bioreactors (MBRs) treating municipal wastewater, *Environ. Sci. Technol.*, 39, 6293-6299 (2005).

[24] Z. Wang, Z. Wu, G. Yu, J. Liu and Z. Zhou, Relationship between sludge characteristics and membrane flux determination in submerged membrane bioreactors, *J. Membr. Sci.*, 284, 87-94 (2006).

[25] Z. Wu, Z. Wang, S. Huang, S. Mai, C. Yang, X. Wang and Z. Zhou, Effects of various factors on critical flux in submerged membrane bioreactors for municipal wastewater treatment, *Sep. Purif. Technol.*, 62, 56-63 (2008).

[26] M. Tokushima, Development for energy–saving MBR technology, *Membrane*, 37, 235-239 (2012).

[27] N. Shimada, J. Morita, M. Higashi, T. Kitagawa and J. Nakajima, Long term pilot MBR test for a newly development flat-sheet membrane made from chlorinated polyvinyl chloride in treatment of kitchen wastewater from a cafeteria, *J. Water Environ. Technol.*, 14, 329-340 (2016).

[28] Q.-V. Bach, V.T. Le, Y.S. Yoon, X.T. Bui, W. Chang, S.W. Chang, H.H. Ngo, W. Guo and D.D. Nguyen, A new hybrid sewage treatment system combining a rolled pipe system and membrane bioreactor to improve the biological nitrogen removal efficiency: a pilot study, *J. Clean. Prod.*, 178, 937-946 (2018).

[29] T. Sano, Y. Koga, H. Ito, L.V. Duc, T. Hama and Y. Kawagoshi, Effects of structural vulnerability of flat-sheet membranes on fouling development in continuous submerged membrane bioreactors, *Bioresour. Technol.*, 304, 123015 (2020).

[30] M. Higashi, J. Morita, N. Shimada and T. Kitagawa, Long-term-hydrophilic flat-sheet microfiltration membrane made from chlorinated poly(vinyl chloride), *J. Membr. Sci.*, 500, 180-189 (2016).

[31] T. Sano and K. Oka, Porous membrane and its production process, *Japanese patent*, P2009-112895A.

[32] H.-H. Chang, S.-C. Chen, D.-J. Lin and L.-P. Cheng, The effect of Tween-20 additive on the morphology and performance of PVDF membranes, *J. Membr. Sci.*, 466, 302-312 (2014).

[33] H. Susanto and M. Ulbricht, Characteristics, performance and stability of polyethersulfone ultrafiltration membranes prepared by phase separation method using different macromolecular additives, *J. Membr. Sci.*, 327, 125-135 (2009).

[34] S. Liu, Y. Chu, C. Tang, S. He and C. Wu, High-performance chlorinated polyvinyl chloride ultrafiltration membranes prepared by compound additives regulated non-solvent induced phase separation, *J. Membr. Sci.*, 612, 118434 (2020).

[35] H. Wu, T. Li, B. Liu, C. Chen, S. Wang and J.C. Crittenden, Blended PVC/PVC-g-PEGMA ultrafiltration membranes with enhanced performance and antifouling properties, *Appl. Surf. Sci.*, 455, 987-996 (2018).

[36] J.S. Kang, K.Y. Kim and Y.M. Lee, Preparation of microporous chlorinated poly (vinyl chloride) membrane in fabric and the characterization of their pore sizes and pore-size distributions, *J. Appl. Polym. Sci.*, 86, 1195-1202 (2002).

[37] M.-H. Xu, R. Xie, X.-J. Ju, W. Wang, Z. Liu and L.-Y. Chu, Antifouling membranes with bi-continuous porous structures and high fluxes prepared by vapor-induced phase separation, *J. Membr. Sci.*, 611, 118256 (2020).

[38] I.M. Wienk, E.E.B. Meuleman, Z. Borneman, T. van den Boomgaard and C.A. Smolders, Chemical treatment of membranes of a polymer blend: mechanism of the reaction of hypochlorite with poly(viny1 pyrrolidone), *J. Polym. Sci. Part A : Polym Chem.*, 33, 49-54 (1995).

[39] J.-J. Qin, M.H. Oo and Y. Li, Development of high flux polyethersulfone hollow fiber ultrafiltration membranes from a low critical solution temperature dope via hypochlorite treatment, *J. Membr. Sci.*, 247, 137-142 (2005).

[40] N. Arahman, T. Maruyama, T. Sotani and H. Matsuyama, Effect of hypochlorite treatment on performance of hollow fiber membrane prepared from polyethersulfone/N-methyl-2-pyrrolidone/Tetronic 1307 solution, *J. Appl. Polym. Sci.*, 110, 687-694 (2008).

[41] N. Arahman, N. Mukramah, S. Maulidayanti and A.O. Putri, The stability of poly(ether sulfone) membranes treated in hot water and hypochlorite solution, *Procedia*

Chem., 16, 709-715 (2015).

[42] Z. Wang, Z. Wu, G. Yu, J. Liu and Z. Zhou, Membrane cleaning in membrane bioreactors: a review, *J. Membr. Sci.*, 468, 276-307 (2014).

[43] H. Sato, A. Shibata, H. Yoshikawa and H. Tamura, Biodegradation mechanisms of non-ionic surfactants evaluated by MALDI-MS, *J. Mass. Spectrom. Soc. Jpn.*, 51, 415-420 (2003).

[44] J.-H. Choi, S.-K. Park and H.-Y. Ng, Membrane fouling in a submerged membrane bioreactor using track-etched and phase-inversed porous membranes, *Sep. Purif. Technol.*, 65, 184-192 (2009).

[45] A. Jena and K. Gupta, Advances in pore structure evaluation by porometry, *Chem. Eng. Technol.*, 33, 1241-1250 (2010).

[46] T. Marino, E. Blasi, S. Tornagahi, E.D. Nicoló and A. Figoli, Polyethersulfone membranes prepared with Rhodiasolv® Polarclean as water soluble green solvent, *J. Membr. Sci.*, 549, 192-204 (2018).

[47] T. Nittami, T. Hitomi, K. Matsumoto, K. Nakamura, T. Ikeda, Y. Setoguchi and M. Motoori, Comparison of polytetrafluoroethylene flat-sheet membranes with different pore sizes in application to submerged membrane bioreactor, *membranes*, 2, 228-236 (2012).

[48] J. Xu and Z.-L. Xu, Poly(vinyl chloride) (PVC) hollow fiber ultrafiltration membranes prepared from PVC/additives/solvent, *J. Membr. Sci.*, 208, 203-212 (2002).

[49] M. Amirilargani, E. Saljoughi and T. Mohammadi, Effects of Tween 80 concentration as a surfactant additive on morphology and permeability of flat sheet polyethersulfone (PES) membranes, *Desalination*, 249, 837-842 (2009).

[50] X. Fan, Y. Su, X. Zhao, Y. Li, R. Zhang, J. Zhao, Z. Jiang, J. Zhu, Y. Ma and Y. Liu,

Fabrication of polyvinyl chloride ultrafiltration membranes with stable antifouling property by exploring the pore formation and surface modification capabilities of polyvinyl formal, *J. Membr. Sci.*, 464, 100-109 (2014).

[51] V.P. Khare, A.R. Greenberg and W.B. Krantz, Vapor-induced phase separation - effect of the humid air exposure step on membrane morphology Part I. Insights from mathematical modeling, *J. Membr. Sci.*, 258, 140-156 (2005).

[52] J.T. Tsai, Y.S. Su, D.M. Wang, L.J. Kuo, J.Y. Lai and A. Deratani, Retainment of pore connectivity in membranes prepared with vapor-induced phase separation, *J. Membr. Sci.*, 362, 360-373 (2010).

[53] Y.S. Su, C.Y. Kuo, D.M. Wang, J.T. Lai, A. Deratani, C. Pochat and D. Bouyer, Interplay of mass transfer, phase separation, and membrane morphology in vapor-induced phase separation, *J. Membr. Sci.*, 338, 17-28 (2009).

Chapter VII

Fabrication of high-performance chlorinated poly(vinyl chloride) flat-sheet membranes using commercially available fluoropolymers as membrane-property modifiers

---

VII.1 Introduction

Membrane bioreactors (MBRs) have been adopted widely in different types of wastewater treatment plants all over the world, resulting in a significant increase in their market share [1,2]. However, MBRs continue to be plagued by membrane fouling which can significantly reduce the permeation flux. In the case of extreme membrane fouling, it becomes necessary to clean or replace the membrane module, which can increase the operation and maintenance costs [1,3]. In general, the fouling propensities of membranes are determined by their characteristics such as the type of material used, surface hydrophilicity, pure water permeability, pore size and distribution, surface porosity, membrane morphology, and surface roughness [4-9]. Therefore, to mitigate membrane fouling, it is essential to develop techniques for controlling the properties of the membranes.

Chlorinated poly(vinyl chloride) (CPVC) flat-sheet microfiltration membranes with a nonwoven polyester fabric as a support layer are used extensively in MBRs [10-13] because of their excellent chemical and mechanical properties. CPVC flat-sheet membranes are generally prepared via water vapor induced phase separation (VIPS), which results in the formation of a symmetric structure both within and on the support layer [11,12]. On the other hand, several studies have reported that blending an

amphiphilic polymer in ultrafiltration and microfiltration membranes can improve the membrane properties such as the surface hydrophilicity and antifouling characteristics [14-17]. Pluronic polymers such as poly(ethylene oxide)-poly(propylene oxide)-poly(ethylene oxide) triblock copolymer are typical commercially available amphiphilic polymers. Therefore, Pluronic polymers are often used as additives in membranes [14,16,17]. However, apart from Pluronic polymers, numerous other types of polymers are also commercially available that can used as polymer additives in membranes. Therefore, to develop a suitable technique for controlling the membrane properties and optimizing their fabrication procedure, it is important to elucidate the differences in the properties of membranes that are prepared using different polymers as additives. In this study, I focused on fluoropolymers whose chemical structures are significantly different from those of Pluronic polymers [18,19]. Thus, fluoropolymers may show unique characteristics as membrane-property modifiers.

With the aim of developing an effective method for controlling the properties of membrane, in this study, CPVC flat-sheet membranes containing commercially available fluoropolymers as additives were prepared by the VIPS method, and their effects on the membrane properties were analyzed.

VII.2 Materials and methods

VII.2.1 Materials

CPVC with a polymerization degree of approximately 800 was purchased from KANEKA Corp., Japan and used to form a membrane. Tetrahydrofuran (THF) and 2-propanol (IPA) were purchased from FUJIFILM Wako Pure Chemical Corp., Japan and used as the solvent and non-solvent, respectively. Unidyne DSN-403N (a perfluoroalkyl

poly(ethylene oxide) adduct compound) and Surflon S-420 (a perfluoroalkyl compound) which were kindly provided by Daikin Industries Ltd., and AGC Seimi Chemical Co., Japan were used as the additive polymers, respectively. For comparison, Pluronic F-108 and L-64 which was kindly provided by Adeka Corp., Japan were used as the Pluronic polymer additives.

VII.2.2 Membrane fabrication

The membranes were prepared from a dope solution containing CPVC, THF, IPA, and different types of additive polymers. The corresponding solution compositions are listed in Table 7-1. The dope solution was prepared by the following procedure. CPVC was dissolved in THF, and the mixture was stirred at 40 °C for 8 h in a water bath to obtain a homogenous solution. This solution was subsequently cooled to 25 °C, followed by adding IPA and the polymer additives to it. The resulting solution was stirred for more than 24 h until a homogenous solution was obtained.

The membranes were prepared via the VIPS method in a room under constant temperature and humidity. A nonwoven polyester fabric with a density of 0.55 g/cm^3 and thickness of 130 μm was used as the support layer. This fabric was dipped into a vessel containing the dope solution and then removed through a clearance gap between two stainless steel rolls that were adjusted to be at a constant distance. The temperature and humidity in the room were maintained at approximately 30 °C and 70%, respectively. The nonwoven polyester fabric impregnated with the dope solution was kept in the room for more than 2 h till it was completely dry, and the membrane structure had solidified.

The viscosities of the dope solutions were measured by a viscometer (BL II, Toki Sangyo Co., Ltd., Japan). All measurements were performed at a constant

Table 7-1 Composition of the dope solutions used for preparing CPVC/polymer-additive membranes

CPVC (g)	THF (g)	IPA (g)	Polymer additive	
			Type	Amount (g)
20	125	55	Control	0
20	125	55	F-108	5
20	125	55	L-64	5
20	125	55	DSN-403N	5
20	125	55	S-420	5

temperature of 25 °C.

VII.2.3 Membrane characterization

VIII.2.3.1 Surface hydrophilicity

The hydrophilicities of the membranes were determined by measuring their contact angles via the sessile drop method by using a contact angle goniometer (DMs-401, Kyowa Interface Science Co., Japan) at a constant temperature of 25 °C.

VII.2.3.2 Pure water permeability

The pure water permeabilities of the membranes were measured by wetting the membranes and using them to filter distilled water. The prepared membranes were placed in a dead-end filtration unit, and distilled water was filtered under a constant pressure of 0.5 bar and temperature of 25 °C. Subsequently, the filtration time for a 100 mL permeate volume was measured. The pure water permeability, L (mL/cm^2·bar·min), was calculated using the following equation [20]:

$$L = \frac{Q}{A \times \Delta t \times \Delta P} \qquad (7-1)$$

where Q is the permeate volume (mL), A is the effective membrane area (cm^2), Δt is the

filtration time (min), and ΔP is the applied transmembrane pressure (bar).

VII.2.3.3 Pore size and distribution

The pore sizes and size distributions of the fabricated membranes were measured by a capillary flow porometer (CFP-1200A, Porous Materials Inc., USA). This apparatus was used to determine the pore diameters of the membranes via the liquid-gas displacement process. The membranes were fully wetted with Galwick which has a low surface tension. The fully wetted membrane was then placed in the sample chamber, and the liquid was extruded from the membrane pores by gradually increasing the air pressure. The flow rate of the air extruded from the membrane pores was measured by a flow meter placed in the apparatus. The mean flow pore diameter, d, was calculated by using the following equation [21]:

$$d = \frac{C\gamma}{p} \qquad (7-2)$$

where C is a constant, γ is the surface tension of Galwick, and p is the differential pressure when the wet flow is half of the dry flow.

VII.2.3.4 Surface morphology and porosity

The surface morphologies of the fabricated membranes were observed via a scanning electron microscope (SEM, TM3030, Hitachi High-Technologies Co., Japan). The surface porosities of the membranes were calculated by binarizing the SEM images of the membrane surfaces by using an image processing software (Image J, National Institutes of Health, USA). In the binarized images, the open-pore areas were designated with black color and the nonporous areas were designated with white color. The surface porosity was determined by the ratio of the total open-pore area to the total surface area.

VII.2.3.5 Surface roughness

The surface roughness of the fabricated membranes were measured by using a portable surface roughness tester (Surftest SJ-410, Mitutoyo Corp., Japan) which uses a contact stylus to make physical contact with the membrane surface. The measurements were performed at a contact force of 7.5×10^{-4} N and a measurement speed of 0.5 mm/s by using a diamond stylus tip. The sampling length was 4 mm. Furthermore, the surface roughness also were analyzed in a narrow area by atomic force microscopy (AFM, AFM5100N, Hitachi High-Technologies Corp., Japan) in the dynamic force mode by suing an SI-DF3P2 (spring constant = 2 N/m) cantilever silicon tip. The scan area was 5 × 5 μm. Both type of measurements were performed in air at room temperature.

VII.3 Results

VII.3.1 Viscosities of dope solutions

Table 7-2 lists the viscosities of the used dope solutions which consisted of CPVC, THF, IPA, and one of the polymer additives. The viscosities of all the dope solutions containing the polymer additives were higher than that of the control solution. Moreover, the viscosities of the dope solutions containing the fluoropolymers as additives were higher than those of the dope solutions containing the Pluronic polymers as additives. In particular, the dope solution containing Surflon S-420 exhibited the highest viscosity.

VII.3.2 Hydrophilicities of fabricated membranes

Table 7-3 lists the water contact angles of the membranes fabricated with and without the different polymer additives. The contact angles of the membranes containing the polymer additives were significantly lower than that of the control membrane.

Table 7-2 Viscosities of the dope solutions

Polymer additive	Control	F-108	L-64	DSN-403N	S-420
Viscosity (mPa·s)	60	66	65	70	84

Table 7-3 Water contact angles of the fabricated membranes after 0 and 180 s

Polymer additive	Contact angle (°)	
time	0 s	180 s
Control	119	117
F-108	33	0
L-64	10	0
DSN-403N	14	0
S-420	35	0

the polymer additives were significantly lower than that of the control membrane. Moreover, the contact angles of all the membranes containing polymer additives reduced to 0° after 180 s. Therefore, it can be concluded that the hydrophilicity of the membranes enhanced due to the polymer additives. However, the hydrophilicities of the membranes with the fluoropolymers were not significantly different from those of the membranes with the Pluronic polymers.

VII.3.3 Pure water permeability of fabricated membranes

Figure 7-1 shows the pure water permeabilities of the membranes with and without the different polymer additives. The pure water permeability of the membrane containing Surflon S-420 was the highest. In contrast, the pure water permeabilities of the membranes with the other polymer additives were lower than that of the control membrane. However, the difference was slight, with the exception of the membrane with Pluronic F-108. According to the Hagen-Poiseuille law, for a constant transmembrane

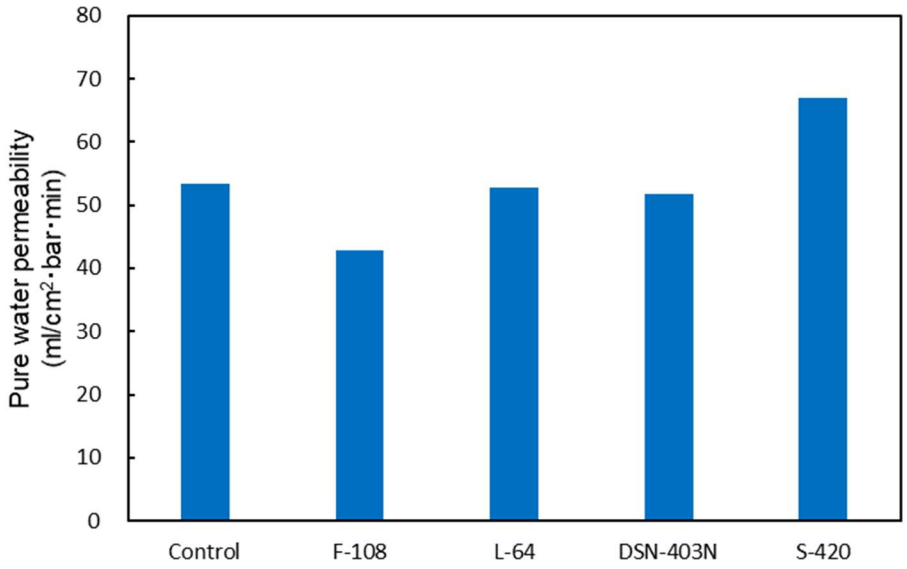

Fig. 7-1 Pure water permeabilities of membranes fabricated using different polymer additives.

pressure, water viscosity, and membrane thickness, the pure water permeability of a membrane is determined by its porosity. In our case, the transmembrane pressure was constant. Furthermore, the viscosity of the water during the measurements also was constant because the measurements were performed at the same temperature. In addition, the membrane thicknesses were also similar (data not shown). Therefore, it can be assumed that the enhanced pure water permeability of the membrane containing Surflon S-420 additive is due to an increase in the porosity of the membrane.

VII.3.4 Pore size and distribution of fabricated membranes

Figure 7-2 shows the mean flow pore sizes of the membranes with and without the different polymer additives. In general, the mean flow pore size is indicative of the average pore size. The pore sizes of all the membranes with the polymer additives were larger than that of the control membrane with the exception of the Pluronic F-108-added

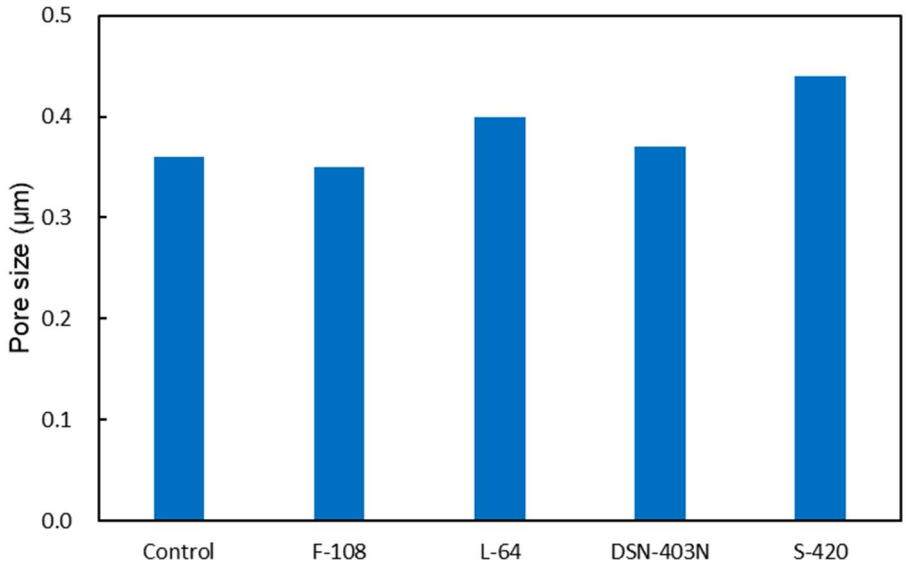

Fig. 7-2 Pore sizes of membranes fabricated using different polymer additives.

membrane. In particular, the pore size of the membrane with Surflon S-420 was significantly larger than those of the other membranes. In contrast, the pore size of the membrane with Pluronic F-108 was slightly smaller than that of the control membrane. The pore size distribution curves of the membranes with and without the polymer additives are shown in Fig. 7-3. The membrane with Surflon S-420 exhibited a broad size distribution, whereas the membranes with the other polymer additives exhibited narrow size distributions.

VII.3.5 Surface morphologies and porosities of fabricated membranes

Figure 7-4 shows the surface morphologies of the membranes with and without the polymer additives. The SEM images show that all the membranes exhibited porous surfaces. In addition, the surface pores of the fluoropolymer-added membranes were much smaller than those of the other membranes. Furthermore, the widths of the additive

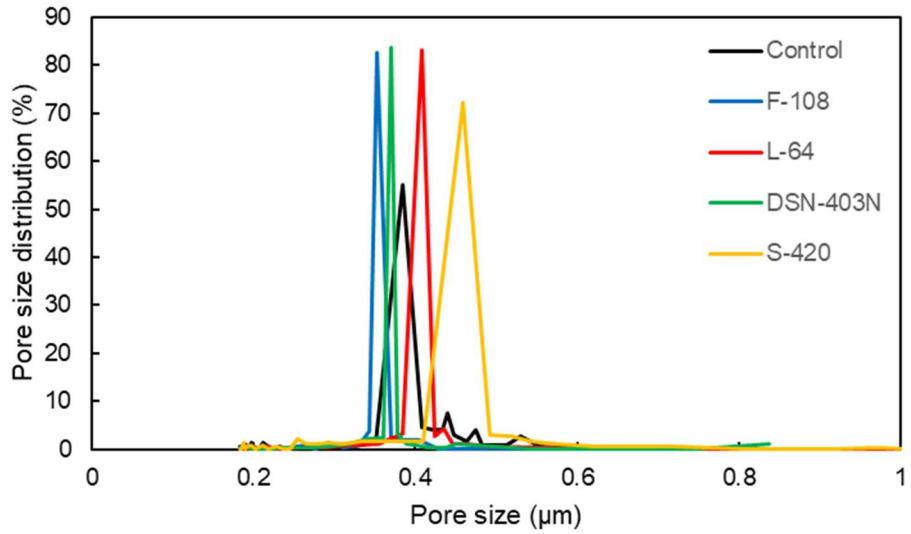

Fig. 7-3 Pore size distributions of membranes fabricated using different polymer additives.

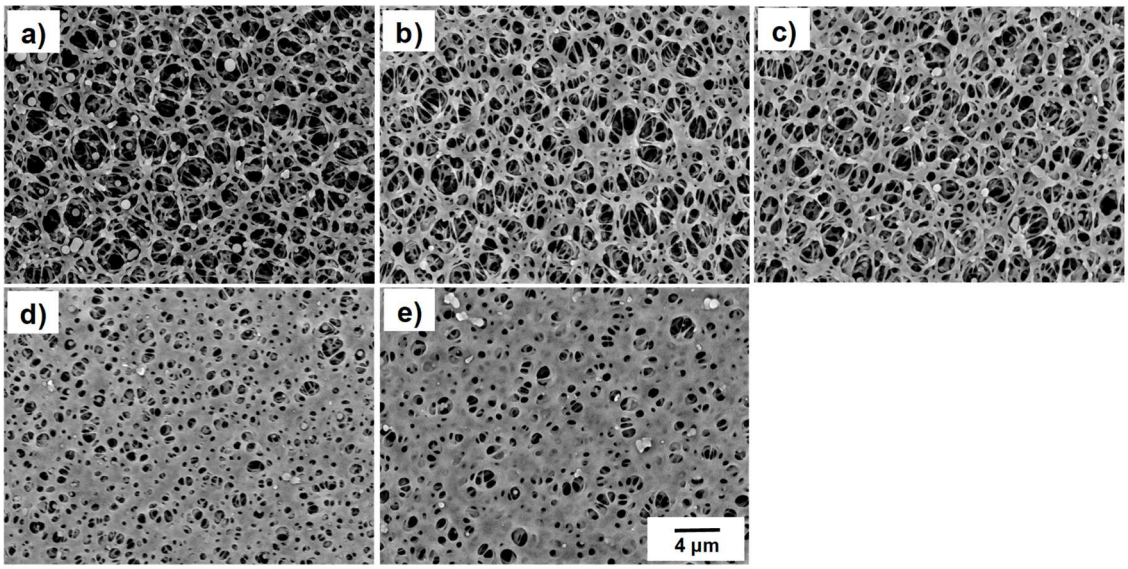

Fig. 7-4 SEM images of the surfaces of membranes fabricated using different polymer additives: a) control membrane, b) Pluronic F-108, c) Pluronic L-64, d) Unidyne DSN-403N, e) Surflon S-420.

polymers surrounding the open pores on the membrane surfaces were greater in the case of Pluronic polymer-added membranes than that in the control membrane.

The surface porosities of the fabricated membranes as calculated from their

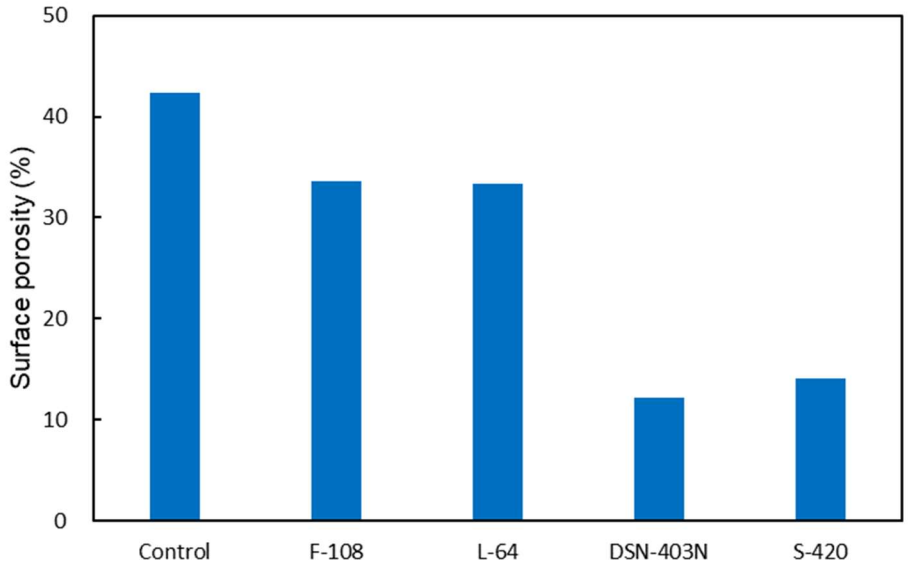

Fig. 7-5 Surface porosities of membranes fabricated using different polymer additives.

binarized images are shown in Fig. 7-5. It was observed that the surface porosities of all the membranes containing the polymer additives were lower than that of the control membrane. This indicates that the area occupied by the pores on the membrane surface decreased. In particular, the surface porosities of the membranes with the fluoropolymers were significantly lower than those of the other membranes containing different additives.

VII.3.6 Surface roughness of fabricated membranes

Figure 7-6 shows the surface roughness line profiles of the membranes with and without the different polymer additives. The surface roughness of the membranes containing the Pluronic polymers were more pronounced than that of the control membrane. Conversely, the fluoropolymer-added membrane surfaces were smoother than that of the control membrane. In particular, the membrane containing Unidyne DSN-403N exhibited the smoothest surface. Figure 7-7 shows AFM images of the fabricated

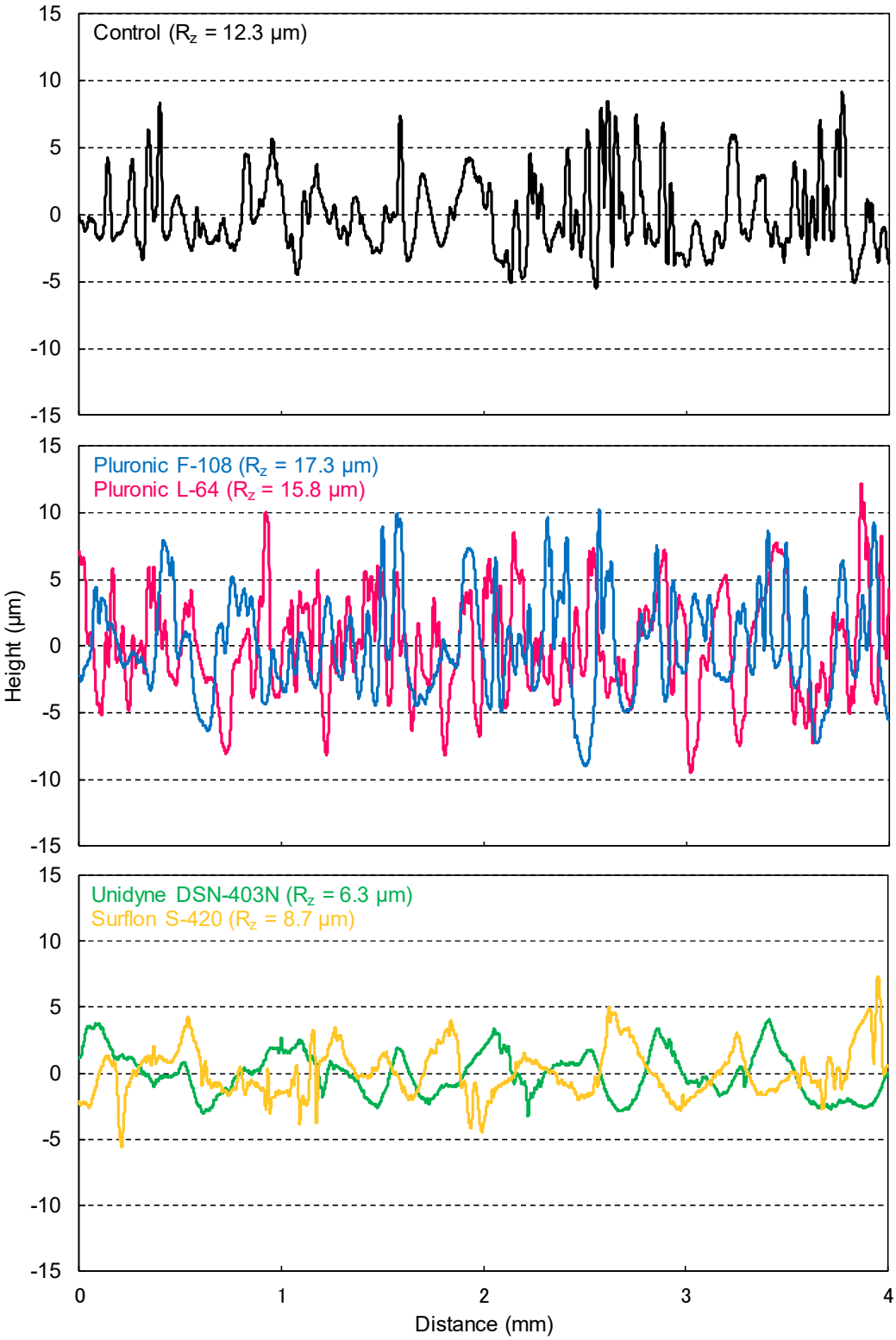

Fig. 7-6 Surface roughness line proflies of membranes fabricated using different polymer additives as determined using surface roughness tester.

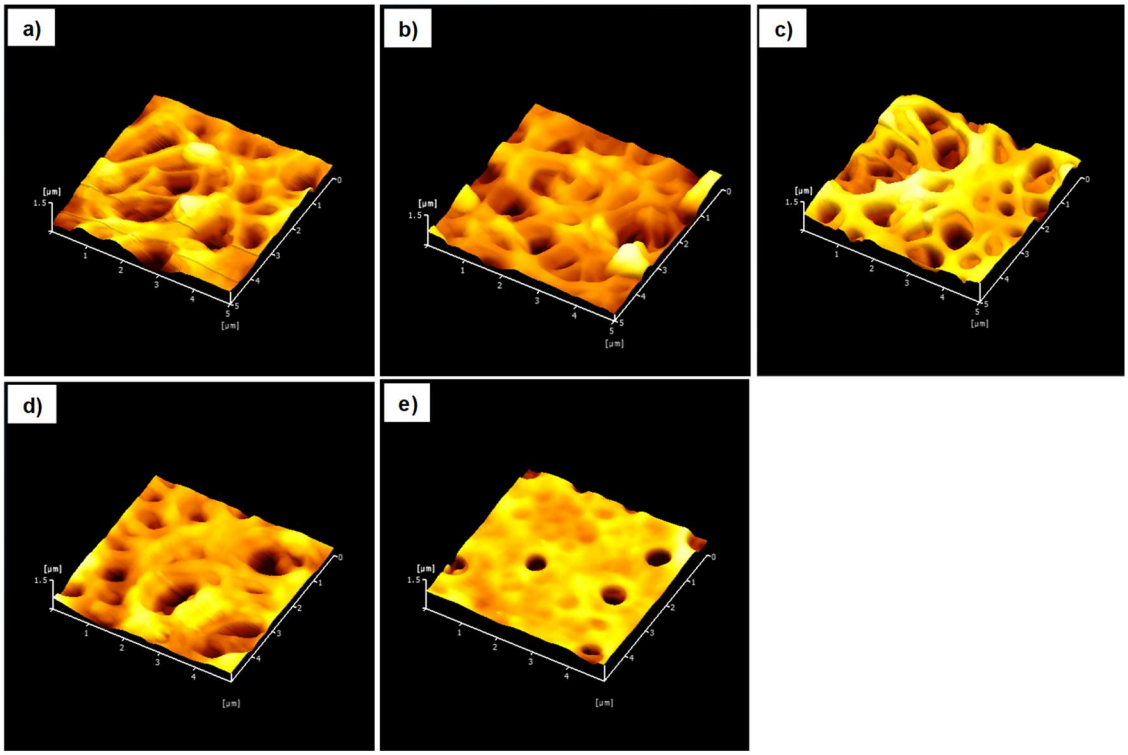

Fig. 7-7 AFM images of membranes fabricated using different polymer additives: a) control membrane, b) Pluronic F-108, c) Pluronic L-64, d) Unidyne DSN-403N, e) Surflon S-420.

membranes. It is clear that the membranes prepared using the fluoropolymers have smoother surfaces. These results are similar to those of the line profile measurements using portable surface roughness tester.

VII.4 Discussion

The membranes that were prepared using the fluoropolymers exhibited structures different from that of the control membrane as well as those of the membranes prepared using the Pluronic polymers. When Surflon S-420 was used as the additive, the surface porosity of the membrane was lower (i.e., the surface was denser), and the surface was smoother than those of the control membrane and the membranes prepared using the

Pluronic polymers. This was observed despite the fact that the Surflon S-420-added membrane showed the highest porosity. Conversely, when Unidyne DSN-403N was used as the additive, the surface porosity of the membrane was the lowest (i.e., the surface was the densest), and the surface was the smoothest, even though this membrane was as porous as the control membrane. In addition, the surface pore sizes of these two membranes were smaller than those of the other membranes. Therefore, it can be concluded that the addition of the fluoropolymers produced membranes that have smoother and denser surfaces as well as show high porosity. I believe that the phenomenon of the formation of a dense membrane surface observed in this study is similar to the evolution of the pore structure because of the coarsening of the polymer-rich phase, as observed in a previous study [17]. The viscosities of the fluoropolymer-mixed dope solutions were higher than those of the other solutions; this may have also contributed to the formation of a dense surface. It is likely that the high viscosities of the former solutions hindered the diffusion of atmospheric water vapor into the dope solution, resulting in a delay in the phase separation and consequently the formation of a denser membrane surface. However, it is known that, when used as leveling agents, fluoropolymers can significantly lower the surface tension in solvent systems. Therefore, this functionality of the fluoropolymers may have aided the formation of smoother membrane surfaces. In general, membranes with denser and smoother surfaces are considered less susceptible to membrane fouling [22,23]. Thus, it can be expected that the membranes containing the fluoropolymers as additives would show excellent antifouling properties in MBRs. The primary purpose of blending Pluronic polymers in membranes is to improve their surface hydrophilicity [14,16]. Considering this aspect, the addition of the fluoropolymers also improved the hydrophilicity of the membrane

surfaces.

Numerous studies have investigated the relationship between the properties of membranes and their fouling propensity. Based on the results of such studies, it is believed that membranes with a higher pure water permeability have a lower fouling propensity in MBRs [20,23]. In our case, only the membrane prepared using Surflon S-420 as an additive showed a higher pure water permeability than that of the control membrane; therefore, it can be expected that of all the membranes fabricated in this study, the Surflon S-420 added membrane would exhibit the best antifouling characteristics in MBRs.

VII.5 Conclusions

In this study, I investigated the effects of different polymer additives on the properties of membranes for MBR applications. I used commercially available fluoropolymers instead of the commonly used amphiphilic polymers such as Pluronic polymers to prepare CPVC membranes by the VIPS method. The addition of fluoropolymers such as Unidyne DSN-403N and Surflon S-420 to the dope solution resulted in membranes that had dense and smooth surfaces and thus would be suitable for MBR applications. Furthermore, it was confirmed that the blending of the fluoropolymers in the dope solution improved the surface hydrophilicity of the fabricated membranes, similar to the case when Pluronic polymers are added. Therefore, this method of using fluoropolymers as additives is suitable for controlling the surface properties of membranes and can be used to fabricate high-performance CPVC flat-sheet membranes that show excellent antifouling properties in MBRs. Thus, this method will aid in developing improved MBRs.

References

[1] P. Le-Clech, V. Chen and T.A.G. Fane, Fouling in membrane bioreactors used in wastewater treatment, *J. Membr. Sci.*, 284, 17-53 (2006).

[2] K. Xiao, S. Liang, X. Wang, C. Chen and X. Huang, Current state and challenges of full-scale membrane bioreactor applications: a critical review, *Bioresour. Technol.*, 271, 473-481 (2019).

[3] W. Yang, N. Cicek and J. Llg, State-of-the-art of membrane bioreactors: worldwide research and commercial applications in North America, *J. Membr. Sci.*, 270, 201-211 (2006).

[4] I.S. Chang, P.L. Clech, B. Jefferson, S. Judd, Membrane fouling in membrane bioreactor for wastewater treatment, *J. Environ. Eng.*, 128, 1018-1029 (2002).

[5] N. Yamato, K. Kimura, T. Miyoshi, Y. Watanabe, Difference in membrane fouling in membrane bioreactors (MBRs) caused by membrane polymer materials, *J. Membr. Sci.*, 280, 911-919 (2006).

[6] P. van der Marel, A. Zwijnenburg, A. Kemperman, M. Wessling, H. Tenmink, W. van der Meer, Influnece of membrane properties on fouling in submerged membrane bioreactors, *J. Membr. Sci.*, 348, 66-74 (2010).

[7] L. Jin, S.L. Ong, H.Y. Ng, Comparison of foluing characteristics in different pore-sized submergd ceramic membrane bioreactors, *Water Res.*, 44, 5907-5918 (2010).

[8] T. Nittami, H. Tokunaga, A. Satoh, M. Takeda, K. Matsumoto, Influence of surface hydrophilicity on polytetrafluoroethylene flat sheet membrane fouling in a submerged membrane bioreactor using two activated sludges with different characteristics, *J. Membr. Sci.*, 463, 183-189 (2014).

[9] T. Miyoshi, K. Yuasa, T. Ishigami, S. Rajabzadeh, E. Kamio, Y. Ohmukai, D. Saeki, J.

Ni, H. Matsuyama, Effect of membrane polymeric materials on relationship between surface pore size and membrane fouling in membrane bioreactors, *Appl. Surf. Sci.*, 330, 331-357 (2015).

[10] K. Saito, N. Hayashi and S. Tanso, A separation system made of a membrane immersion process for wastewater treatment, *Yuasa Jiho*, 91, 21-30 (2001).

[11] M. Higashi, J. Morita, N. Shimada and T. Kitagawa, Long-term-hydrophilic flat-sheet microfiltration membrane made from chlorinated poly(vinyl chloride), *J. Membr. Sci.*, 500, 180-189 (2016).

[12] T. Sano, Y. Koga, H. Ito, L.V. Duc, T. Hama and Y. Kawagoshi, Effects of structural vulnerability of flat-sheet membranes on fouling development in continuous submerged membrane bioreactors, *Bioresour. Technol.*, 304, 123015 (2020).

[13] M. Tokushima, Development for energy–saving MBR technology, *Membrane*, 37, 235-239 (2012).

[14] W. Zhao, Y. Su, C. Li, Q. Shi, X. Ning and Z. Jiang, Fabrication of antifouling polyethersulfone ultrafiltration membranes using Pluronic F127 as both surface modifier and pore-forming agent, *J. Membr. Sci.*, 318, 405-412 (2008).

[15] H. Rabiee, S.M.S. Shahabadi, A. Mokhtare, H. Rabiei and N. Alvandifar, Enhancement in permeation and antifouling properties of PVC ultrafiltration membranes with addition of hydrophilic surfactant additives: Tween-20 and Tween-80, *J. Environ. Chem. Eng.*, 4, 4050-4061 (2016).

[16] M.-H. Xu, R. Xie, X.-J. Ju, W. Wang, Z. Liu and L.-Y. Chu, Antifouling membranes with bi-continuous porous structures and high fluxes prepared by vapor-induced phase separation, *J. Membr. Sci.*, 611, 118256 (2020).

[17] T. Sano, S. Yamamoto, I. Kokubo, N. Murakami and K. Saito, Effects of Pluronic

TR-702 on chlorinated poly(vinyl chloride) flat-sheet membranes prepared by water vapor induced phase separation, *Membrane*, 46, 44-52 (2021).

[18] S. Ohtoshi, Synthesis and specific properties of fluoro-surfactants, *Sekiyu Gakkaishi*, 32, 277-285 (1989).

[19] Y. Saito, Pluronic surfactants, *Nippon Yuka Gakkaishi*, 49, 1071-1079 (2000).

[20] J.-H. Choi, S.-K. Park and H.-Y. Ng, Membrane fouling in a submerged membrane bioreactor using track-etched and phase-inversed porous membranes, *Sep. Purif. Technol.*, 65, 184-192 (2009).

[21] T. Marino, E. Blasi, S. Tornagahi, E.D. Nicoló and A. Figoli, Polyethersulfone membranes prepared with Rhodiasolv® Polarclean as water soluble green solvent, *J. Membr. Sci.*, 549, 192-204 (2018).

[22] M. Hashino, T. Katagiri, N. Kubota, Y. Ohmukai, T. Maruyama and H. Matsuyama, Effect of membrane surface morphology on membrane fouling with sodium alginate, *J. Membr. Sci.*, 366, 258-265 (2011).

[23] T. Tsuyuhara, Y. Hamamoto, T. Miyoshi, K. Kimura and Y. Watanabe, Influence of membrane properties on physically reversible and irreversible fouling in membrane bioreactors, *Water Sci. Technol.*, 61, 2235-2240 (2010).

Chapter VIII

Conclusions

Membrane bioreactors (MBRs) are promising treatment techniques, especially for wastewater, including dense suspensions and high salinity. However, membrane fouling is still a critical issue for continuous application and has hampered the further spread of MBRs. Establishing membrane fouling mitigation techniques for MBRs is essential for the further spread of MBRs. On the other hand, I believe that the development of membrane fouling mitigation technique alone is not enough for the further spread of MBRs. One of the solutions for this problem is to create new roles for MBRs. I focus on the removal of microplastics, which has become a major environmental issue in recent years. MBRs have excellent microplastics removal performance compared to conventional wastewater treatment plants. Therefore, to further popularize MBRs, I studied the development of a membrane suitable for removing microplastics. In the first part of this study (Chapters II, III, IV, and V), I investigated the membrane properties that have sufficient durability to remove microplastics and mitigate membrane fouling. In the latter part of this study (Chapters VI and VII), I developed a technique for preparing a membrane with such membrane properties.

In Chapter II, the relationship between fouling development in a continuous laboratory-scale MBR and the membrane material was investigated using flat-sheet membranes prepared from four materials: polyvinylidene difluoride (PVDF), chlorinated poly(vinyl chloride) (CPVC), polytetrafluoroethylene (PTFE), and polyethersulfone (PES). Furthermore, the characteristics of the suspension liquid in a laboratory-scale

MBR were compared with those of samples from actual wastewater treatment plants. In addition to the characteristics of the membrane material, the structural vulnerability of the membranes had a determining effect on fouling development. The PVDF membrane showed the highest transmembrane pressure during MBR operation and its surface experienced significant damage because of the shearing stress caused by aeration, resulting in the penetration of the membrane by the fouling compounds. The characteristics of the suspension liquid in the laboratory-scale MBR were similar to those in the MBR at a night-soil treatment plant and the aeration tank of a sewage treatment plant.

In Chapter III, I investigated in detail the three types of membranes except for PVDF membrane used in Chapter II and clarified the mechanical durability and antifouling property of these membranes. Its purpose is to indicate the type of membrane suitable for removing microplastics in MBR. Microplastics have received increasing attention as substances of potential risk due to their adverse effect on ecosystems and human health in recent years. MBRs have excellent microplastic removal performance compared to conventional wastewater treatment plants (WWTPs). Meanwhile, there is a possibility that the membrane materials themselves become the source of microplastics when they deteriorate. Therefore, it is important to consider not only the antifouling performance for wastewater treatment but also the mechanical durability of the membranes to reduce microplastic production; thus; promoting application of MBRs. In this study, the mechanical durability and antifouling performance of the three kinds of membranes, CPVC, PTFE, and PES used in a laboratory-scale submerged MBR for almost two months, was explored. The experiment was carried out in a laboratory-scale submerged MBR with effective working volume of 6.8 L. Synthetic wastewater was

prepared with D-glucose, meat extract, polypeptone, and inorganic salts, and was fed to the reactor. The mixed liquor suspended solids (MLSS) was constantly maintained within 11000-12500 mg/L. Significant breakage and rupture on the surface of the PES membrane and notable changes in the parameters such as pore size and surface roughness related to the membrane structure were observed through MBR operation. Contrarily, for the CPVC and PTFE membranes, only a slight change in the membrane structure and properties was observed. These results indicated that the PES membrane was more susceptible to damage by the shearing force with aeration for MBR than the other membranes. Therefore, the durability of the PES membrane was the lowest among the membranes studied, indicating high microplastic production risk, even though all three membranes have the same antifouling performance. This is the first report of changes in the membrane characteristics and morphology related to mechanical durability and the membrane fouling problem under MBR operation.

In Chapter IV, the relationship between membrane fouling development was investigated using originally prepared CPVC flat-sheet membranes with different pore sizes in MBRs, and fouling development mechanism was demonstrated. Under the conditions in this study, the optimal membrane pore size for suppressing fouling development was determined to be in the range of 0.31-0.57 μm. Further, irreversible fouling is closely related to the capture of protein-like compounds inside the membrane; in contrast, reversible fouling was due to gel and cake layers formed on the membrane surface. Moreover, the membrane pore size directly and indirectly affected both reversible and irreversible fouling through the mutual relationship with other membrane characteristics such as the surface roughness. Finally, the optimal pore size of the membrane for suppressing fouling development is determined by the total filtration

resistance caused by irreversible and reversible fouling phenomena.

In Chapter V, the influence of the surface hydrophilicity of the membranes on fouling development in a continuous laboratory-scale MBR was investigated using two types of symmetric PTFE flat-sheet membranes with similar membrane properties, except for surface hydrophilicity. The hydrophilicity of a membrane has so far been considered an important factor contributing to fouling phenomena. In general, a hydrophobic membrane has a higher fouling development than a hydrophobic membrane; however, there is no conclusion in this matter because many contradictory results have also been reported. In addition, only a few studies have revealed the influence of membrane hydrophilicity on fouling development in an MBR for a long operation period. Therefore, in this chapter, the influence of the surface hydrophilicity of the membrane on fouling development was investigated using a laboratory-scale MBR with PTFE flat-sheet membranes to confirm the influence of membrane hydrophilicity on fouling development. No remarkable difference in the change in transmembrane pressure was observed between hydrophilic and hydrophobic PTFE membranes, indicating that the hydrophilicity of the membrane had little influence on the fouling phenomena. The relationship between hydrophilicity and pore-forming resistance was suggested; however, the dominant factor in membrane fouling was cake layer resistance. The adsorption of protein-like compounds, which were present in the suspension liquid, inside the membrane contributed to the pore fouling resistance based on the results of extracellular polymeric substance measurement and three-dimensional excitation-emission matrix analysis.

In Chapter VI, a method for improving the membrane properties by adding an amphiphilic Pluronic block copolymer to the membrane was developed. In general, membrane properties such as porosity and surface morphology significantly affect fouling

in MBRs. Amphiphilic Pluronic block copolymers have attracted attention in recent years due to their use during membrane preparation, which has resulted in improved membrane properties. This chapter focuses on establishing a technique to improve membrane properties by adding Pluronic TR-702 to prepare a CPVC flat-sheet membrane suitable for use in an MBR. The deterioration of Pluronic TR-702 was expected during long-term MBR applications. Therefore, Pluronic TR-702 was removed from the membranes before evaluation. The pure water permeability, pore size and distribution, surface morphology, surface porosity, and the influence of the additive on the membrane thickness were investigated. Excessive addition of Pluronic TR-702 to the dope solution led to the preparation of membranes with larger pore sizes that were unsuitable for MBRs. On the contrary, appropriate addition increased the pore size and thickness of the membranes and decreased the surface porosity with increasing additive content. When the concentration of Pluronic TR-702 was 50 wt/wt%, a membrane with a suitable pore size for use in MBRs was prepared. This method is a useful technique for improving the properties of membranes used in MBRs.

In Chapter VII, a method for improving the membrane properties by adding a fluoropolymer to the membrane was developed. The porosity, surface hydrophilicity, and morphology of the membranes significantly affect their fouling propensity in MBRs. The use of polymers as additives is an effective strategy for improving the properties of membranes. In this chapter, I developed a technique to improve the membrane properties by using Unidyne DSN-403N and Surflon S-420, which are fluoropolymers, as novel polymer additives to prepare CPVC flat-sheet membranes suitable for MBR applications. The blending of these fluoropolymers in the dope solution produced membranes that exhibited dense and smooth surfaces and were appropriate for use in MBRs. The

membrane prepared using Surflon S-420 showed a higher pure water permeability than that of the membrane prepared using Unidyne DSN-403N. Thus, the former membrane would exhibit better antifouling properties. This method of blending a fluoropolymer is useful for preparing high-performance CPVC flat-sheet membranes for MBRs.

Publications related to this dissertation

Journal papers

1. Toshio Sano, Yoshiki Koga, Hiroaki Ito, Luong Van Duc, Takehide Hama, Yasunori Kawagoshi: Effects of structural vulnerability of flat-sheet membranes on fouling development in continuous submerged membrane bioreactors, Bioresource Technology, 304, 123015 (2020).

2. Toshio Sano, Shunsuke Yamamoto, Ituki Kokubo, Naoki Murakami, Kenichi Saito: Effects of Pluronic TR-702 on chlorinated poly(vinyl chloride) flat-sheet membranes prepared by water vapor induced phase separation, Membrane, 46, 44-52 (2021).

3. Toshio Sano, Hiroki Mizui, Itsuki Kokubo, Kouhei Shintaku, Shunsuke Yamamoto, Naoki Murakami, Kenichi Saito: Fabrication of high-performance chlorinated poly(vinyl chloride) flat-sheet membranes using commercially available fluoropolymers as membrane-property modifiers, GS Yuasa Technical Report, 18(1), 23-30 (2021).

4. Toshio Sano, Hiroaki Ito, Kei Ishida, Akira Sato, Luong Van Duc, Yasunori Kawagoshi, Effect of surface hydrophilicity of symmetric polytetrafluoroethylene flat-sheet membranes on membrane fouling in a submerged membrane bioreactor, Japanese Journal of Water Treatment Biology, 57, 79-89 (2021).

5. Toshio Sano, Yasunori Kawagoshi, Itsuki Kokubo, Hiroaki Ito, Kei Ishida, Akira Sato, Direct and indirect effects of membrane pore size on fouling development in a submerged membrane bioreactor with a symmetric chlorinated poly(vinyl chloride) flat-sheet membrane, Journal of Environmental Chemical Engineering, 10, 107023 (2022).

6. Toshio Sano, Hiroaki Ito, Kei Ishida, Akira Sato, Yasunori Kawagoshi, Mechanical durability and fouling development of flat-sheet membranes in submerged membrane bioreactor, Japanese Journal of Water Treatment Biology, in press.

International conference proceedings

1. Toshio Sano, Hiroaki Ito, Takehide Hama, Luong Van Duc, Yasunori Kawagoshi: Influence of hydrophilicity on membrane fouling in submerged membrane bioreactor with polytetrafluoroethylene flat-sheet membranes, Proceedings of the 2019 international conference on climate change, disaster management and environmental sustainability, 351-356, September 19-21, 2019, Kumamoto University, Japan.

Domestic conference proceedings

1. Shunsuke Yamamoto, Kenchi Saito, Toshio Sano: Effects of Pluronic surfactants concentration as additives on performance of flat-sheet chlorinated poly(vinyl chloride) membrane, Proceedings of the SCEJ 82nd Annual Meeting, PD375, March 6-8, 2017, Shibaura Institute of Technology, Tokyo

2. Yoshiki Koga, Toshio Sano, Hiroaki Ito, Yasunori Kawagoshi: Comparison of fouling occurrence in membrane bioreactor using chlorinated polyvinyl chloride (CPVC), polyvinylidene fluoride (PVDF), polyethersulfone (PES), polytetrafluoroethylene (PTFE), Proceedings of the 51th Annual Conference of JSWE, 1-F-09-2, March 15-17, 2017, Kumamoto University, Kumamoto

3. Yoshiki Koga, Toshio Sano, Shota Watanabe, Hiroaki Ito, Takehide Hama, Yasunori Kawagoshi: Relationship between the membrane materials and the fouling occurrence in submerged membrane bioreactor, Proceedings of the 54th Annual Meeting of Japanese Society of Water Treatment Biology, B-08, November 8-10, 2017, Osaka University, Osaka

4. Toshio Sano, Yoshiki Koga, Shota Watanabe, Hiroaki Ito, Takehide Hama, Yasunori Kawagoshi: Effect of pore size of CPVC flat-sheet membranes on fouling propensity in a submerged membrane bioreactor, Proceedings of the 54th Annual Meeting of Japanese Society of Water Treatment Biology, B-07, November 8-10, 2017, Osaka University, Osaka

5. Toshio Sano, Yoshiki Koga, Hiroaki Ito, Takehide Hama, Yasunori Kawagoshi: Study of fouling occurrence in different pore sized submerged membrane bioreactors, Proceedings of the 52nd Annual Conference of JSWE, 2-D-09-2, March 15-17, 2018, Hokkaido University, Hokkaido

6. Yoshiki Koga, Toshio Sano, Hiroaki Ito, Takehide Hama, Yasunori Kawagoshi: Study on fouling occurrence factors of membranes with different materials in submerged membrane bioreactor, Proceedings of the 52nd Annual Conference of JSWE, 2-D-09-3, March 15-17, 2018, Hokkaido University, Hokkaido

7. Shota Watanabe, Yoshiki Koga, Hiroaki Ito, Luong Van Duc, Takehide Hama, Yasunori Kawagoshi, Toshio Sano: Study on influence of membrane materials and properties on fouling occurrence in submerged membrane bioreactor, Proceedings of the 2017 research presentation of JSWE Kyushu Okinawa branch, 1-1-5, March 10, Kumamoto University, Kumamoto

8. Shunsuke Yamamoto, Naoki Murakami, Kenichi Saito, Toshio Sano: Effects of surfactants as additives on chlorinated poly(vinyl chloride) membrane, Proceedings of the SCEJ 50th Autumn Meeting, CC113, September 18-20, 2018, Kagoshima University, Kagoshima

9. Yaunori Kawagoshi, Toshio Sano, Hiroaki Ito, Takehide Hama, Luong Van Duc: Discussion on the relationship between the membrane materials and the changes in transmembrane pressure in submerged membrane bioreactor, Proceedings of the 56th Annual Meeting of Japanese Society of Water Treatment Biology, B-11, November 8-10, 2019, Kanazawa Institute of Technology, Ishikawa

10. Kyota Fujimoto, Hiroaki Ito, Luong Van Duc, Takehide Hama, Yaunori Kawagoshi, Toshio Sano, Relationship between hydrophilicity of PTFE membrane and fouling behavior in submerged MBR, Proceedings of the 2019 research presentation of JSWE Kyushu Okinawa branch, B3-4, February 20, The University of Kitakyushu, Fukuoka

11. Toshio Sano, Hiroaki Ito, Luong Van Duc, Takehide Hama, Yasunori Kawagoshi: Influence of surface hydrophilicity of membranes on membrane fouling in submerged membrane bioreactor, Proceedings of the SCEJ 85th Annual Meeting, D203, March 15-17, 2020, Kansai University, Osaka

12. Toshio Sano, Shunsuke Yamamoto: Effects of Pluronic TR-702 as additive on pore-forming of CPVC flat-sheet membranes prepared by VIPS, Proceedings of the SCEJ 85th Annual Meeting, I119, March 15-17, 2020, Kansai University, Osaka

Patent

1. Toshio Sano, Keiichi Oka: Porous membrane and its production process, Japanese Patent P2009-112895A

Acknowledgement

This dissertation is the results of the work which I have accomplished in six years. I am greatly indebted to many people whose support, advice and encouragement allowed me to complete this work.

Firstly, I would like to thank my supervisor and a respectable researcher Professor Yasunori Kawagoshi for your guidance, support, advice and encouragement. Your enthusiasm for work and your integrated insight into research have given me great help. I would also like thank Assistant Professor Hiroaki Ito for his generous support during the experiment.

I am grateful for Professor Gozo Tsujimoto, Associate Professor Takehide Hama (Graduate School of Agriculture, Kyoto University), Associate Professor Shigeru Morimura, Associate Professor Akira Sato, Associate Professor Kei Ishida and Dr. Luong Van Duc (Graduate School of Engineering, Osaka University). I am grateful that this work was accomplished with the cooperation of many students and graduate student in the Kawagoshi's laboratory as collaborators.

I would like to thank Mr. Shuji Kido, the former president of Yuasa Membrane Systems Co., Ltd. for giving me such an opportunity. This dissertation includes some of the developments achieved together with Yuasa Membranes Systems colleagues. I also thank them.

Special thanks to my wife, two sons and daughter. They cheered me up and gave me mental and emotional support.